The Non-inflammatory Role of Macrophage Migration Inhibitory Factor in Regulating Insulin Resistance and Hypertriglyceridemia

By

Yiheng Huang

A Thesis submitted to the Faculty of Graduate Studies of The University of Manitoba in partial fulfilment of the requirements of the degree of

Doctor of Philosophy

College of Pharmacy

University of Manitoba

Winnipeg

ABSTRACT

Insulin resistance (IR) and hypertriglyceridemia are two major symptoms of metabolic dysfunction, which are regulated by endocrine function and lipid storage in white adipose tissue (WAT). Macrophage migration inhibitory factor (MIF) is a pro-inflammatory cytokine regulating metabolic dysfunction. We currently identified how adipose MIF regulated IR and hypertriglyceridemia through the following mechanisms.

(1) MIF is involved in the development of non-inflammatory IR by a cross-talk between preadipocyte factor 1+ (Pref-1+) cells and adipocytes in WAT.

Pref-1 expression is negatively associated with circulating MIF levels in obese human subjects and animal models in the absence of adipose inflammation. Pref-1 is released from Pref-1+ cells including M2 (anti-inflammatory) macrophages, endothelial cells or progenitors in WAT. Its release inhibits MIF derived from both Pref-1+ cells and adipocytes by binding with integrin β1 and inhibiting the mobilization of p115. High palmitic acid (PA) induces protease-activated receptor 2 (PAR2) expression in Pref-1+ cells, thereby downregulating Pref-1 expression and release in an AMP-activated protein kinase (AMPK)-dependent manner. The loss of Pref-1 increases adipose MIF secretion contributing to non-inflammatory IR in obesity. In contrast, treatment with Pref-1 blunts the increase in circulating plasma MIF levels and subsequent IR induced by a high palmitic acid diet (PD).

(2) MIF inhibits lipoprotein lipase (LPL) that catalyzes the degradation of plasma triglyceride (TG) and upregulates adipose lipid storage.

LPL hydrolyzes circulating TG to release free fatty acids (FFAs) and it promotes lipid storage in WAT. Obesity-associated high PAR2 expression is inversely correlated with LPL expression in WAT, leading to hypertriglyceridemia. MIF reduces LPL expression and activity in adipocytes. High circulating MIF levels in mice models with PD feeding or high MIF expression

suppress adipose LPL, which is associated with increased plasma TG levels. However, the low adipose LPL expression and activity is reversed in *Par2*$^{-/-}$ mice. Thus, high PA increased activation of PAR2, facilitating adipose MIF secretion, and then resulted in low LPL-induced hypertriglyceridemia.

We identified the mechanisms of MIF in mediating IR and hypertriglyceridemia in both human subjects and animal models. Our translational research will provide important clinical implications for the development of new therapeutic strategies for metabolic syndrome.

ACKNOWLEDGEMENTS

I would like to express my deepest gratitude to my supervisor Dr. Dake Qi for his lasting guidance to my Ph.D. study journey. I am deeply indebted to the support of the experimental skills and animal supply from our lab manager/technician Yadan Qi. I am so grateful to all the lab members I worked with in Dr. Qi's lab for their accompany and support to go through this journey together.

I would like to extend my sincere thanks to my committee member, Dr. Garry Shen and Dr. Lucy Marzban for their kindness and great suggestions about my Ph.D. study. I also appreciate all the collaborators as follow. Dr. Richard Bucala and Dr. Lin Leng from Yale University gave us transgenic mice and key experimental materials and protocols and technical support. Dr Lawrence H. Young from Yale university and Dr Brian Rodrigues from University of British Columbia supported the current study with brilliant suggestions. Dr John McGuire from Western University gave us the transgenic mice as a gift. Dr. Guang Sun from Memorial University gave us the opportunity of the second use of human samples. Dr. Jacqueline L. Vanderluit from Memorial University and her graduated Ph.D. student, now a medical student in Memorial University, Dr. Kathleen E. Fifield, help me with immunofluorescence labeling and imaging.

I am also thankful for technical support from core facilities in University of Manitoba and Memorial University. I am grateful to the instructors of the courses I took during my Ph.D. study, such as Dr. John Smeda and Dr. Van Vliet from Memorial University. Thank should also go to the funding support from the CIHR, NSERC and CSC.

I could not have undertaken this journey without the recommendation of Dr Gonglin Hou from Zhejiang Sci-Tech University and Dr. Donghong Cui from Shanghai Jiao Tong University. Last but not least, I appreciate the long-lasting support from my dear family members and friends.

TABLE OF CONTENTS

LIST OF FIGURES

LIST OF TABLES

ABBREVIATIONS

ABC	ATP-binding cassette
ABCA1	ABC transporter subfamily 1
AC	Adipocytes
ACC	Acetyl-CoA carboxylases
AgRP	Agouti-related protein
AICAR	5-Aminoimidazole-4-carboxamide ribonucleotide
Akt/PKB	Protein kinase B
AMPK	AMP-activated protein kinase
ANGPTL	Angiopoietin-like
ANOVA	Analysis of variance
Apo	Apolipoprotein
aP2/FABP4	Adipocyte protein 2
AT	Adipose tissue
AT/BW	Adipose tissue weight/body weight
ATGL	Adipose triglyceride lipase
BAT	Brown adipose tissue
BDG	(1,3)(1,6)-beta-D-glycans
BDNF	Brain-derived neurotropic factor
BMI	Body mass index
BSA	Bovine serum albumin
BW	Body weight
CaMKKβ	CaM-dependent protein kinase kinase beta
CCR/MCP-1	CC motif chemokine receptor

cDNA	Complementary DNA
CD	Cluster of differentiation
CXCR	CXC chemokine receptor
DAG	Diacylglycerol
DGAT	Diglyceride acyltransferase
DNL	de novo lipogenesis
ELISA	Enzyme-linked immunosorbent assay
ER	Endoplasmic reticulum
ERK	Extracellular signal-regulated kinase
FA	Fatty acid
FAHFA	Fatty acid esters of hydroxy fatty acid
FASN	Fatty acid synthase
FABP4	Fatty-acid-binding protein 4
FBS	Fetal bovine serum
FFA	Free fatty acid
FoxO1	Forkhead box protein O1
FPLC	Fast protein liquid chromatography
F2RL1/PAR2	F2R like trypsin receptor 1
Gapdh	Glyceraldehyde-3-phosphate dehydrogenase
GLUT4	Glucose transporter type 4
GPIHBP1	Glycosylphosphatidylinositol-anchored high-density lipoprotein–binding protein 1
GPR	G-protein coupled receptor
GTT	Glucose tolerance test
G3P	Glycerol-3-phosphate

h	Hour
HE	Hematoxylin and eosin
HFD	High-fat diet
HL	Hepatic lipase
HOMA IR	Homeostatic model assessment for insulin resistance
HREB	Health Research Ethics Board
HSL	Hormone-sensitive lipase
IBMX	3-Isobutyl-1-methylxanthine
IDL	Intermediate-density lipoprotein
IgG	Immunoglobulin G
IL	Interleukin
IL-1R1	IL-1 receptor 1
i.p.	Intraperitoneal
IR	Insulin resistance
ITT	Insulin tolerance test
ITGA5	Integrin alpha 5
ITGB1	Integrin beta 1
i.v.	Intravenous
IVC	Individually ventilated cage
LDL	Low-density lipoprotein
LDL-C	LDL-cholesterol
LMF1	Lipase maturation factor 1
LPL	Lipoprotein lipase
LPS	Lipopolysaccharide

LYVE1	Lymphatic vessel endothelial hyaluronan receptor 1
MΦ	Macrophage
MAG	Monoacylglycerol
MCP 1	Monocyte chemoattractant protein 1
MGL	Monoacylglycerol lipase
MIF	Macrophage migration inhibitory factor
Mif lung Tg/Mif Tg	Mif lung transgenic mice
mTORC2	Mechanistic target of rapamycin complex 2
NC	Normal chow
PA	Palmitic acid
PAR2	Protease-activated receptor 2
PBS	Phosphate buffered saline
PD	High palmitic acid diet
Pik3r1	Phosphoinositide-3-kinase regulatory subunit 1
PPARγ	Peroxisome proliferator-activated receptors gamma
Pref-1	Preadipocyte factor 1
Pref-1 C	Pref-1 cells
PTEN	Phosphatase and tensin homologue
qPCR	Quantitative polymerase chain reaction
RBP-4	Retinol binding protein-4
rMIF	Recombinant MIF
RNA	Ribonucleic acid

rPref-1	Recombinant Pref-1
SD	Standard deviation
siRNA	Small interfering RNA
SIRT1	Sirtuin 1
SM	Skeletal muscle
SVF	Stromal vascular fraction
TG	Triglyceride
TNFα	Tumor necrosis factor alpha
Val66Met	Valine with a methionine at codon 66
VLDL	Very-low-density lipoprotein
WAT	White adipose tissue
WT	Wild type
12,13-diHOME	12,13-dihydroxy-9Z-octadecenoic acid
2fLI	2-furoyl-LIGRLO-NH2
3T3D	3T3 differentiated adipocytes
3T3U	3T3 undifferentiated Pref-1 + cells
9-PAHSA	Palmitic-acid-9-hydroxy-stearic-acid

CHAPTER 1: INTRODUCTION

There are mainly two types of adipose tissue in mammals, white and brown, with different morphology and functions of adipocytes. WAT stores lipids and supplies FFAs to other organ systems. However, brown adipose tissue (BAT) oxidizes fatty acids (FAs) within the brown adipocytes to contribute to thermogenesis.

In addition to storing excess energy, WAT is an endocrine organ that affects metabolic dysfunction by releasing cell-signalling molecules, “adipokines” (1). WAT involves adipocytes and many non-adipocyte cells, including endothelial cells, pericytes, adipose precursor cells, macrophages, etc. Due to the different proportions of adipocytes and non-adipocytes, WAT in different parts of the human body has different abilities to secrete adipokines (2). To meet the increased storage demands during obesity, preadipocytes differentiate into mature adipocytes (adipogenesis), and adipocytes can expand in size (hypertrophy). Alterations in adipocyte number and morphology during obesity not only accommodate excess energy by lipid uptake, esterification, and lipolysis but also contribute to changes in adipose immune conditions and adipokines release.

In the setting of metabolic dysfunction, WAT releases cytokines that can recruit and activate resident and non-resident immune cells, leading to the development of inflammation. These cytokines also act directly on the insulin signalling pathway, attenuating insulin signalling and leading to IR. However, IR is not always associated with adipose inflammation. It can precede macrophage accumulation and adipose inflammation (3). Furthermore, anti-inflammatory treatments have failed to improve insulin sensitivity in animal models and human subjects (4, 5). These data suggest that non-inflammatory adipose events may also play a crucial role in the development of IR. BAT has a potential role in combating metabolic dysfunction, so WAT browning also offers an important strategy against IR.

The capacity of lipid storage in WAT also affects the levels of plasma TG. LPL is a key enzyme facilitating TG breakdown to release FFAs for storage in WAT (6). Therefore, the alteration of adipose LPL expression and activity may contribute to the occurrence of hypertriglyceridemia during metabolic dysfunction (7).

1.1 WHITE ADIPOSE TISSUE AND INSULIN RESISTANCE

1.1.1 Lipid Dynamic in White Adipose Tissue and Insulin Sensitivity

During fasting, exercise, cold exposure or hormone stimulation, stored lipids in WAT are hydrolyzed into FFAs and glycerol (8). This process is called “lipolysis”, which promotes the release of FFAs into circulation to meet the requirement of whole-body energy consumption (Figure 1-1). On the other hand, in a postprandial state, lipolysis is inhibited while the increased FFA or glucose uptake promotes “lipogenesis” to store extra lipid or glucose in circulation and prevent ectopic lipid storage, hyperlipidemia or hyperglycemia (Figure 1-1). Both lipolysis and lipogenesis in WAT have been implicated in the development of systemic IR.

1.1.1.1 Lipolysis and insulin resistance

Normally, WAT lipolysis is inhibited by insulin. Thus, IR increases lipolysis levels. However, a surgical injury with hemorrhagic shock and counterregulatory hormone (epinephrine) infusion stimulates adipocyte lipolysis, IR and hyperglycemia (9). Inhibition of lipolysis abolished the stress-induced IR and hyperglycemia (9), suggesting that lipolysis may also contribute to the development of IR. FAs produced by adipocyte lipolysis have been postulated to exacerbate IR. Human studies indicated that inhibition of basal lipolysis reduces fatty acid turnover and improves insulin sensitivity without altering fat mass (10). Three enzymes, including adipose triglyceride lipase (ATGL), hormone-sensitive lipase (HSL), and monoglyceride lipase (MGL), work stepwise to complete hydrolysis of TG (Figure 1-1). Among them, ATGL global knockout mice are severely defective in lipolysis and can resist high-fat diet (HFD)-induced IR (11, 12). HSL insufficiency or

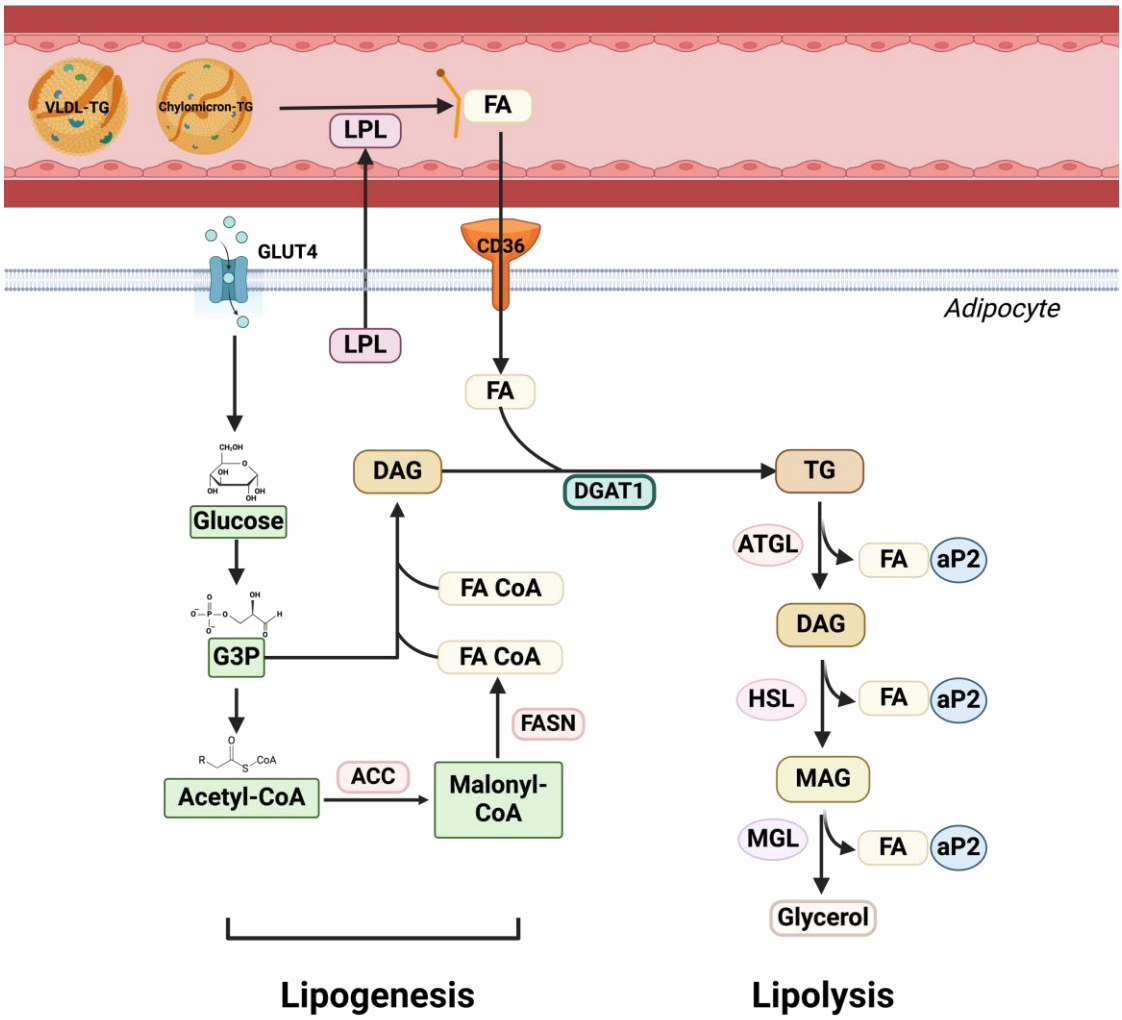

Figure 1-1. Lipid dynamic in WAT. Following feeding, the increased FFA or glucose uptake promotes "lipogenesis" to store extra energy in WAT. However, during fasting, exercise, cold exposure or hormone stimulation, stored lipids in adipose tissue are hydrolyzed into FFAs and glycerol. This process is called "lipolysis", which promotes the release of FFA into circulation to meet the requirement of whole-body energy consumption.

deficiency also improves insulin sensitivity without altering body weight, fat mass, or adipose inflammation (10, 13). Adipocyte protein 2 (aP2, also called FABP4) is a fatty acid carrier protein mainly expressed in adipocytes and macrophages (14, 15) (Figure 1-1). aP2 functions to move FAs out of adipocytes and promote lipolysis. aP2-deficient mice develop obesity but no IR after feeding a HFD (16). These inhibitory effects of lipolysis by knockdown of ATGL, HSL or aP2 are associated with reduced fatty acid turnover, thereby improving glucose metabolism and insulin signalling in WAT and skeletal muscle (17, 18).

1.1.1.2 Lipogenesis and insulin resistance

Lipid accumulation in adipocytes depends on the conversion of FAs and glycerol into TG or *de novo* lipogenesis (DNL) (19) (Figure 1-1). In the first process, LPL degrades circulating TG (embedded in very-low-density lipoprotein (VLDL) or chylomicrons) to release FAs, which are further transported into adipocytes via FA transporters (such as cluster of differentiation 36 (CD36)) (6, 20). Three FAs and a glycerol backbone undergo esterification to form TG. DNL involves the synthesis of FA from acetyl-CoA and the subsequent esterification of FA and glycerol. Acetyl-CoA carboxylases 1 (ACC1) converts acetyl-CoA to malonyl-CoA, which is transformed into palmitate by fatty acid synthase (FASN), an essential rate-limiting enzyme in DNL (21, 22). Palmitate can be further converted to other complex FAs through elongation and desaturation processes (23).

The degree of IR was inversely correlated with *LPL mRNA* in abdominal subcutaneous fat of human subjects (24). Overexpression of adipose LPL improves insulin sensitivity by selectively upregulating peroxisome proliferator-activated receptors gamma (PPARγ)-regulated genes without increasing fat mass in diet-induced obesity (25). However, adipose-specific LPL deficiency reduced the uptake of chylomicron TG into BAT and lung but had no effect on WAT (7). Deletion of adipose LPL does not affect glucose uptake in other tissues, such as liver and heart (7). However, adipose-specific LPL knockout mice with muscle LPL overexpression have

increased glucose uptake in visceral adipose tissue rather than subcutaneous adipose tissue or BAT (7), suggesting a complex role of LPL in regulating glucose metabolism.

CD36 recruits circulating FAs into adipocytes. CD36 expression levels in human subcutaneous and visceral adipose tissue correlate with BMI as well as circulating glucose and insulin levels (26). Inherited CD36 deficiency or single nucleotide polymorphisms in the *CD36* gene are associated with lipid abnormalities that induce IR and diabetes (27-30). Independently regulated promoters generate six CD36-encoding transcripts, with adipocyte-specific CD36 transcript 1C predicting systemic and tissue-specific insulin sensitivity in adipose, liver and muscle, suggesting that CD36 expression in adipocytes can counteract IR (31). In fact, blocking CD36 function reversed HFD-induced visceral fat accumulation and IR in obese mice carrying a brain-derived neurotropic factor (BDNF)-valine with a methionine at codon 66 (Val66Met) variant (32), suggesting that not only CD36 expression but also its function is related to the development of IR.

Diglyceride acyltransferases (DGATs) are a group of enzymes that catalyzes the terminal and committed steps of triglyceride synthesis. The expression of DGAT1 in human adipose tissue is closely related to insulin sensitivity and obesity (33, 34). Adipose-specific DGAT1 knockout mice exhibit glucose intolerance associated with the activation of endoplasmic reticulum (ER) stress with HFD (35, 36). However, mice deficient in DGAT2 in adipocytes had normal TG storage and glucose metabolism after feeding a HFD (35). These data suggest that DGAT1 but not 2 promotes adipogenesis in WAT, thereby preventing ectopic fat storage and IR.

DNL from adipocytes is also associated with the regulation of whole-body insulin sensitivity (37). FASN is a rate-limiting enzyme that regulates DNL in WAT. Most previous human studies have shown that FASN expression is inversely correlated with IR (33, 38, 39). However, one study showed a positive correlation between FASN gene expression and IR (40). Interestingly, in an animal model of diet-induced obesity, loss of FASN in white and brown

adipocytes upregulated glucose tolerance, energy expenditure, and increased brown fat-like adipocytes in subcutaneous adipose tissue, as well as resistance to diet-induced obesity (41, 42).

1.1.2 Adipose Endocrine Function and Insulin Sensitivity

1.1.2.1 Adipose endocrine function

In addition to serving as an energy storage organ, WAT has also been identified as the largest endocrine system regulating metabolic homeostasis. The first hormone released by adipose tissue, leptin, was discovered in 1994. In the ensuing decades, an increasing number of fat-derived proteins, including hormones or cytokines, known as “adipokines”, were found to be involved in the development of metabolic dysfunction. For example, leptin, a “hunger hormone” produced from adipocytes, suppresses appetite and regulates energy homeostasis (43). A paucity of WAT significantly reduces plasma leptin release from WAT, resulting in severe IR and fatty liver (44), suggesting that the endocrine function of WAT is critical for regulating metabolic abnormalities. So far, many adipokines have been found to be expressed and released from well-functioning WAT under physiological and pathologic conditions, including leptin, adiponectin, resistin, pro-cytokines and novel family of lipids, etc. Regulation of these adipokines significantly contributes to the development of IR and other metabolic abnormalities during obesity.

1.1.2.2 Obesity and alterations in adipose endocrine functions

Obesity is associated with endocrine changes in WAT, which in most cases are reversed with weight loss, suggesting that these endocrine changes are a direct consequence of obesity (45). WAT in obesity undergoes marked alterations in the secretion of adipokines (Figure 1-2). Adiponectin and omentin have beneficial effects on maintaining metabolic homeostasis through enhancing insulin sensitivity and resisting inflammation (46, 47). Their expression and release in WAT are significantly reduced in obesity and type 2 diabetes (48, 49). In contrast, serum leptin levels were significantly increased due to leptin resistance, which was positively associated with

IR in obesity (50). Resistin and chemerin are also increased following obesity (51, 52), and they induce IR by downregulating adipogenesis or upregulating inflammation in WAT (53-56). Retinol binding protein-4 (RBP-4) is a lipocalin that transports small hydrophobic molecules (57) and promotes adipose inflammation and IR (58). RBP-4 has been found to be positively correlated with body mass index (BMI) and glucose concentration (59). More importantly, WAT also expresses and secretes a variety of cytokines during obesity, including tumor necrosis factor alpha (TNFα), interleukin 6 (IL-6), IL-1α and IL-1β, etc (60, 61). Alterations in the expression and release of these cytokines significantly contribute to the development of IR by exacerbating adipose inflammation.

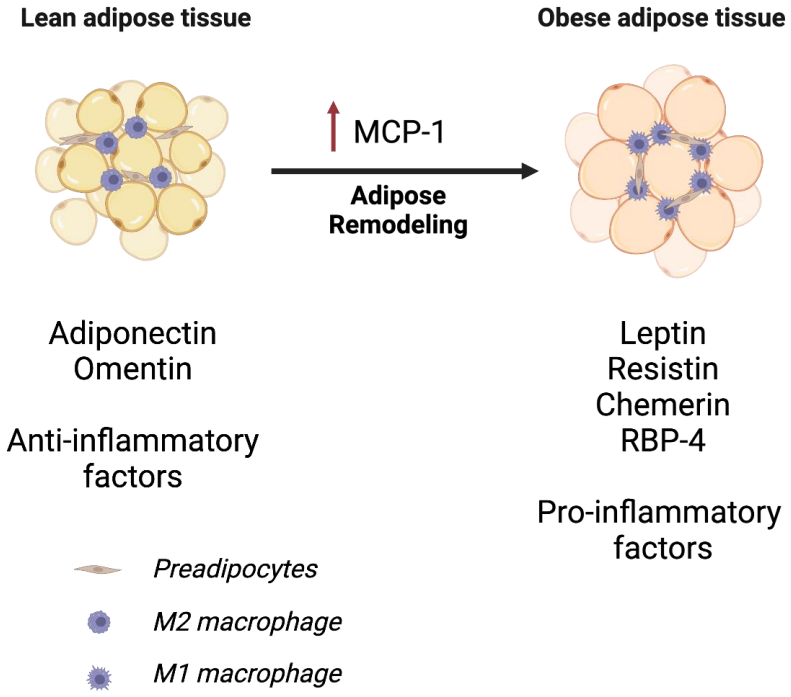

Figure 1-2. Chronic inflammation in WAT. Obesity leads to adipose remodeling and subsequent alterations in adipokine release. Lean WAT containing M2 macrophages releases hormones, including adiponectin and omentin, and anti-inflammatory factors. Upon adipose remodeling, enlarged WAT during obesity recruits M1 inflammatory macrophages and releases leptin, resistin, chemerin, RBP-4 and pro-inflammatory factors.

1.1.2.3 Lipokines and insulin resistance

Other than adipokines, WAT can also release signaling lipid species, lipokines, to modulate whole-body metabolic homeostasis. One group of lipokines is branched fatty acid esters of hydroxy fatty acids (FAHFAs), of which palmitic-acid-9-hydroxy-stearic-acid (9-PAHSA) is studied the most. 9-PAHSA improves whole-body insulin sensitivity without body weight alteration (62). Mechanically, 9-PAHSA improves adipose glucose uptake and pancreatic glucose-stimulated insulin secretion through activation of G-protein coupled receptor 120 (GPR120) and GPR40, respectively (62, 63). Another lipokine, called 12,13-dihydroxy-9Z-octadecenoic acid (12,13-diHOME), is highly secreted from BAT and facilitates fatty acid uptake in BAT and skeletal muscle following cold exposure and exercise (64, 65).

1.1.3 Chronic Inflammation in White Adipose Tissue and Insulin Resistance

Over the past few decades, chronic adipose inflammation has been considered an important theory for IR mechanism (66). Chronic obesity is accompanied by adipose inflammation, which is characterized with adipocyte dysfunction, immune cell infiltration, and cytokine release (67, 68). Many factors may be involved in triggering adipose inflammation, such as dietary FAs, adipose hypoxia, and intestinal microbiota-regulated production of lipopolysaccharide (66). Obesity increases chemokine release, which promotes immune cell recruitment and adipose inflammation (69, 70) (Fig. 2). Thus, deficiency of the CC motif chemokine receptor 2 (CCR2, known as MCP-1) in mice significantly suppressed macrophage infiltration and improved insulin sensitivity in adipose tissue following HFD feeding (71). Infiltration and activation of neutrophils, macrophages and T cells further exacerbate adipose inflammation (72-74). There are two types of macrophages in adipose tissue, M1 and M2 macrophages (Fig. 2). Under normal physiological conditions, M2-type macrophages predominate and secrete anti-inflammatory cytokines in WAT. However, during obesity-associated adipose inflammation, M1 macrophages accumulate in WAT and secrete pro-inflammatory cytokines (75).

Inflammation has various effects on remodeling adipose functions in regulating metabolic homeostasis, referred as "homeostatic inflammation" (76) (Fig. 2). Macrophages are involved in angiogenesis (77), clearance of dead adipocytes (78) and thermogenesis (79). The recruitment, infiltration, and accumulation of bone marrow-derived (lymphatic vessel endothelial hyaluronan receptor 1) LYVE-1+ macrophages in the apical region of epididymal adipose tissue promotes the formation of a dense vascular network (80). Conversely, sirtuin 1 (SIRT1) deficiency in WAT reduces macrophage infiltration and differentiation, resulting in reduced extracellular matrix and attenuated expression of vascular endothelial growth factor and angiogenic factors (77). Macrophages are also involved in the clearance of dead adipocytes in epididymal adipose tissue following HFD feeding (78, 81). Dying adipocytes typically release lipid droplets that attract macrophages to sequester and clear the local lipid content in the interstitial space (82). Cold exposure activates catecholamine-secreting macrophages, which induce thermogenesis in BAT and lipolysis in WAT (79). Cold stress also induces WAT browning by recruiting M2 macrophages (83).

More importantly, during adipose inflammation, macrophage infiltration promotes cytokine release, attenuating insulin sensitivity in adipocytes through autocrine/paracrine effects. TNF-α is known as an insulin receptor inhibitor and can directly lead to IR (84). In addition to insulin signaling and glucose uptake, TNF-α also plays a key role in lipolysis and FFA uptake, thereby impairing insulin sensitivity indirectly (85). Thus, long-term adipose inflammation may play an important role in the development of obesity-associated IR.

1.1.4 Evidence of Non-Inflammatory Insulin Resistance in White Adipose Tissue

1.1.4.1 Insulin resistance is not always coupled with adipose inflammation

Adipose inflammation is strongly associated with IR, but not always. For instance, thermoneutrality-induced adipose inflammation does not seem to affect IR significantly (86). In HFD-fed mice, systemic and tissue-specific IR in liver, skeletal muscle and WAT might develop

prior to signs of adipose inflammation (87). Similarly, a recent study demonstrated that obesity-related IR could potentially precede an increase in macrophage accumulation in WAT (3). In a larger animal model (rabbit), whole-body IR has been detected following 10 weeks of HFD without significant changes in subcutaneous lipid metabolism or the status of adipose inflammation (88). Furthermore, a recent human study suggested a positive correlation between adipose IR levels and the size of subcutaneous and femoral adipocytes, but not necessarily with cytokine gene expression or macrophage markers of adipose inflammation (89). Taken together, these findings imply that insulin resistance is not always coupled with adipose inflammation, and that inflammation may primarily affect long-term HFD-induced IR in animal models (90).

1.1.4.2 Inconsistent effects of anti-inflammatory therapy in insulin resistance

Over the past decades, anti-inflammatory strategies have been tested in basic and clinical research. Many of these focus on cytokines, such as TNF-α, IL-6, IL-1β, and IL-10 as therapeutic targets for IR. However, the results have been inconsistent and even disappointing.

1.1.4.2.1 Tumor necrosis factor-α

Although TNF-α has been found to directly induce IR, transgenic deficiency of TNF-α was not sufficient to improve insulin sensitivity in obese mouse models (91). Interestingly, deletion of the TNF-α receptor even further impairs insulin sensitivity in HFD-fed wild-type (WT) or db/db mice (92). Clinical trials by blocking the effect of TNF-α failed to improve insulin sensitivity (93-99), suggesting that blocking TNF-α is not a favorable strategy for the treatment of IR. However, the treatment against TNF-α improves insulin sensitivity without changing body composition in patients with rheumatoid arthritis, suggesting that IR associated with inflammatory diseases may be beneficial from anti-TNFα treatment (100-102).

1.1.4.2.2 Interleukin-6

IL-6 has exhibited pleiotropic effects on metabolic homeostasis. Both genetic deficiency and overexpression of IL-6 in mice deteriorate hepatic inflammation and IR induced by HFD feeding (103, 104). However, expression of human IL-6 in mice improves insulin sensitivity and attenuates weight gain following a HFD (105), suggesting a beneficial effect of human IL-6 on IR. Indeed, infusion of human IL-6 increases lipolysis and enhances insulin sensitivity in healthy or diabetic subjects (106, 107). However, a previous study also indicated that single dose intravenous (i.v.) injection of anti-IL-6 receptor blocker, tocilizumab improved insulin sensitivity in non-diabetic patients with rheumatoid arthritis (108).

1.1.4.2.3 Interleukin-1β

Similar as TNF-α, IL-1β also impairs insulin signaling in adipocytes and liver-derived cells (109-111). Thus, deletion of IL-1β receptor, IL-1 receptor 1 (IL-1R1), significantly attenuated adipose inflammation while improved whole-body insulin sensitivity in mice fed with either normal chow (NC) or HFD (112). Deficiency of caspase 1, an upstream activator of IL-1β, also resisted HFD-induced insulin resistance (113). Clinical studies also showed that blockage of IL-1β improved hyperglycemia as well as insulin sensitivity in patients with type 2 diabetes (114).

1.1.4.2.4 Interleukin-10

IL-10 is a critical anti-inflammatory cytokine mainly secreted by M2 macrophages. Overexpression of IL-10 in murine skeletal muscle prevents aging-associated IR (115). However, neither deletion of IL-10 from the hematopoietic system (116) nor administration of IL-10 affects insulin sensitivity in HFD-induced obese mice (117). Furthermore, increased circulating IL-10 and adipose IL-10 expression did not improve IR in obese human subjects following 4-week (1,3)(1,6)-beta-D-glycans (BDG) consumption (118). These data suggest that anti-inflammatory cytokines such as IL-10 are not effective in improving insulin sensitivity.

1.1.4.2.5 Anti-inflammatory drugs

Clinical evidence shows that anti-inflammatory drugs, such as salicylates, aspirin and dexamethasone, can indeed improve insulin sensitivity. Decades ago, high doses of salicylates or aspirin were found to control hyperglycemia in diabetic patients (119, 120). In young healthy male subjects, short-term dexamethasone treatment significantly improved insulin sensitivity (121). However, both high-dose aspirin and dexamethasone have severe side effects that limit their therapeutic potential. Despite the positive effects of statins on atherosclerosis through their anti-inflammatory effects, their exploitation on IR has been dismal (122). High-dose statins even increase the risk of diabetes (123).

1.1.4.3 Insulin resistance may induce adipose inflammation

IR may contribute to the development of adipose inflammation. Adipose-specific phosphatase and tensin homologue (PTEN) deficiency or heterozygous deletion of phosphoinositide-3-kinase regulatory subunit 1 (Pik3r1) improves insulin sensitivity in mice, which is associated with reduced macrophage accumulation, proinflammatory expression, and chemokine secretion in WAT after HFD feeding (124, 125). Conversely, disrupting adipose insulin signaling via knockout of Akt isoforms or mechanistic target of rapamycin complex 2 (mTORC2) exacerbates IR and adipose inflammation (3, 126). mTORC2-knockout mice have higher MCP1 expression in adipocytes, which may trigger monocyte infiltration and subsequent differentiation into M1 macrophages (3). IR-associated activation of forkhead box protein O1 (FoxO1) may also upregulate the expression of the pro-inflammatory cytokine IL-1b, leading to adipose inflammation (127).

The variable relationship between adipose inflammation and IR (89) suggests that non-inflammatory adipose events may also play a crucial role in the development of IR. However, the underlying molecular and cellular mechanisms leading to these observations remain largely unclear.

1.2 WHITE ADIPOSE TISSUE AND HYPERTRIGLYCERIDEMIA

1.2.1 The Origination of Circulating Triglycerides

Circulating triglycerides are majorly derived from intestine and liver, packed in the forms of lipoproteins, such as chylomicrons and $VLDL_1$, respectively. In the postprandial state, chylomicrons containing a TG core, phospholipids, cholesterol and lipoprotein apolipoprotein B-48 (apoB48) are generated from enterocytes of the small intestine and secreted into the circulation through lacteal endothelial gaps (128). Hepatic TG is synthesized by accumulating FAs from adipose lipolysis, hepatic *de novo* lipogenesis, diet and hepatic TG-rich lipoprotein uptake (129). Given the evidence that adipose lipolysis contributes to approximately 80% of circulating FA pool, adipose lipolysis seems the most important source of hepatic TG (130). TG accumulation facilitates the synthesis and secretion of $VLDL_1$ containing a large amount of TG and apoB100 (131).

1.2.2 The Clearance of Circulating Triglycerides

Plasma TG in $VLDL_1$ and chylomicrons are broken down to release FFAs through LPL and hepatic lipase (HL). LPL is highly expressed in adipose tissue, skeletal muscle and heart. It is synthesized in parenchymal cells but translocated to capillary endothelial cells for their functions to hydrolyze plasma TG to release FFAs (6). With the effect of LPL, chylomicrons become chylomicron remnants, and $VLDL_1$ becomes a smaller molecule, $VLDL_2$ which is further degraded to intermediate-density lipoprotein (IDL) (132). HL, mainly expressed in hepatocyte and endothelial cells in the liver, subsequently converts IDL into low-density lipoprotein (LDL) (133). Eventually, plasma LDL rich in cholesterol is taken up by the liver and excreted as cholesterol or bile acid through the bile (134).

1.2.3 Hypertriglyceridemia

Hypertriglyceridemia is one of core symptoms of metabolic syndrome, affecting 25% of adults in American. Hypertriglyceridemia is diagnosed with plasma TG level above 1.7mmol/L

(128). Clinical studies showed that hypertriglyceridemia is an important risk factor for cardiovascular diseases, independent of plasma cholesterol levels (135, 136). Kinetic studies have demonstrated the mechanisms of dysregulation of plasma TG levels, including increased liver derived $VLDL_1$ and inhibited clearance of TG from the circulation (137, 138). Interestingly, delayed clearance of TG contributes approximately 50% of the increase in total plasma TG levels, suggesting that any mechanism facilitating plasma TG clearance might be potential and important for the treatment of hypertriglyceridemia.

LPL expression is important to regulate TG clearance. Thus, familial LPL deficient patients had tremendously elevated plasma TG levels (139). However, other genes which facilitate LPL synthesis and functions are also involved in the development of hypertriglyceridemia (140, 141), such as lipase maturation factor 1 (LMF1) and glycosylphosphatidylinoitol-anchored high-density lipoprotein–binding protein 1 (GPIHBP1). LMF1 is required for the folding and assembly of LPL protein, while GPIHBP1 transports synthesized LPL from parenchymal cells to its functional location, the surface of capillary endothelial cells (140, 142). Mutations on both genes results in hypertriglyceridemia (141, 143). Many other mediators also regulate LPL activity, including apoC-I, apoC-II, apoC-III, angiopoietin-like 3 (ANGPTL3), ANGPTL4, ANGPTL8, etc. Any changes in them can modulate plasma TG levels (144).

1.2.4 Pharmacological Therapies for Hypertriglyceridemia

Today, there is no effective medications for the therapy of hypertriglyceridemia in the clinical practice. Statins are the most commonly used medications for reducing plasma LDL-cholesterol (LDL-C) but they also reduce plasma TG levels around 5-15% (128). Fibrates, the activators of PPARα also reduce plasma TG levels around 25-45% leading to a reduction of cardiovascular disease risk (128). However, the combination of statins and fibrates failed to further reduce cardiovascular disease risk compared with monotherapy (128, 145). Omega-3-fatty acids may also decrease plasma TG levels (145).

1.2.5 The Regulatory Functions of White Adipose Tissue in Hypertriglyceridemia

Animals in the absence of WAT demonstrated severe insulin resistance and increased triglyceride storage in the liver and muscle (146). However, transplantation of WAT into these mice reverses these metabolic abnormalities (147), suggesting that WAT is a key organ system to regulate plasma TG levels. Both adipogenesis and lipolysis in WAT may contribute to the occurrence of hypertriglyceridemia. Insulin resistance in WAT promotes lipolysis that relatively facilitates hepatic overproduction of the triglyceride-rich $VLDL_1$ particles (148). Adipose LPL is also associated with metabolic dysfunction and hypertriglyceridemia. Patients with insulin resistance had lower adipose LPL activity compared with control group (149). Weight loss significantly upregulated adipose LPL gene expression and activity (150). Adipose specific LPL deficient mice demonstrated increased plasma TG levels with either NC or HFD (7), suggesting the fundamental influence of adipose LPL in regulating plasma TG levels.

1.3 MACROPHAGE MIGRATION INHIBITORY FACTOR

1.3.1 The Introduction of Macrophage Migration Inhibitory Factor

Although MIF is one of the first cytokines discovered almost 60 years ago (151), its function as an inflammatory regulator was not specified until 1993 (152). MIF is a 114-amino-acid non-glycosylated protein (12.5kDa) that is released from immune cells, including monocytes, macrophage, T cells, B cells, *etc* (153). In addition to immune system, MIF is also ubiquitously expressed in adipose tissue (154), brain (155), heart (156) and so on, suggesting its wider biological functions in addition to immune effects. MIF is constantly synthesized and stored in an intracellular pool and it can be released following stimulation (153). Due to the lack of an amino-terminal leader sequence, MIF is released by non-conventional protein-secretion pathway mediated by ATP-binding cassette (ABC) transporter subfamily 1 (ABCA1) (157) and Golgi-associated protein p115 (158). Secreted MIF mediates intracellular signaling pathways through

endocytosis or interacting with cell membrane receptors, such as CD74 (159), CXC chemokine receptor 2 (CXCR2), CXCR4 (160) and CXCR7 (161).

MIF has multifaceted roles in different pathological conditions. MIF deteriorates many inflammatory and autoimmune diseases, such as atherosclerosis (162), sepsis (163) and rheumatoid arthritis (164). However, MIF also facilitates the clearance of invading pathogens by upregulating pro-inflammatory cytokines release and mediating macrophage response (165). MIF also has protective effects in neurodegenerative disorders (166) and ischemia-reperfusion injury occurred in the heart (167) and kidney (168).

1.3.2 Macrophage Migration Inhibitory Factor and Metabolic Dysfunction

MIF plays a key role in regulating metabolic homeostasis. MIF stimulates insulin secretion in pancreatic β-cells and upregulates glycolysis in skeletal muscle (169). However, our previous study indicated that MIF upregulated agouti-related protein (AgRP) expression in the hypothalamus, leading to hyperphagia following olanzapine treatment in mice (154). Moreover, obesity and insulin resistance are positively associated with plasma MIF levels (170, 171) that could be reversed by weight loss (172). Adipose MIF expression is augmented in obese individuals (173, 174) and both adipocytes and preadipocytes in WAT can release MIF (175). MIF attenuates insulin signaling, leading to IR in WAT (176). These data together suggest that WAT may be a key source of circulating MIF in obesity and adipose derived MIF may play a fundamental role in regulating metabolic dysfunction.

As a pro-inflammatory cytokine, MIF may regulate the development of metabolic dysfunction through mediating adipose inflammation. MIF KO mice demonstrated reduced body weight gain and IR associated with attenuated adipose inflammation following HFD feeding (177). However, a recent study indicated that IR precedes the initiation of adipose inflammation (3). More importantly, plasma MIF levels are correlated with IR and type 2 diabetes independent of

other immune markers (178). Taken together, MIF may have both inflammatory and non-inflammatory effects on regulating metabolic dysfunction.

1.4 RESEARCH RATIONALE AND OBJECTIVES

WAT is a key organ system regulating energy storage, but it also has endocrine functions. Metabolic overload during obesity regulates lipolysis and lipogenesis in WAT, which in turn affect circulating TG levels and attenuate whole-body insulin sensitivity. Alterations in adipokine profile following obesity also lead to whole body IR. Thus, WAT may mediate both IR and hypertriglyceridemia.

MIF is an evolutionarily conserved cytokine and upstream regulator of the innate immune response (179) but it is also associated with metabolic dysfunction (177). The effect of MIF on metabolic dysfunction is associated with adipose inflammation. However, a recent study showed that IR precedes the initiation of adipose inflammation, suggesting an important role of non-inflammatory WAT in early stage of metabolic dysfunction (3). Given the evidence that MIF is released from non-immune cells in WAT, such as preadipocytes and adipocytes, we highly suspect that MIF may also have a non-inflammatory role in mediating metabolic dysfunction in WAT. Thus, our research for the first time investigates the novel role of MIF in regulating IR and hypertriglyceridemia in the absence of adipose inflammation.

To investigate the potential mechanisms, my current research includes the following objectives:

1. To investigate non-inflammatory mechanisms of adipose MIF release and its role in the development of IR.

2. To demonstrate the role of adipose derived MIF in regulating LPL and plasma TG levels.

CHAPTER 2 A PREADIPOCYTE FACTOR-1-CONTROLLED NON-INFLAMMATORY MECHANISM OF INSULIN RESISTANCE

2.1 INTRODUCTION

IR in obesity is considered to arise from inflammation in WAT (180). However, anti-inflammatory therapies have failed to improve insulin sensitivity in animal models and human subjects (4, 5). Recent studies further indicate that obesity-induced IR may occur without any change in systemic or tissue inflammation (3, 181). IR can develop before macrophage accumulation and WAT inflammation (3), suggesting a proximate role of non-inflammatory adipose events in the initiation of IR. However, the underlying molecular and cellular mechanisms responsible for these observations remain largely unknown.

MIF is an evolutionarily conserved cytokine and upstream regulator of the innate immune response (179). However, MIF also has non-immune effects in the regulation of metabolic pathways and in myocardial stress and injury (169, 182, 183). Emerging work has shown that circulating MIF levels are significantly elevated in obesity, while weight loss reduces plasma MIF levels (172). *MIF* gene expression in abdominal fat, including visceral and subcutaneous adipose tissue is positively associated with waist circumference or body fat percentage in obesity (173, 174). These findings suggest WAT as a potential source of circulating MIF.

In accord with previous paradigms regarding the pathogenesis of obesity, MIF expression in WAT is thought to arise from infiltrating macrophages (177, 184). However, experimental findings also indicate that non-immune cells, such as progenitor adipocytes and adipocytes also release MIF under both physiologic and pathologic conditions (175, 185), indicating an independent role for non-inflammatory mechanisms of adipose MIF production. At the current time, the pathways mediating non-inflammatory MIF release as well as their contribution to IR remain to be determined.

Pref-1 is a transmembrane protein that is highly expressed in non-adipocyte cells in WAT. Pref-1 is cleaved by TNFα-converting enzyme to generate a soluble form, which acts as an autocrine/paracrine factor. Pref-1 was originally reported to regulate metabolism by inhibiting *PPAR*γ expression and adipogenesis (186). Mice with high levels of soluble Pref-1 in WAT have a reduced fat mass and hypertriglyceridemia (187). Mice lacking Pref-1 show augmented fat deposition and obesity (188). However, other investigators have reported that *pref-1* overexpression may improve glucose homeostasis during metabolic stress without changing adipogenesis (189). Thus, the details of the actions of the Pref-1 signaling pathway in regulating metabolism, especially in IR, have yet been clearly defined.

The present study investigates the hypothesis that reduced Pref-1 expression and release mediate IR by increasing MIF release from non-inflammatory cells in WAT. The collective findings, in both animal models and specimens from obese human subjects, reveal a functional interaction between Pref-1+ cells and adipocytes in WAT. FAs and HFD reduce Pref-1 expression through activation of PAR2, with loss of Pref-1 leading to an increase in the extracellular release of MIF and plasma MIF levels.

Hypothesis: To investigate non-inflammatory release of MIF from WAT and its role in the development of IR.

Objective 1: To identify the role of non-inflammatory adipose MIF release in the development of IR.

Objective 2: To determine the molecular mechanism of non-inflammatory MIF release from WAT in cells.

Objective 3: To confirm the molecular mechanism of non-inflammatory adipose MIF release and its effect on IR in animal models.

2.2 METHODS

2.2.1 Human Subjects

Human mRNA samples were obtained from a previous overfeeding study to investigate the effects of a positive energy balance on endocrine factors and glucose and lipid metabolism, which has been approved by Newfoundland and Labrador Health Research Ethics Board (HREB) (190). We also obtained an ethic approval for a secondary use of these samples for the current study (Research portal File# 20200635). All study-related procedures were carried out with written informed consent. The male subjects (Caucasian) including 10 lean (age: 23.3 ± 2.2) and 10 obese (age: 24.3 ± 3.3) were from the city of St. John's and surrounding area in Newfoundland and Labrador, Canada. All of the subjects agreed to undergo an adipose tissue biopsy for the current mRNA studies. Peripheral venous blood was collected from lean and obese subjects and plasma MIF level was determined with an enzyme-linked immunosorbent assay (ELISA) method according to the protocol from R&D Systems, USA.

2.2.2 Mice

All experiments involving mice were conducted in accordance with the Guide for the Care and Use of Laboratory Animals of the National Institutes of Health and were approved by the Internal Animal Committee Review Board of Memorial University of Newfoundland and University of Manitoba. *Par2*$^{-/-}$, Mif lung transgenic mice (*Mif* lung Tg) and littermate WT mice with a pure C57BL/6 background (from 20 to 28 weeks of age) were maintained at the Health Science Center Animal Facility in Memorial University of Newfoundland and University of Manitoba, Canada. Only male mice were utilized in this study. WT mice (20 weeks) with or without transplantation were housed in individually ventilated cages (IVCs) with an artificial 12:12 hr light: dark cycle at room temperature and fed with either NC or PD (41% palmitic oil; #170100, Envigo Teklad Diets) for 8 weeks. Mice were then fasted for six hours, and fasting blood glucose levels were determined from tail venous blood; 2mg/g body glucose or 0.75U/kg insulin then was injected intraperitoneal

(i.p.) respectively and blood glucose values were obtained at 0, 15, 30, 60, 90 and 120 min. Serum FFA and TG were measured by commercial kits purchased from Wako.

2.2.3 Cell Culture

3T3-L1 cells, derived from male mouse embryos, were purchased from ATCC and passage 6-15 of these cells were used in the study. 3T3-L1 undifferentiated cells were cultured in DMEM (11965092, Gibco) with 10% newborn calf serum (16010159, Gibco) and they were differentiated in DMEM containing 10% fetal bovine serum (FBS, 26140079, Gibco), 0.5 mM 3-Isobutyl-1-methylxanthine (IBMX, I7018, Sigma-Aldrich), 0.25 µM dexamethasone (D4902m, Sigma-Aldrich), and 1 µg/ml insulin (I5500, Sigma-Aldrich). Before the experiments, both 3T3-L1 undifferentiated and differentiated cells were briefly serum-starved in DMEM-0.5% newborn calf serum or FBS for 8 hours.

2.2.4 Visceral Adipose Tissue Transplantation

All male donor mice (*Par2*$^{-/-}$ or WT) at 18 weeks of age were euthanized and their intra-abdominal perigonadal (epididymal) visceral fat depots were isolated and kept in cold saline for the maximum of 30 min until transplantation. Male recipient mice (*Par2*$^{-/-}$ or WT, 18 weeks) were anesthetized, and their endogenous epididymal fat pads were removed in both sides. The donor fats were then carefully transplanted into the visceral cavity. Recipient mice will be fed with NC till 20 weeks of age and then they will receive either NC or PD for 8 weeks.

2.2.5 Recombinant Mouse Preadipocyte Factor-1 Infusion by Mini-pump

Male WT mice at 20 weeks were initially fed with PD for 4 weeks. Jugular vein was then cannulated and recombinant mouse Pref-1 (24µg/day/kg) or vehicle was injected via a mini-osmotic pump implanted in a subcutaneous pocket (Alzet model 1004) into the mice accompanied with PD feeding for the following 4 weeks.

2.2.6 Isolation of Stromal Vascular Fraction and Adipocyte Fractions from White Adipose Tissue

Abdominal fat was excised and digested with 1mg/ml type I collagenase (type I collagenase, LS004196, Worthington Biochemical Company, NJ) for 30min at 37°C. After digestion and centrifugation, the buoyant adipocytes were collected while the cell pellet was retrieved for the stromal vascular fraction (SVF).

2.2.7 Flow Cytometry

SVF was resuspended in 1% BSA PBS solution and analyzed by flow cytometry. Briefly, SVF was stained with the following antibodies: CD45.2-PerCP (eBioscience; catalog 45-0454-80); F4/80-PE (eBioscience; catalog 12-4801-80); CD11b-APC eFluor 780 (eBioscience; catalog 47-0112-80); CD11c-PE-Cy7 (eBioscience; catalog 25-0114-81); CD206-Alexa Fluor™ 488 (Invitrogen; catalog 53-2061-80); CD301–Alexa Fluor 647 (AbD Serotec; catalog MCA2392A647T); CD31-FITC (Invitrogen; catalog RM5201); CD34-PE (Invitrogen; catalog MA5-17831); anti-Pref-1 antibodies (R&D; catalog MAB8634) and (Invitrogen; catalog MA5-15915); anti-PAR2 antibody (Abcam; catalog 180953); anti-MIF antibody (ab187064; Abcam); antIRabbit Alexa Fluor® 488 (Jackson ImmunoResearch; catalog 711-545-152); antIRabbit Alexa Fluor™ 647 (Invitrogen; catalog A-21244); anti-Mouse Alexa Fluor® 647 (Jackson ImmunoResearch; catalog 715-605-150). Flow cytometry was performed on a CytoFLEX flow cytometer (Beckman Coulter) and the data were analyzed by using FlowJo v10 software (Becton Dickinson).

2.2.8 Gene Expression and Phosphorylated and Total Protein Levels Analysis

Transcript levels for the mouse and human genes of *F2rl1 (PAR2)*, *Mif (MIF)*, *pref-1 (PREF1)*, *PPARγ(PPARG)*, *ITGB1, ITGA5, Tnfa (TNF), Il6 (IL6) and Il1b (IL1B)*, etc were measured by qPCR. The primer sequences have been listed in Table S2-1 and S2-2. Briefly, RNAs were extracted by TRIzol™ Reagent (Invitrogen) and iScript cDNA Synthesis Kit (Bio-Rad)

was used to synthesize complementary DNA (cDNA). SsoAdvanced™ Universal SYBR® Green Supermix (Bio-Rad) was performed to measure gene expression levels in the QuantStudio 6 Flex System (Applied Biosystems). The delta–delta Ct method was used to quantify gene expressions normalized by *Gapdh*.

Phosphorylation and total protein levels of extracellular signal-regulated kinase (ERK), AMPK and ACC, the contents of MIF, p115, integrin β1 (ITGB1) and integrin α5 (ITGA5) in WAT or cells, and the released levels of p115 in cell culture medium were evaluated by Western blot. Protein extracts were performed in a lysis buffer containing cOmpleteTM, EDTA-free Protease Inhibitor Cocktail (ROCHE). According to the manufacturer's instructions, protein concentrations were examined using Bio-Rad Protein Assay Dye Reagent (Bio-Rad). Protein quantification was performed by using an iBright™ CL1500 Imaging System (Invitrogen). Plasma MIF levels and released MIF levels in cell culture medium were determined with an ELISA method according to the protocol from R&D Systems, USA.

2.2.9 Immunostaining

Immunohistochemistry was performed to identify MIF accumulation in WAT. Immunofluorescence staining was performed on either WAT sections (30μm) or 3T3-L1 cell line cultured on chamber slides. Primary antibodies to the following antigens were used: anti-Pref-1 antibody (R&D; catalog AF8277); PAR2 antibody (Abcam; catalog ab180953); anti-MIF antibody (Torrey Pines Biolabs; catalog TP234) and (R&D; catalog MAB2892); anti-p115 antibody (Proteintech; catalog 13509-1-AP); anti-Pref-1 antibody (Invitrogen; catalog MA5-15915) and anti-ITGB1 (Invitrogen, 14-0292-82). Following the incubation with primary antibodies, the sections were washed three times for 15 min with phosphate-buffered saline and then incubated for 1 h at room temperature with secondary antibodies. Finally, the images were obtained with an Olympus confocal microscope.

2.2.10 Protease-activated Receptor 2 and AMP-activated Protein Kinase Knockdown by siRNA

To temporarily silence PAR2 and AMPK expression in 3T3-L1 undifferentiated cells, 10nM *F2rl1* siRNA (PAR2 siRNA, s65793, ThermoFisher), 30μM AMPK Alpha 1/2 siRNA (sc-45313, Santa Cruz) or non-silencing control siRNA (AM4611, ThermoFisher) was transfected into the cells by using Lipofectamine™ RNAiMAX Transfection Reagent (13778075, Invitrogen) in medium without newborn calf serum and antibiotics. Following 6 hours of transfection, cells were cultured in DMEM with 10% newborn calf serum for 48 hours.

2.2.11 Quantification and Statistical Analysis

For the human study, Kolmogorov-Smirnov test was used to examine the data normal distribution. The difference in metabolic indicators and qPCR results between lean and obese groups was analyzed using *t*-test. All significant levels were two-tailed tested, and a P value of less than 0.05 was considered as statistically significant.

The food intake, body weight gain, glucose tolerance test (GTT) and insulin tolerance test (ITT) data in mice were analyzed by multivariate ANOVA. Wherever appropriate, One-way ANOVA with post hoc Tukey's tests or 2-tailed Student's *t*-test was used to determine differences between group mean values. The level of statistical significance was set at $P<0.05$.

Table S2-1. The description of mouse PCR primer sequences.

Gene Name	Sequences (5' – 3')
Mif	CGG ACC GGG TCT ACA TAC A TCA AGC GAA GGT GGA ACC GTT
pref-1	CTG TGT CAA TGG AGT CTG CAA G CTA CGA TCT CAC AGA AGT TGC
PPARγ	TGT TAT GGG TGA AAC TCT GGG AGA GCT GAT TCC GAA GTT GG
Fabp4	GTG ATG CCT TTG TGG GAA CCT GGA AG TCA TAA ACT CTT GTG GAA GTC ACG CC
ITGB1	CTG TGG GTG AAT TGT TGC CTA ATC TTT TAA TGT GTC TGT TTG C
ITGA5	TTG CCT GAG TTC CAT CCA AGG CAG AAT CCG GGA GCC TTT GC
F2rl1	AAC ATC ACC ACC TGT CAC GA CAC GTA GGC AGA CGC AGT AA
Tnfa (TNF-α)	CAG GCG GTG CCT ATG TCT C CGA TCA CCC CGA AGT TCA GTA G
Il6 (IL-6)	GAG GAT ACC ACT CCC AAC AGA CC AAG TGC ATC ATC GTT GTT CAT ACA
Il1b (IL-1β)	TGG TGT GTG ACG TTC CCA TT CAG CAC GAG GCT TTT TTG TTG
GAPDH	ATG TGT CCG TCG TGG ATC TGA TGC CTG CTT CAC CAC CTT CTT

Table S2-2. The description of human PCR primer sequences.

Gene Name	Sequences (5' – 3')
MIF	CGG ACA GGG TCT ACA TCA A CTT AGG CGA AGG TGG AGT T
PREF1	CTG GAC GGT GGC CTC TAT GAA TG ATC ATC CAC GCA GGT GCC TC
PPARG	ACA GAC AAA TCA CCA TTC GT CTC TTT GCT CTG CTC CTG
TNF (TNF-α)	TGT AGC CCA TGT TGT AGC AAA CC GAG GAC CTG GGA GTA GAT GAG GTA
IL6 (IL-6)	TGG CTG AAA AAG ATG GAT GCT TCT GCA CAG CTC TGG CTT GT
IL1B (IL-1β)	CAG AAG TAC CTG AGC TCG CC AGA TTC GTA GCT GGA TGC CG
β-actin	CCT GTA CGC CAA CAC AGT GC ATA CTC CTG CTT GCT GAT CC

2.3 RESULTS

2.3.1 Preadipocyte Factor-1 Regulates Non-inflammatory Macrophage Migration Inhibitory Factor Release from White Adipose Tissue Which Induces Insulin Resistance

Abdominal adipose tissue samples were collected from lean (age: 23.3 ± 2.2; BMI<25kg/m^2) and obese (age: 24.3 ± 3.3; BMI>30kg/m^2) human subjects with metabolic dysfunction (Figure S2-1). Subject-to-subject variability was detected within the recruited subjects, but the two groups nevertheless showed similar expression in WAT of the inflammatory mediators: *TNF* (TNFα), *IL1B* (IL-1β) and *IL6* (IL-6) (Figure 2-1A). The obese group, however, had evidence of higher homeostatic model assessment for insulin resistance (HOMA IR) scores and lower adipose *PREF1* (Pref-1) gene expression (Figure 2-1B-C). The reduction in *PREF1* gene expression additionally was not accompanied by any change in *PPARG* (PPARγ) gene expression (Figure 2-1D). *MIF* gene expression in the sampled adipose was equivalent in both lean and obese groups (Figure 2-1E) and did not correlate with BMI (Figure S2-2). Nevertheless, the obese subjects had higher plasma MIF concentration (Figure 2-1F) that correlated positively with the subject's IR (Figure 2-1G). More interestingly, adipose *PREF1* gene was negatively associated with plasma MIF levels (Figure 2-1H), suggesting that Pref-1 expression in WAT may negatively modulate the release of adipose MIF and influence plasma MIF levels (Figure 2-1F).

To investigate whether Pref-1 mediates non-inflammatory MIF release, we employed a non-inflammatory mouse model of obesity. Male WT mice (20-week-old) were fed a PD for eight weeks, which induced obesity (Figure S2-3) without altering either the gene expression of the pro-inflammatory (M1) macrophage markers [*Tnfa* (TNF-α), *Il1b* (IL-1β) and *Il6* (IL-6)] or the macrophage polarization (M1/M2) ratio in subcutaneous or visceral adipose tissues (Figure S2-4 and Figure 2-1I-J). In comparison to their counterparts fed a NC diet, these obese mice exhibited IR (Figure 2-1K) that was accompanied by a downregulation of Pref-1 gene and protein expression in abdominal adipose tissue (Figure S2-5A and Figure 2-1L-M). The reduced Pref-1

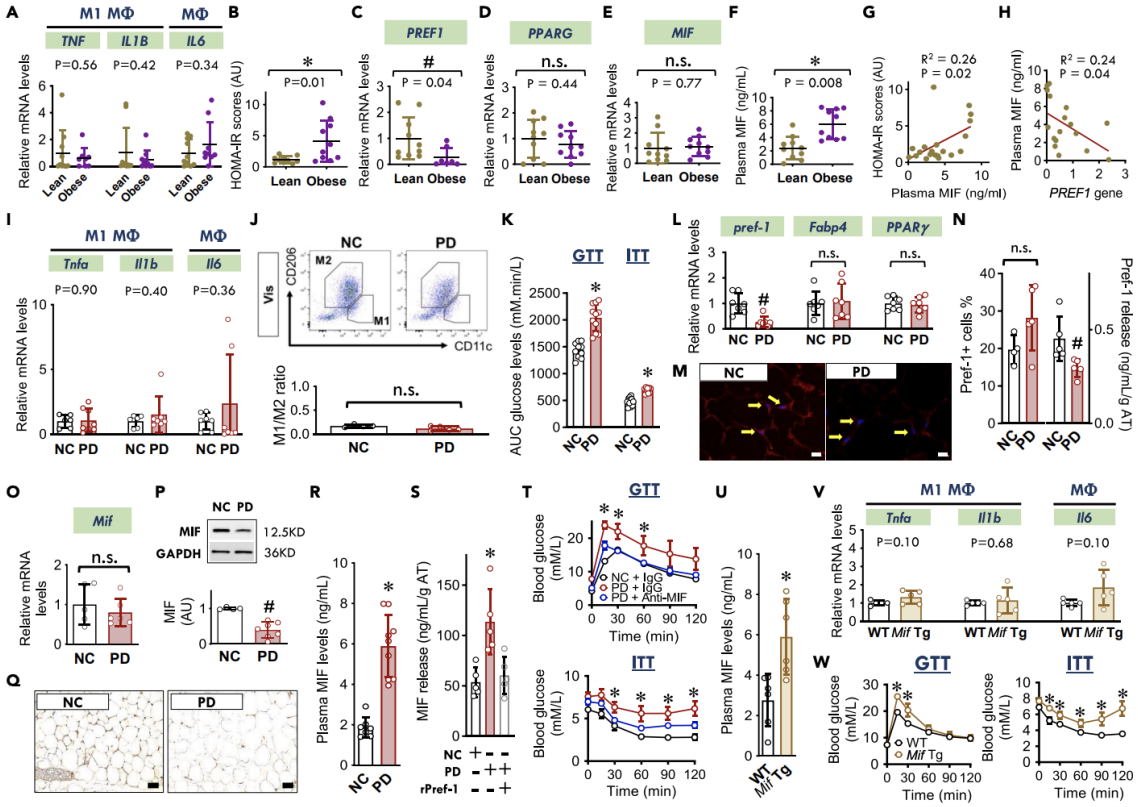

Figure 2-1. Pref-1 regulates non-inflammatory MIF release from WAT which induces IR. (**A**) *TNF* (TNF-α), *IL1B* (IL-1β) and *IL6* (IL-6) mRNA expression in biopsied WAT from male subjects including lean (age: 23.3 ± 2.2; BMI ≤ 25 kg/m^2) (N = 10) and obese individuals (age: 24.3 ± 3.3; BMI > 30 kg/m^2) (N = 10). (**B**) HOMA-IR scores of recruited lean and obese individuals evaluated by plasma glucose and insulin levels. (**C**-**F**) *PREF1* (Pref-1) (**C**), *PPARG* (PPARγ) (**D**) and *MIF* (**E**) mRNA expression in biopsied WAT and plasma MIF levels (**F**) from recruited lean and obese individuals. (**G** and **H**) The correlation between HOMA-IR scores and plasma MIF levels, and the correlation between *PREF1* mRNA expression and plasma MIF levels. (**I**) Pro-inflammatory macrophage (M1 MΦ) markers: *Tnfa* (TNF-α) and *Il1b* (IL-1β), and general inflammatory (MΦ, macrophages) marker: *Il6* (IL-6) in visceral epididymal adipose tissue collected from WT mice (20-week-old) fed with NC or a PD for 8 weeks. (**J**) The ratio of M1/M2 was evaluated by flow cytometry. (**K**) Insulin sensitivity was quantified by i.p. GTT and ITT. (**I** and **M**) Adipose *pref-1*, *FABP4* and *PPARγ* mRNA expression (**L**) and Pref-1 immunofluorescence staining (**M**) from WT mice (20-week-old) fed with NC or PD for 8 weeks (Arrows, Pref-1 (red); Scale bars, 20 μm). (**N**) Pref-1+ cells sorted by flow cytometry from SVFs (left) and Pref-1 release from visceral adipose tissues (right) isolated from NC and PD groups. (**O** to **Q**) MIF gene and protein expression in WAT isolated from NC and PD groups (Scale bars, 20 mm). (**R**) Plasma MIF levels in NC and PD groups. (**S**) MIF release from WATs isolated from NC and PD groups in the presence or absence of recombinant Pref-1 proteins (2.5μg/ml). (**T**) Insulin sensitivity quantified by GTT and ITT in PD groups following MIF neutralization with anti-MIF antibody (20 mg/kg, i.p. twice a week). (**U**) Plasma MIF levels in 25-week-old WT and *Mif* lung Tg mice. (**V**) Pro-inflammatory macrophage (M1 MΦ) markers: *Tnfa* (TNF-α) and *Il1b* (IL-1β), and general inflammatory (MΦ, macrophages) marker: *Il6* (IL-6) in visceral epididymal adipose tissue collected from 25-week-old WT and *Mif* lung Tg mice. (**W**) Insulin sensitivity quantified by GTT and ITT in 25-week-old WT and *Mif* lung Tg mice. All data are presented as mean ± SD. $^{\#}$P ≤ 0.05 reduction vs. lean subjects in (**C**), vs. NC group in (**N**), and (**P**); *P ≤ 0.05 increase vs. lean subjects in (**B**) and (**F**), vs. NC group in (**K**) and (**R**), vs. WT group in (**U**) and (**W**), vs. other groups in (**S**) and (**T**). The n.s. represents no significance.

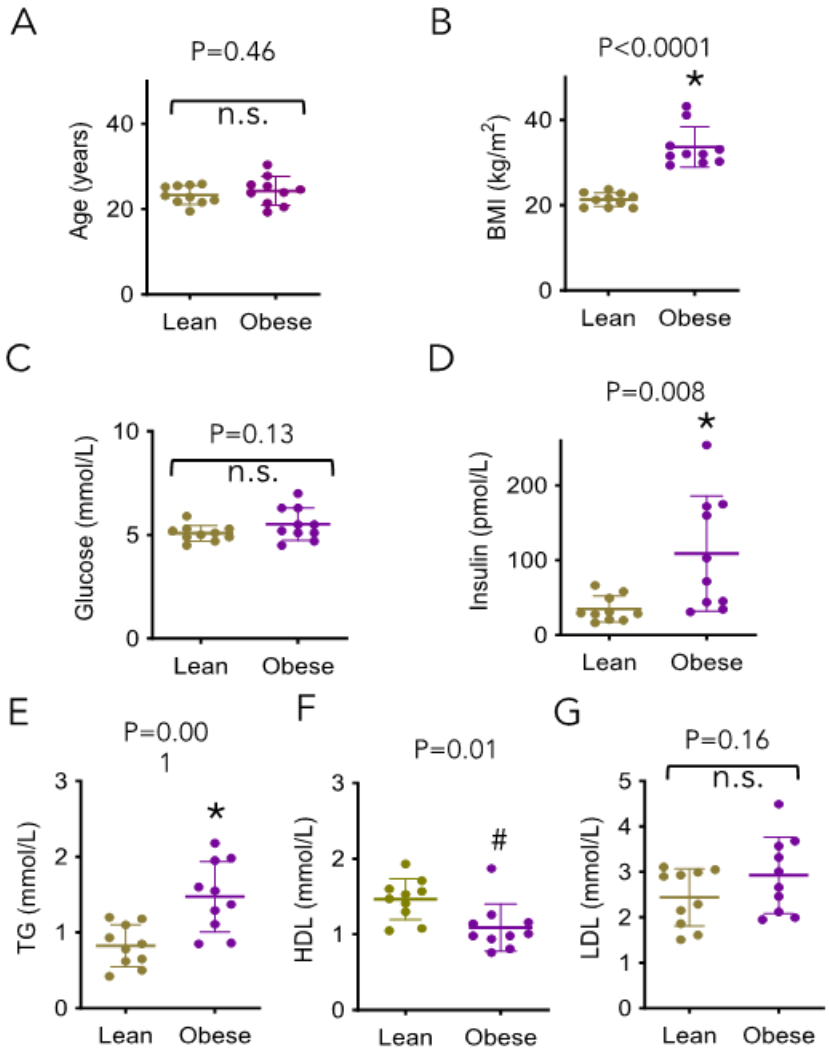

Figure S2-1. The general characteristics of human subjects. 20 male subjects including 10 lean and 10 obese were recruited for the current experiment. Mean ± SD in all the panels; *P<0.05 increase vs. Lean group; #P<0.05 reduction vs. Lean group. The n.s. represents no significance.

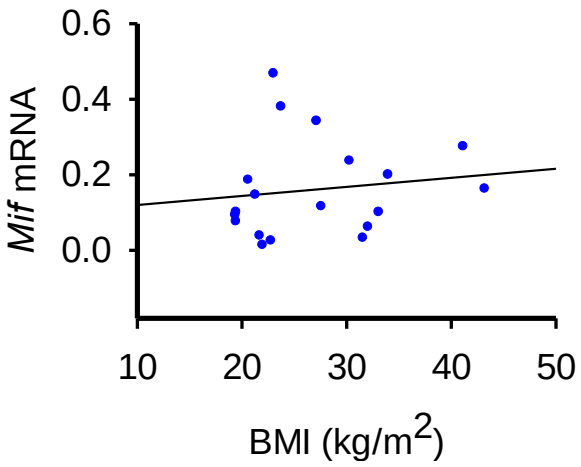

Figure S2-2. BMI is not correlated with adipose MIF gene expression in human subjects.

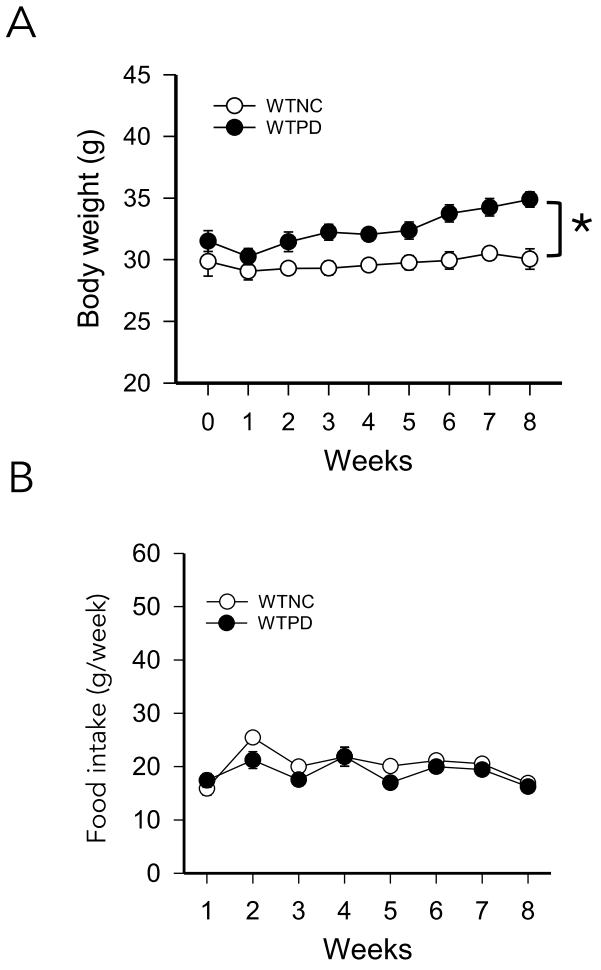

Figure S2-3. High palmitic acid diet feeding induces obesity in WT mice. WT mice at 20 weeks were fed with NC or PD diet for eight weeks. Body weight (A) and food intake (B) was monitored every week. Mean ± SD in all the panels; *P<0.05 represents an overall increase vs. NC following 2-week PD feeding.

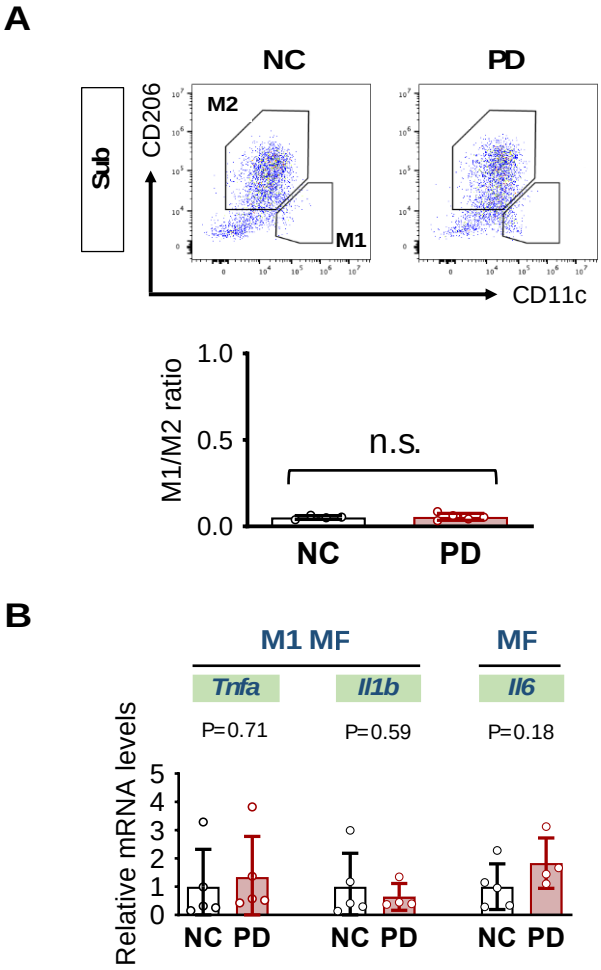

Figure S2-4. High palmitic acid diet feeding is not associated with inflammation in subcutaneous adipose tissue. WT mice at 20 weeks were fed with NC or PD for 8 weeks. M1/M2 ratio (A) and gene expression of *Tnfa*, *Il1b* and *Il6* (B) in femoral adipose tissue were quantified by flow-cytometry and qPCR. Mean ± SD in all the panels; the n.s. represents no significance.

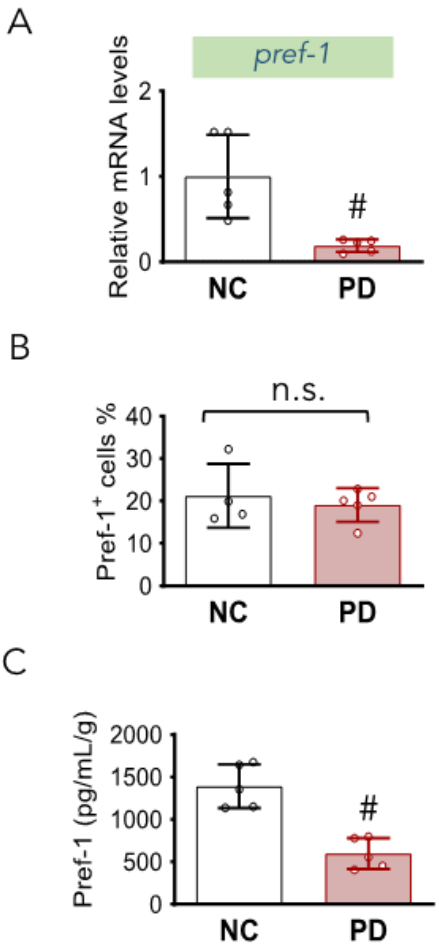

Figure S2-5. The effects of high palmitic acid diet on Pref-1 expression and release in subcutaneous adipose tissue. PD reduces pref-1 gene expression (A) without affecting the number of Pref-1+ cells (B) in femoral adipose tissue. PD also decreases Pref-1 release from subcutaneous adipose tissue (C). Mean ± SD in all the panels; #P<0.05 decrease vs. NC; the n.s. represents no significance.

expression was not associated with any change in the expression of adipogenic genes, such as *Fabp4* and *PPARγ* (Figure 2-1L) or the number of Pref-1+ cells (Figure 2-1N and Figure S2-5B). In the group fed PD, Pref-1 release from isolated WATs was significantly lower than in the group fed NC (Figure 2-1N and Figure S2-5C). The reduction of Pref-1 expression and release was not associated with changes in *Mif* gene expression (Figure 2-1O), however, there was a decrease in adipose MIF protein content (Figure 2-1P-Q) that was associated with an increase in circulating plasma MIF levels (Figure 2-1R). Pref-1 is cleaved at the cell membrane leading to the release of its active component (186). To further define whether Pref-1 regulates adipose MIF release, isolated WAT from NC and PD groups were treated with or without recombinant, bioactive Pref-1 protein (rPref-1, 2.5 μg/ml) for 24 h. The PD group demonstrated increased MIF release compared to the NC group; this was inhibited by rPref-1 (Figure 2-1S), suggesting a crucial role of Pref-1 in inhibiting MIF release from WAT.

In order to better define the role of circulating MIF in PD-induced IR, we assessed the actions of neutralizing anti-MIF antibody administration. Anti-MIF significantly improved whole-body and adipose insulin sensitivity and attenuated obesity in PD group (Figure 2-1T and Figure S2-6). In reciprocal experiments, increasing plasma MIF concentrations in a mouse model, overexpressing MIF in lung (*Mif* lung Tg mice (*Mif* Tg)), demonstrated that high circulating MIF levels (Figure 2-1U) are associated with IR and hypertriglyceridemia in the absence of alterations in inflammatory gene expression in adipose tissue (Figure 2-1V-W and Figure S2-7). These data together support the role of MIF in regulating IR in the absence of adipose inflammation.

2.3.2 Preadipocyte Factor-1 Inhibits Macrophage Migration Inhibitory Factor Release from Both Adipose Preadipocyte Factor-1+ Cells and Adipocytes

We isolated the cell populations that express and potentially release Pref-1 in WAT from male mice. Most of these cells co-stained with CD34, CD31 and CD45 (Figure 2-2A), suggesting

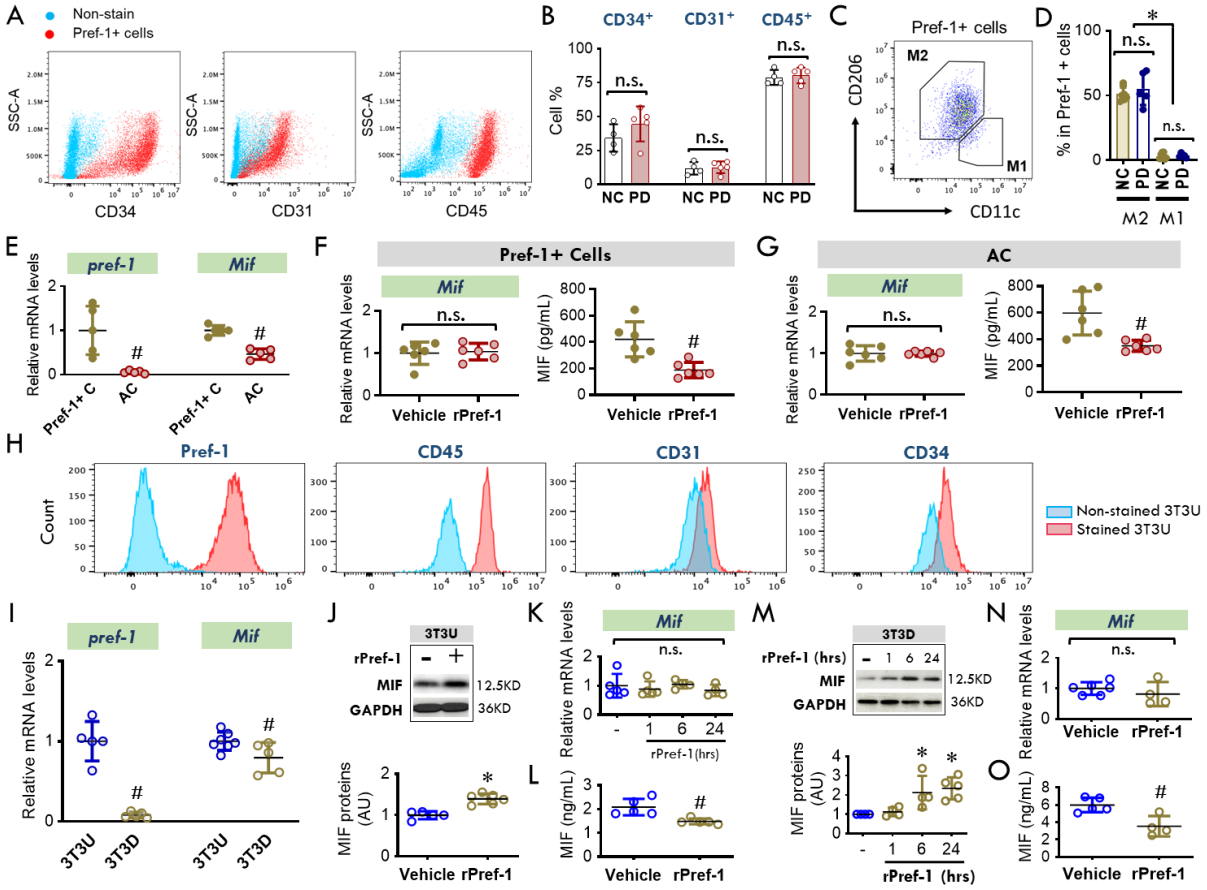

Figure 2-2. Pref-1 inhibits MIF release from both adipose Pref-1+ cells and adipocytes. (**A**) Cells with CD34+, CD31+ or CD45+ in Pref-1+ cells isolated from WAT in 20-week WT mice by flow cytometry. (**B**) The percentages of CD34+, CD31+ or CD45+ cells in Pref-1+ cells following 8-week NC or PD diet feeding. (**C** and **D**) M1 macrophages ($CD45^+F4/80^+CD11b^+CD11c^+$) and M2 macrophages ($CD45^+F4/80^+CD11b^+CD206^+$) were identified in Pref-1+ cells from NC and PD groups by flow cytometry. (**E**) Gene expression of *pref-1* and *Mif* in isolated Pref-1+ cells (Pref-1+ C) and adipocytes (AC) quantified by qPCR. (**F** and **G**) *Mif* gene expression and its release in isolated Pref-1+ cells and adipocytes following the treatment of mouse rPref-1 protein (2.5μg/ml) for 24 hours. (**H**) 3T3-L1 undifferentiated cells were identified with Pref-1, CD45, CD31 and CD34 antibodies by flow cytometry. (**I**) The genetic quantifications of *pref-1* and *Mif* in 3T3-L1 undifferentiated (3T3U) and differentiated (3T3D) cells. (**J**-**O**) 3T3U and 3T3D were incubated with or without rPref-1 for 24h and MIF protein content (**J** and **M**), gene expression (**K** and **N**) and release (**L** and **O**) were measured by western blot, qPCR and ELISA, respectively. All data are presented as mean ± SD. *P ≤ 0.05 increase and $^{\#}$P ≤ 0.05 reduction vs. Vehicle. The n.s. represents no significance.

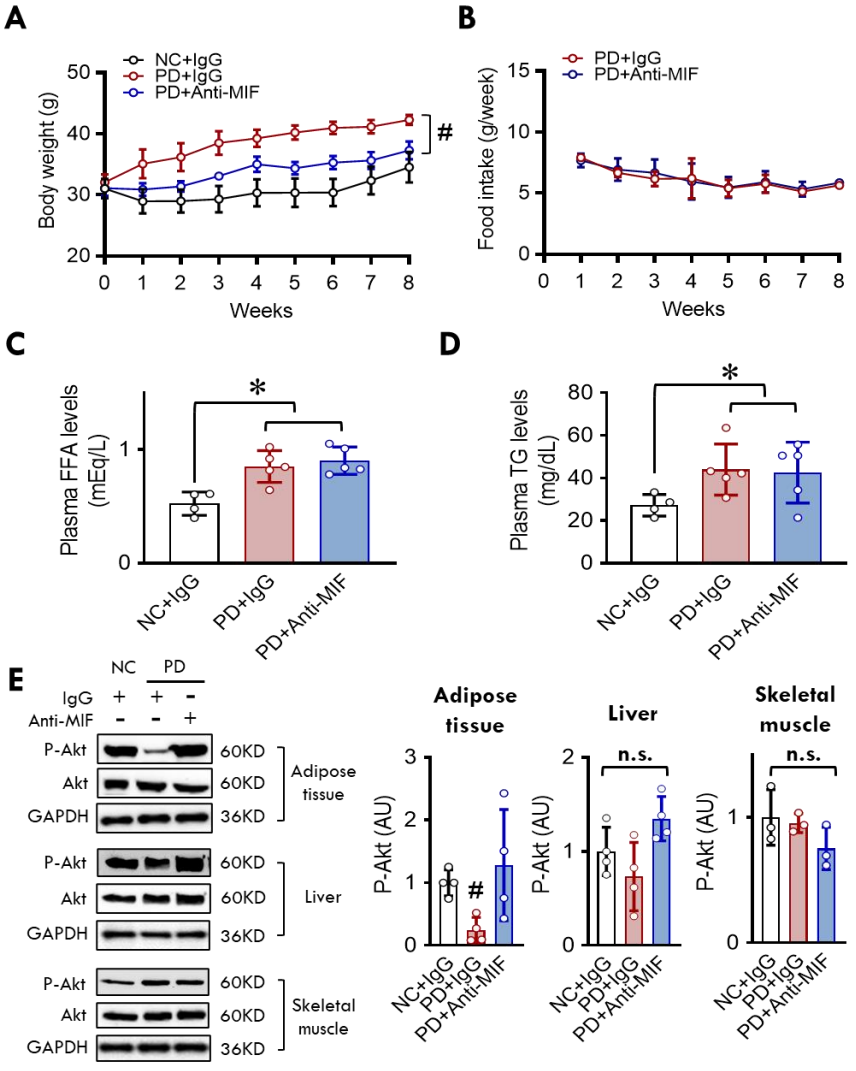

Figure S2-6. Anti-MIF antibody reverses high palmitic acid diet induced IR. Neutralization of circulating MIF with anti-MIF antibody reduces body weight gain (A) without affecting food intake (B), plasma FA (C) and TG (D) levels following PD feeding. The Akt phosphorylation in WAT, liver and skeletal muscle was shown in (E). Mean ± SD in all the panels; #P<0.05 decrease vs. PD+IgG; *P<0.05 increase vs. NC+IgG in (C and D), vs other groups in (E); the n.s. represents no significance.

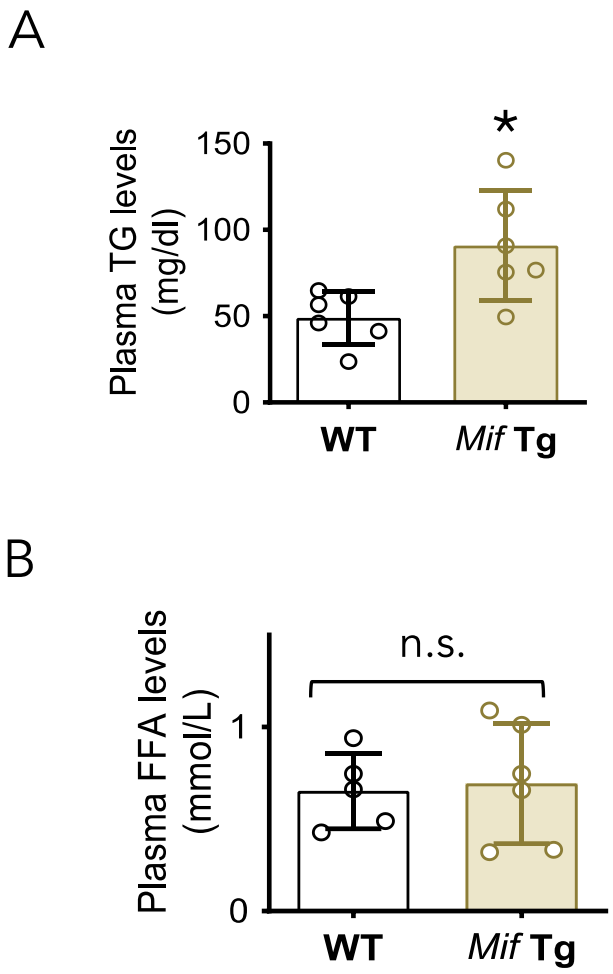

Figure S2-7. The plasma levels of TG and FFA in WT and *Mif* lung Tg mice. Mean ± SD in all the panels; *P<0.05 increase vs. WT, the n.s. represents no significance.

the characteristics of progenitor cells (*e.g.,* CD34), endothelial cells (*e.g.,* CD31), and immune cells (e.g., CD45). The components of CD34+, CD31+ and CD45+ cells in the total Pref-1+ cells were unchanged following PD feeding (Figure 2-2B). We also identified that M2 rather than M1 macrophages express Pref-1 (Figure 2-2C-D). PD feeding did not affect the proportion of the M2 cells present amongst the Pref-1+ population of cells (Figure 2-2D).

Although both Pref-1+ cells (Pref-1 C) and mature adipocytes (AC) isolated from WAT express MIF, MIF expression was lower in the mature adipocytes (Figure 2-2E). Pref-1 is associated with inflammatory factors in obese humans in both subcutaneous and omental adipose tissue (191). We tested whether secreted Pref-1 protein may regulate MIF release from Pref-1+ cells and adipocytes. Following treatment with rPref-1 protein (2.5 µg/ml for 24h), both cell types showed reduced MIF secretion in the absence of a change in *Mif* mRNA content (Figure 2-2F-G), implicating Pref-1 in the crosstalk between Pref-1+ cells and adipocytes and its action to inhibit MIF release.

Pref-1 was originally cloned from 3T3-L1 precursor fibroblasts, which also express CD45, CD31 and CD34 (Figure 2-2H) as isolated adipose Pref-1+ cells (Figure 2-2A). *Mif* mRNA expression was reduced when the precursor fibroblasts (Pref-1+ 3T3U) were differentiated into adipocytes (3T3D) (Figure 2-2I), which mimicked the pattern of *Mif* expression observed in Pref-1+ cells versus mature adipocytes in healthy mouse WAT (Figure 2-2E). Following rPref-1 treatment of 3T3-L1 precursor fibroblasts, we observed a significant increase in MIF protein but not *Mif* mRNA content (Figure 2-2J-K). Interestingly, MIF concentration in conditioned media was reduced after rPref-1 treatment (Figure 2-2L). We also investigated the possible paracrine role of Pref-1 in regulating MIF release from 3T3-L1 adipocytes. Following rPref-1 treatment, MIF protein content increased in 3T3-L1 differentiated adipocytes in a time-dependent manner (Figure 2-2M), mimicking the observations in precursor cells that an increase in MIF protein is not

associated with changes in *Mif* mRNA levels (Figure 2-2N), but rather with reduced MIF release into the medium (Figure 2-2O).

Based on these findings in primary cells and cell lines, we suggest that secreted Pref-1 inhibits MIF release from both Pref-1+ cells and mature adipocytes in an autocrine/paracrine manner.

2.3.3 Preadipocyte Factor-1 Inhibits Macrophage Migration Inhibitory Factor Secretion by Interaction with the Cell Membrane Protein, Integrin 1β, and Inhibiting P115, a Cofactor for Macrophage Migration Inhibitory Factor Release

To investigate the cellular mechanisms by which Pref-1 regulates MIF release, we examined the 3T3-L1 precursor fibroblast model of adipocyte differentiation. MIF lacks a signal sequence and is secreted from cells by a non-conventional pathway for protein export (192). The Golgi-associated protein, p115, is an intracellular binding partner of MIF that is co-secreted with MIF (158). The deletion of p115 from monocytes/macrophages reduces the release of MIF but no other cytokines following inflammatory stimulation or intracellular bacterial infection (158). We observed that rPref-1 treatment of 3T3-L1 undifferentiated Pref-1+ cells (3T3U) for 24 h significantly reduced the release of p115 (Figure 2-3A) and MIF (Figure 2-2L) into medium; this occurred in the absence of inflammatory stimulation and was associated with an increase in intracellular p115 content (Figure 2-3A). Pref-1 also inhibits lipopolysaccharide (LPS) triggered MIF release (Figure 2-3C) by inhibiting p115 release (Figure 2-3A). We studied the cellular distribution of MIF in 3T3-L1 Pref-1+ cells by immunofluorescence staining and found that MIF and p115 appeared to co-localize in the cytoplasm (Figure 2-3B). Upon LPS stimulation, both MIF and p115 staining was more diffuse in the cytoplasm, and staining intensity was reduced following the addition of rPref-1 (Figure 2-3B), suggesting a role for Pref-1 in inhibiting MIF release by interfering with the cytoplasmic interaction of MIF and p115. In 3T3-L1 differentiated adipocytes (3T3D), Pref-1 also reduced basal p115 release, which was associated with an

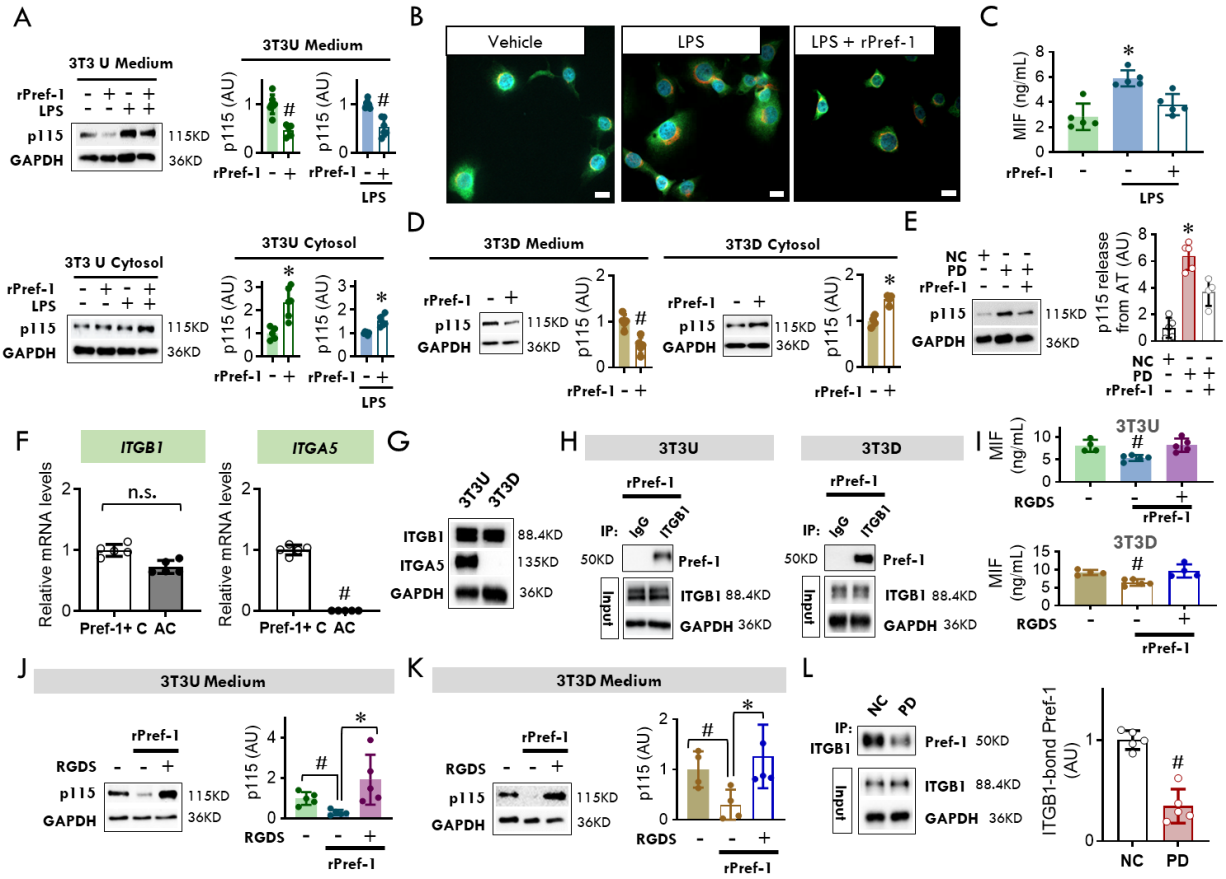

Figure 2-3. Pref-1 inhibits MIF secretion by interaction with the cell membrane protein, integrin 1β, and inhibiting p115, a cofactor for MIF release. (**A**) 3T3U Pref-1+ cells were treated with or without rPref-1 (2.5μg/ml) in the absence or presence of LPS (5μg/ml) for 24 hours. p115 was then quantified in cytosol and medium by western blot. (**B**) MIF (green) and p115 (red) were visualized by immunofluorescence staining in 3T3-L1 undifferentiated Pref-1+ cells following vehicle or LPS treatment. The nucleus was stained by DAPI (blue), (Scale bars, 10 μm). (**C**) MIF release from 3T3-L1 undifferentiated Pref-1+ cells following vehicle or LPS treatment in the presence or absence of rPref-1. (**D**) p115 in cytosol and medium of 3T3D quantified by western blot following rPref-1 treatment for 24 hours. (**E**) p115 release from WATs isolated from NC and PD groups in the presence of absence of rPref-1 (2.5μg/ml). (**F**) The gene expression of ITGB1 and ITGA5 in Pref-1+ cells and adipocytes isolated from WT visceral adipose tissue. (**G**) ITGB1 and ITGA5 genes in 3T3U and 3T3D. (**H**) In 3T3U and 3T3D, immunoprecipitation was performed with negative-control antibody (IgG) or anti-ITGB1 following the treatment of rPref-1. Immunoprecipitated proteins were then detected by anti-Pref-1 antibody. (**I**-**K**) MIF and p115 release from 3T3U and 3T3D following the treatment of rPref-1, in the presence or absence of integrin inhibitor, RGDS peptide (100μM). (**L**) Following NC or PD feeding, visceral adipose tissues isolated from WT mice were initially immunoprecipitated with anti-ITGB1 antibody and the immunoprecipitated proteins were further detected by anti-Pref-1 antibody. All data are presented as mean ± SD. *P ≤ 0.05 increase and #P ≤ 0.05 reduction vs. Vehicle, Pref-1+ cells, IgG, NC, or all other groups. The n.s. represents no significance.

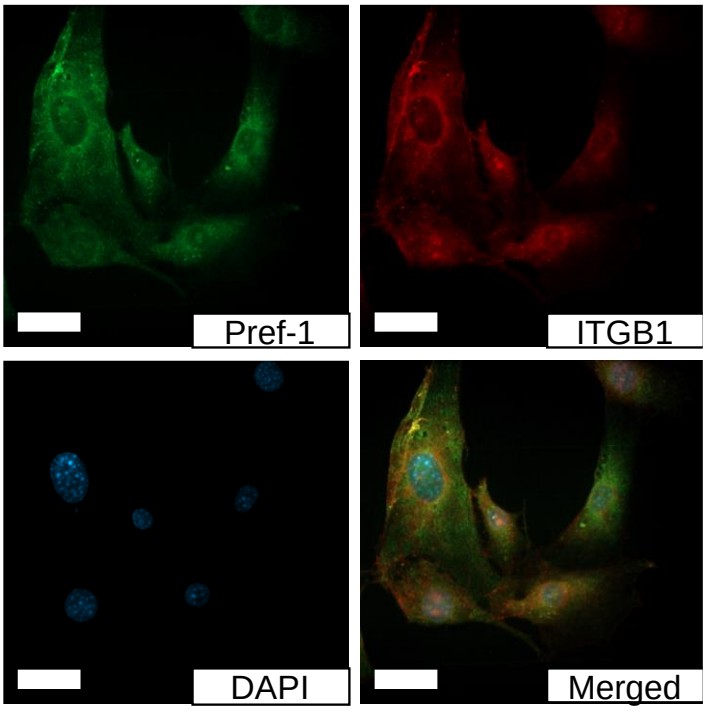

Figure S2-8. Pref-1 and ITGB1 are colocalized in 3T3-L1 undifferentiated (Pref-1+) cells (Scale bars: 20 μM).

increase in cytosolic p115 content (Figure 2-3D). The reduction in p115 release is associated with reduced MIF release (Figure 2-2O), which is consistent with prior observations describing the role of p115 in MIF export (158). In parallel with changes with MIF release (Figure 2-1S), the PD fed group demonstrated increased adipose p115 release when compared to the NC group, and this effect was reduced following rPref-1 treatment (Figure 2-3E). Taken together, these data suggest that Pref-1 inhibits MIF release by the intermediation of p115 in both Pref-1+ cells and adipocytes in WAT.

Pref-1 signaling is associated with the activation of the classic fibronectin receptor, integrin $\alpha5/\beta1$ (193). ITGB1 is highly expressed in both Pref-1+ cells and adipocytes but ITGA5 is only expressed in Pref-1+ cells (Figure 2-3F-G). Given the evidence that Pref-1 regulates MIF release in both cell types (Figure 2-2), we hypothesized that ITGB1 activation may be an essential component in Pref-1 regulation of MIF release. Indeed, Pref-1 binds to ITGB1 in both 3T3-L1 undifferentiated Pref-1+ cells and 3T3-L1 differentiated adipocytes (Figure 2-3H and Figure S3-8). The inhibition of integrin receptor function significantly reversed Pref-1 inhibition of MIF and p115 release from both cell types (Figure 2-3I-K). In mice, PD feeding significantly reduced adipose Pref-1 expression and release (Figure 2-1L-N) when compared to the NC group, and this effect was associated with a reduction in the binding of Pref-1 with ITGB1 (Figure 2-3L). The data together suggest that Pref-1 regulates MIF release from WAT through binding with ITGB1 in both Pref-1+ cells and adipocytes.

2.3.4 Protease-activated Receptor 2 Activation and Expression Modulate Preadipocyte Factor-1 in an AMP-activated Protein Kinase-dependent Manner in Preadipocyte Factor-1+ Cells

PAR2 is a unique GPR that is encoded by the *F2rl1* gene. *F2rl1* is highly expressed in isolated Pref-1+ cells rather than adipocytes (Figure 2-4A). In Pref-1+ cells, PAR2 protein was expressed peripherally and along the plasma membrane, while Pref-1 showed a diffuse cytosolic

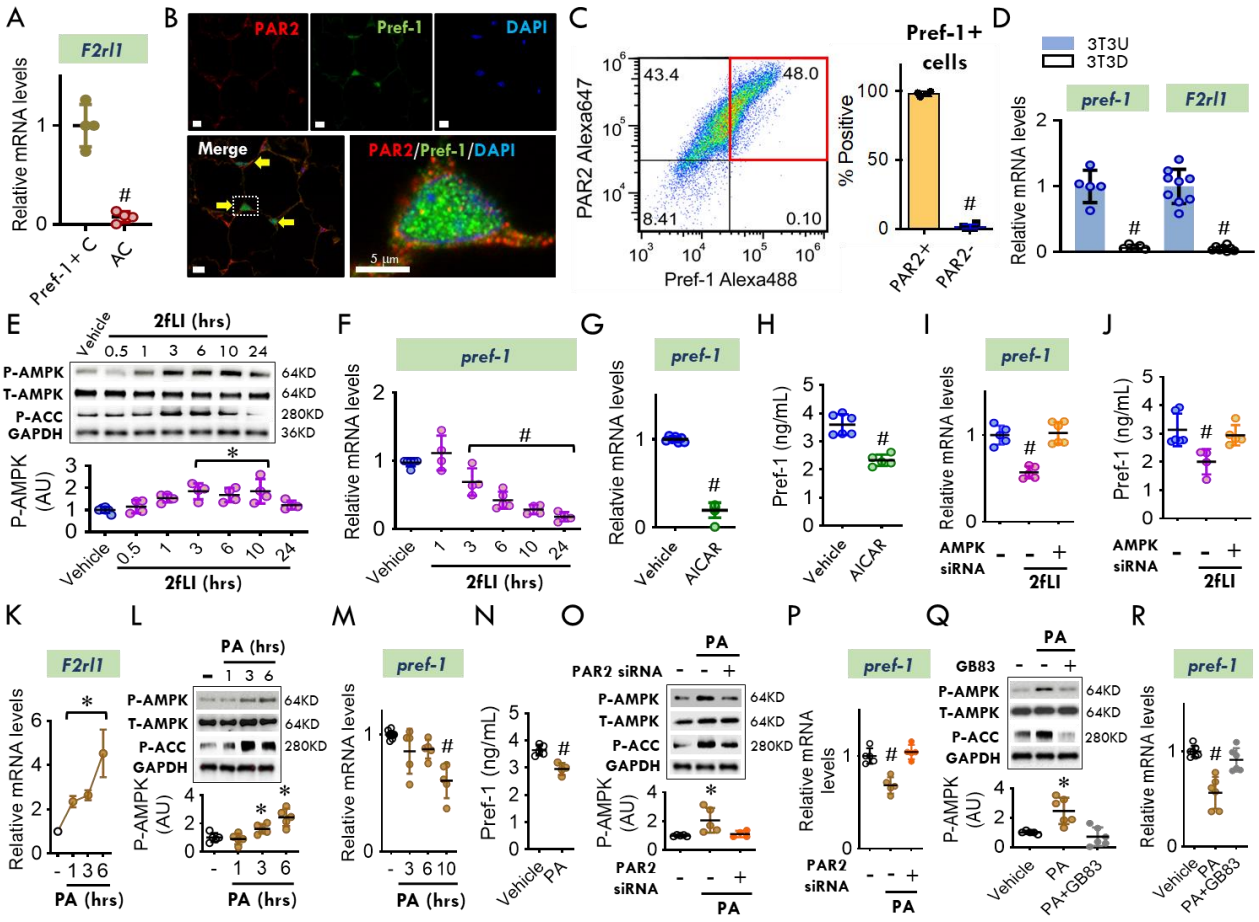

Figure 2-4. PAR2 activation and expression modulate Pref-1 in an AMPK-dependent manner in Pref-1+ cells. (**A**) The mRNA expression of *F2rl1* (PAR2) and *Mif* in isolated Pref-1+ cells (Pref-1+ C) and adipocytes (AC) from 25-week-old WT mouse visceral adipose tissue. (**B**) Colocalization of PAR2 (red) and Pref-1 (green) in WT mouse visceral adipose tissue. (Arrows indicate colocalization. Yellow scale bars, 20 μm, white scale bar: 5 μm). (**C**) Scatter-dot plot and quantification of flow cytometry analysis of PAR2 and Pref-1 in mouse SVF cells. (**D**) The *pref-1* and *Par2* transcript levels were quantified in 3T3U and 3T3D cells. (**E** and **F**) AMPK activation (**E**) and *pref-1* mRNA expression (**F**) in 3T3-L1 undifferentiated cells cultured with 2fLI (30 nM) for 0.5-24 h. (**G** and **H**) Pref-1 mRNA expression (10 h) (**G**) and release in the cell media (24 h) (**H**) in 3T3-L1 undifferentiated cells incubated with AICAR (0.25 mM) for 10-24 h. (**I** and **J**) Pref-1 expression (**I**) and release (**J**) in 3T3-L1 undifferentiated cells (Pref-1+ cells) cultured with or without 2fLI (30 nM) for 24 h following knockdown of AMPKα1 and α2 isoforms by siRNA. (**K**-**N**) *F2rl1* (PAR2) mRNA expression (**K**), AMPK phosphorylation (**L**), *pref-1* mRNA expression (**M**) and Pref-1 release (24 h) (**N**) in 3T3-L1 undifferentiated cells (Pref-1+ cells) incubated with high PA (200 μM) for 1-24 h. (**O** and **P**) AMPK activity (6 h) (**O**) and *pref-1* mRNA expression (10 h) (**P**) in 3T3-L1 undifferentiated cells incubated with or without high PA treatment following knockdown of PAR2 by siRNA. (**Q** and **R**) AMPK activity (6 h) (**Q**) and *pref-1* mRNA expression (10 h) (**R**) in 3T3-L1 undifferentiated cells following high PA treatment with or without the PAR2 inhibitor, GB83 (5 μM). All data are presented as mean ± SD. 2-tailed Student's *t* test in (**A**), (**C**), (**D**), (**G**), (**H**) and (**N**), and one-way ANOVA plus Tukey in the rest of data were used for statistical analysis. *P ≤ 0.05 increase vs. Vehicle in (**E**) and (**L**); vs. other groups in (**O**) and (**Q**); #P ≤ 0.05 reduction vs. Pref-1+ C in (**A**), PAR2+ in (**C**) and 3T3U in (**D**); vs. Vehicle in (**F**), (**G**), (**M**) and (**N**), vs. other groups in (**I**), (**J**), (**P**) and (**R**).

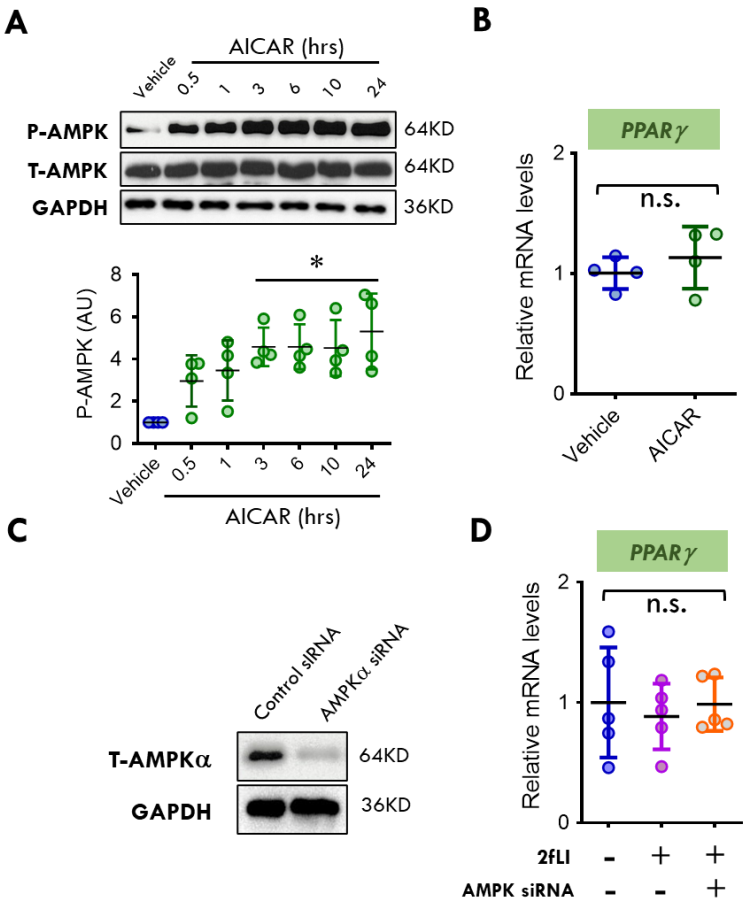

Figure S2-9. The regulation of AMPK activation does not affect PPARγ gene expression in undifferentiated 3T3-L1 cells. The undifferentiated 3T3-L1 cells were incubated with AMPK activator, AICAR (0.25mM) for 0.5 to 24 hours and then AMPK was evaluated by immunoblotting with phosphor- and total AMPKα antibodies (A). (B) *PPARγ* gene expression was evaluated by qPCR. AMPKα was knockdown by AMPKα siRNA (C) in undifferentiated 3T3-L1 cells and *PPARγ* expression (D) was measured with and without 2fLI treatment by qPCR. Mean ± SD in all the panels; *P<0.05 increase vs. Vehicle; the n.s. represents no significance.

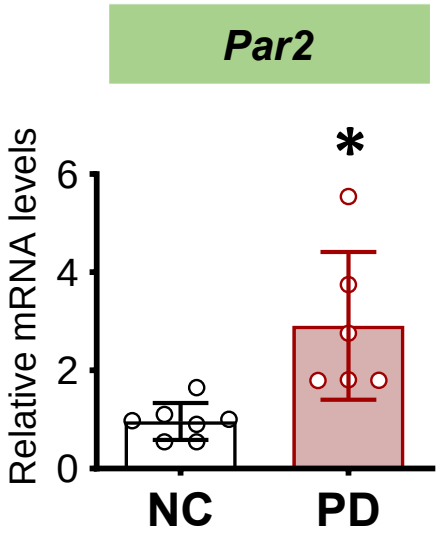

Figure S2-10. High palmitic acid diet (PD) feeding upregulates PAR2 expression in visceral adipose tissue. Mean ± SD in the panel; *P<0.05 increase vs. normal chow (NC).

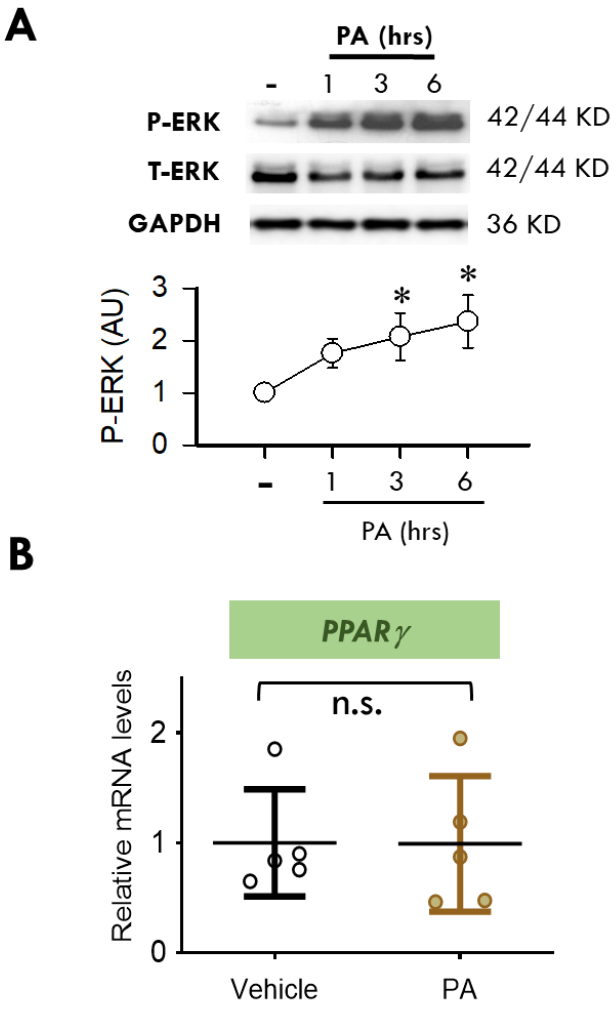

Figure S2-11. ERK phosphorylation and PPARγ gene expression following high palmitic acid treatment in 3T3-L1 undifferentiated cells. The undifferentiated 3T3-L1 cells (Pref-1+ cells) were incubated with or without high PA (200μM) from 1 to 6 hours and then the isolated protein was immunoblotted with phosphorylated ERK and total ERK antibodies (n=6 each group) (A). *PPARγ* gene expression (B) was evaluated by qPCR. Mean ± SD in all the panels; *P< 0.05 increase vs. Vehicle, the n.s. represents no significance.

staining pattern (Figure 2-4B). Quantitative flow-cytometry of freshly isolated SVF cells showed that almost all Pref-1+ cells were also PAR2 positive (Figure 2-4C-D) confirming that Pref-1+ cells express PAR2.

PAR2 activation leads to downstream phosphorylation of AMPK at its Thr^{172} activation site (194). The pharmacologic activation of PAR2 with the PAR2 activating peptide, 2-furoyl-LIGRLO-NH2 (2fLI, 30 nM) increased AMPK phosphorylation in a time-dependent manner in Pref-1+ cells (Figure 2-4E). The *pref-1* mRNA expression was downregulated over the same time frame (Figure 2-4F). Activating AMPK with the activator 5-Aminoimidazole-4-carboxamide ribonucleotide (AICAR) (Figure S2-9A) also downregulated *pref-1* mRNA expression in Pref-1+ cells (Figure 2-4G). AMPK-mediated downregulation of *pref-1* in turn reduced Pref-1 release from Pref-1+ cells (Figure 2-4H). Knocking down AMPK (Figure S2-9C) in Pref-1+ cells prevented the PAR2-induced reduction in *pref-1* expression (Figure 2-4I) and Pref-1 release (Figure 2-4J). These findings establish a requisite role for AMPK in PAR2-mediated *pref-1* downregulation in Pref-1+ cells. Pref-1 downregulates *PPARγ* expression which impedes differentiation of adipocyte precursor cells into mature adipocytes (186). However, when we examined *PPARγ* expression, we found no change in *PPARγ* levels in 3T3-L1 undifferentiated cells despite activation of AMPK and reduced *pref-1* expression (Figure S2-9B and D). Thus, these results indicate that PAR2-induced regulation of AMPK and pref-1 expression occurs independently of *PPARγ* expression.

PD upregulates PAR2 expression in WAT (Figure S2-10). We investigated whether high PA concentrations modulate the PAR2/AMPK/Pref-1 pathway in Pref-1+ cells. Undifferentiated 3T3-L1 cells incubated with a high concentration of PA (200μM) upregulated *F2rl1* (PAR2) expression (Figure 2-4K) in conjunction with activation of downstream ERK phosphorylation (Figure S2-11A). PA also increased AMPK phosphorylation (Figure 2-4L), which was accompanied by a reduction in *pref-1* gene expression and Pref-1 release into the culture media (Figure 2-4M-N). PA addition, however, did not alter *PPARγ* gene expression in these Pref-1+

cells (Figure S2-11B). To examine whether PAR2 activation had an obligatory role in PA-induced AMPK activation and downstream inhibition of *pref-1* expression, undifferentiated 3T3-L1 cells were treated with high PA in the presence of the PAR2-specific inhibitor GB83 (5 μM) or following PAR2 knockdown by siRNA. Both pharmacologic and siRNA inhibition of PAR2 abolished AMPK activation and blocked the PA treatment induced reduction in *pref-1* gene expression (Figure 2-4O-R).

2.3.5 Protease-activated Receptor 2 Controls Macrophage Migration Inhibitory Factor Release from Preadipocyte Factor-1+ Cells and Adipocytes Through Preadipocyte Factor-1

We further investigated whether PAR2 regulates MIF release. We treated 3T3-L1 undifferentiated Pref-1+ cells with 2fLI (30 nM) and observed decreased MIF protein content (Figure 2-5A) but no change in *Mif* mRNA levels (Figure 2-5B). In parallel, we found that MIF content in the media was significantly increased following the addition of 2fLI (Figure 2-5C). These findings suggest that PAR2 may augment cellular MIF release in Pref-1+ cells without altering *Mif* gene expression, thereby reducing intracellular MIF content. Pref-1 inhibits MIF release from Pref-1+ cells and thus, Pref-1 may mediate the functional interaction between the PAR2 and MIF pathway. To test this hypothesis, we activated the PAR2 pathway pharmacologically with 2-fLI in the presence or absence of Pref-1 in Pref-1+ cells. PAR2 activation enhanced MIF release and reduced cellular MIF content, and these effects were reversed by the addition of rPref-1 (Figure 2-5D and F). *Mif* gene expression remained unchanged (Figure 2-5E). This observation additionally appeared only in Pref-1+ cells. In contrast, MIF expression and content were not affected by 2fLI in 3T3-L1 differentiated Pref-1 negative adipocytes (Figure 2-5G), which have negligible *Par2* expression (Figure 2-4D).

With increased PAR2 expression following high PA treatment (Figure 2-4K), MIF content

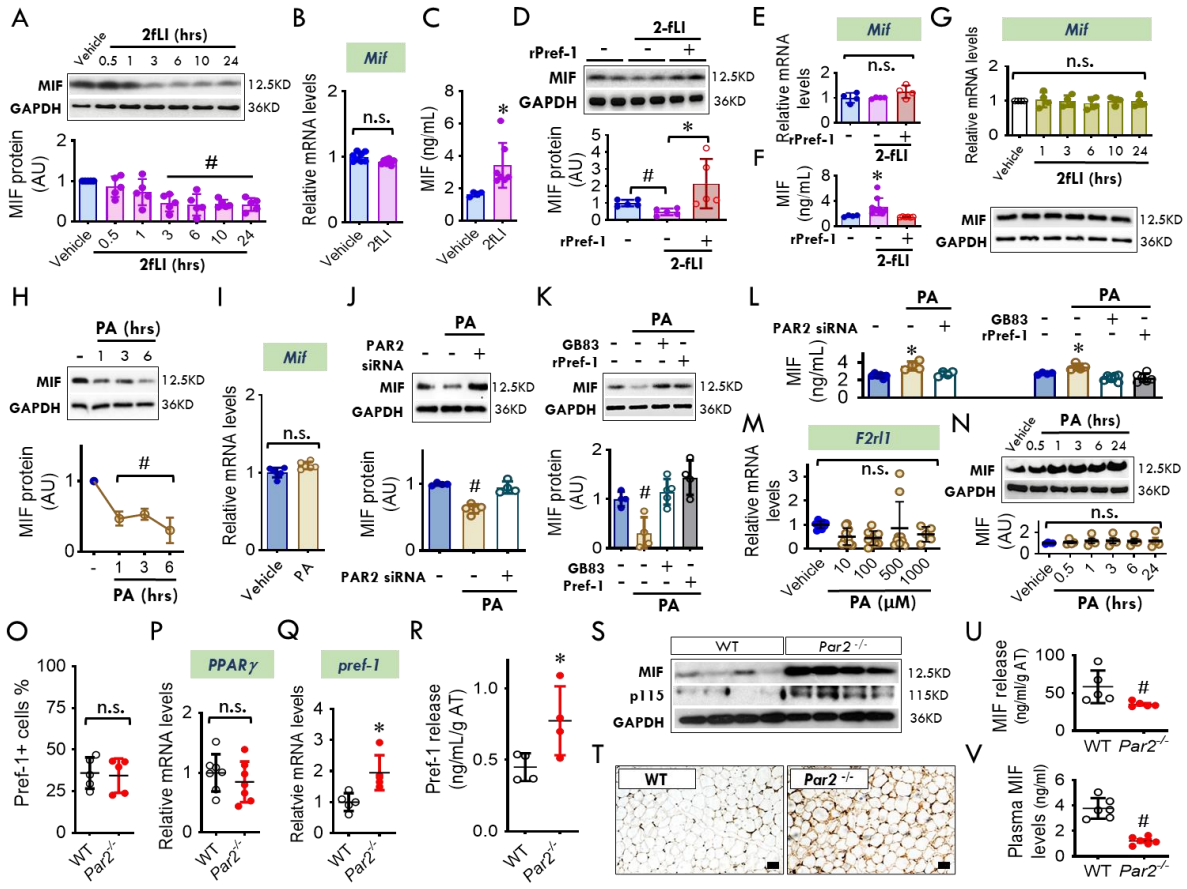

Figure 2-5. PAR2 controls MIF release from Pref-1+ cells and adipocytes through Pref-1. (**A**-**C**) MIF protein (**A**), mRNA expression (24 h) (**B**) and release in the medium (24 h) (**C**) following PAR2 activator, 2fLI (30 nM) treatment for 0.5-24 h in 3T3-L1 undifferentiated cells. (**D**-**F**) MIF protein (**D**), mRNA expression (**E**) and release levels (**F**) following 2-fLI treatment (30 nM) with or without rPref-1 (2.5 μg/ml) for 24 h. (**G**) MIF mRNA and protein expression following 2fLI (30 nM) treatment for 1-24 h in 3T3-L1 differentiated cells. (**H** and **I**) MIF protein (**H**) and gene expression (**I**) in 3T3-L1 undifferentiated cells (Pref-1+ cells) following high PA (200μM) treatment for 24h. (**J**-**L**) Following knocking down PAR2 with siRNA or inhibition of PAR2 with its antagonist, GB83 (5 μM), cellular MIF levels were quantified in the presence or absence of high PA with or without rPref-1 (**J** and **K**). MIF release in the medium was measured by ELISA in (**L**). (**M** and **N**) *F2rl1* (PAR2) gene (**M**) and MIF protein (**N**) levels in differentiated 3T3-L1 adipocytes following variable concentrations of PA for 24 hours. (**O**-**Q**) In 25-week WT and *Par2*$^{-/-}$ mice, the percentages of adipose Pref-1+ cells were quantified by flow cytometry (**O**). The gene expression of *PPARγ* and *pref-1* was evaluated by qPCR (**P** and **Q**). (**R**-**V**) Visceral adipose tissues isolated from WT and *Par2*$^{-/-}$ mice were cultured in PBS for 24 hours at 37°C. Pref-1 and MIF proteins were assessed by ELISA in the medium (**R** and **U**) while cellular MIF and p115 levels were measured by western blot (**S**) and immunohistochemistry staining (Scale bars, 20 μm) (**T**). Plasma MIF levels were quantified by ELISA (**V**). All data are presented as mean ± SD. 2-tailed Student's *t* test in (**B**), (**C**), (**I**), (**O**-**R**), (**U**) and (**V**), and one-way ANOVA plus Tukey in the rest of data for statistical analysis. *P ≤ 0.05 increase vs. Vehicle in (**C**); vs. other groups in (**F**) and (**L**); vs. 2FLI+Vehicle in (**D**); vs. WT in (**Q**) and (**R**). #P ≤ 0.05 reduction vs. Vehicle in (**A**), (**D**) and (**H**); vs. other groups in (**J**) and (**K**); vs. WT in (**U**) and (**V**). The n.s. represents no significance.

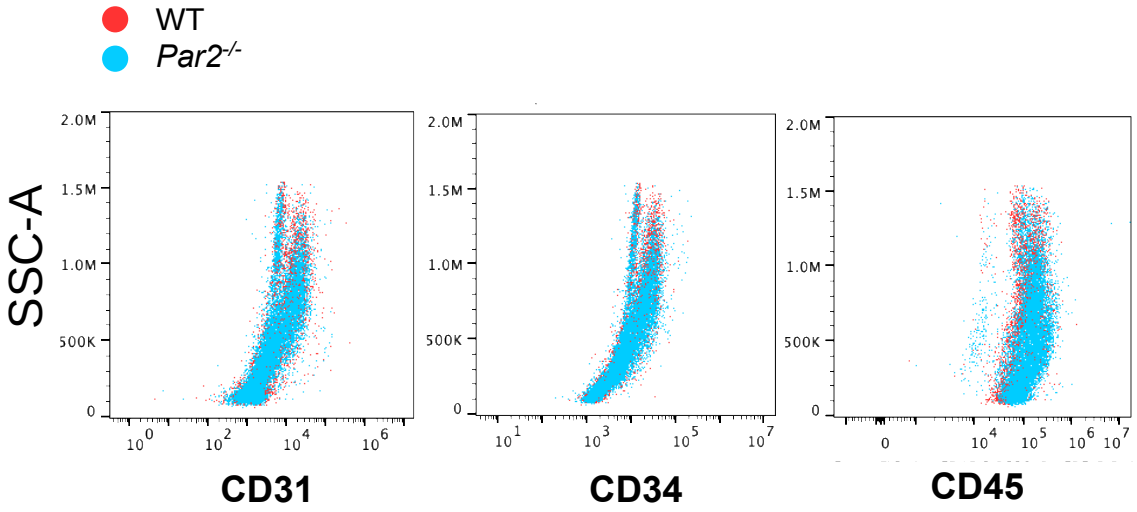

Figure S2-12. Cells with CD31+, CD34+ or CD45+ in Pref-1+ cells isolated from visceral adipose tissue in 25-week WT and *PAR2*$^{-/-}$ mice by flow cytometry.

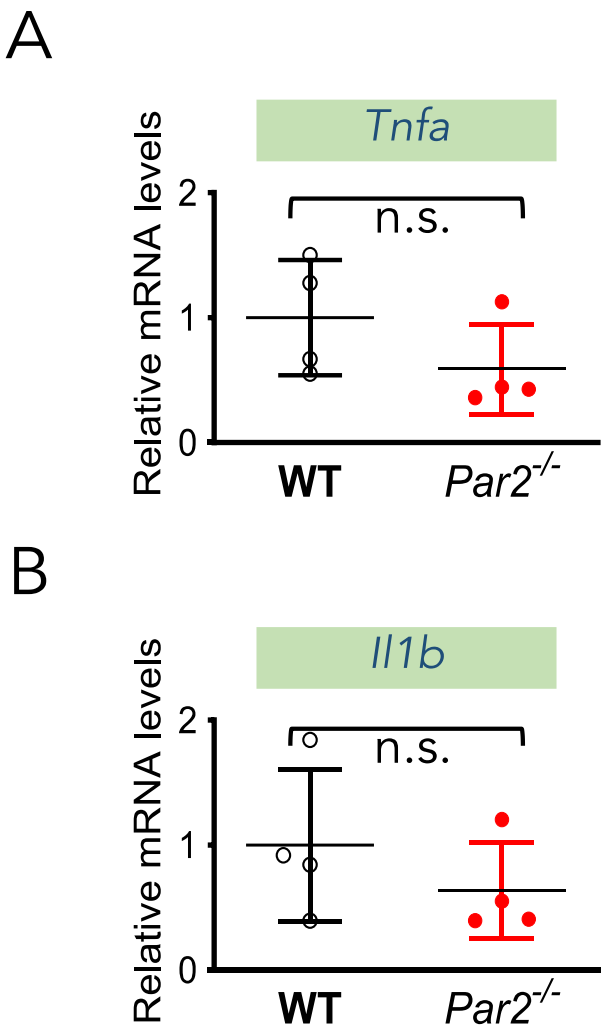

Figure S2-13. The gene expression of inflammatory factors in visceral adipose tissues from 25-week WT and Par2$^{-/-}$ mice. *Tnfa* (A) *and Il1b* (B) gene expression was evaluated by qPCR. Mean ± SD in all the panels; the n.s. represents no significance.

in 3T3-L1 undifferentiated Pref-1+ cells was decreased in a time-dependent manner (Figure 2-5H) and this reduction occurred without changes in *Mif* gene expression (Figure 2-5I). To examine whether PA-downregulated MIF content requires PAR2 expression and activation, PAR2 knockdown and inhibition were performed. Both siRNA and pharmacologic inhibition of PAR2 reversed PA-induced depletion of cellular MIF and this inhibition was blocked by the addition of rPref-1 (Figure 2-5J-K). In parallel, high PA augmented MIF release, but this effect of PA could be reversed by blockade of PAR2 (Figure 2-5L). In contrast, in 3T3-L1 differentiated adipocytes, high PA did not trigger *F2rl1* (PAR2) gene expression or alter cellular MIF content (Figure 2-5M-N).

We also found that in the absence of PAR2 expression, there was no evident alteration in either adipose Pref-1+ cell populations and characteristics or PPARγ expression (Figure 2-5O-P and Figure S2-12), however, there was an increase in both *pref-1* mRNA expression (Figure 2-5Q) and Pref-1 release (Figure 2-5R). PAR2 deficiency upregulated adipose content of MIF and p115 (Figure 2-5S-T), which was associated with a decrease in both MIF release from WAT (Figure 2-5U) and circulating MIF levels (Figure 2-5V). These *in vivo* data further suggest that the PAR2/Pref-1 signaling pathway may play a key role in regulating MIF accumulation and release from WAT even in the absence of inflammation (Figure S2-13).

2.3.6 Protease-activated Receptor 2 Deficiency in White Adipose Tissue or Addition of Preadipocyte Factor-1 Decreases Non-inflammatory Adipose Macrophage Migration Inhibitory Factor Release and Improves Insulin Sensitivity

We next transplanted visceral (epididymal) adipose tissue from WT to WT, *Par2*$^{-/-}$ to WT or WT to *Par2*$^{-/-}$ mice respectively (Figure 2-6A, Figure S2-14 and S2-15) (195). Following a PD feeding, plasma Pref-1 levels were significantly reduced in the group of WT to WT while *Par2*$^{-/-}$ adipose tissue transplantation into WT mice reversed the effect of PD (Figure 2-6B). In parallel, PD increased plasma MIF levels, IR, body weight and adipose tissue mass, and these effects

were all inhibited by *Par2*$^{-/-}$ adipose tissue transplantation into WT mice (Figure 2-6C-G). Additionally, we found no evidence of adipose inflammation after PD feeding, indicating that this was a non-inflammatory mechanism (Figure 2-6H).

In an additional separate experiment, 20-week-old male WT mice were initially fed with either NC or a PD for 4 weeks. The mice were implanted subsequently with an osmotic pump filled with vehicle or rPref-1 for 4 weeks of infusion with continued PD feeding (Figure 2-6I and Figure S16). We observed that administration of Pref-1 significantly blocked the reduction of plasma Pref-1 levels induced by PD feeding (Figure 2-6J). There were no associated changes in *PPAR*γ expression (Figure 2-6K) to suggest that infusion of Pref-1 might affect adipogenesis. However, Pref-1 administration augmented the adipose content of MIF and p115 (Figure 2-6L) and circulating plasma MIF levels were reduced (Figure 2-6M). These results suggested that exogenous Pref-1 infusion inhibits MIF release from WAT. Pref-1 infusion attenuated IR during PD (Figure 2-6N), despite no evident change in body weight gain, adipose tissue weight and adipocyte size compared to the PD group with vehicle infusion (Figure 2-6O-Q). As in the study of *Par2*$^{-/-}$ adipose tissue transplantation, Pref-1 infusion did not affect inflammatory gene expression (Figure 2-6R). These findings indicate that Pref-1 treatment reverses non-inflammatory IR by downregulating adipose MIF release.

In summary, these data support a novel, inflammation-independent PAR2/Pref-1/MIF pathway that acts between Pref-1+ cells and mature adipocytes to regulate WAT MIF release in obesity related IR (Figure 2-6S).

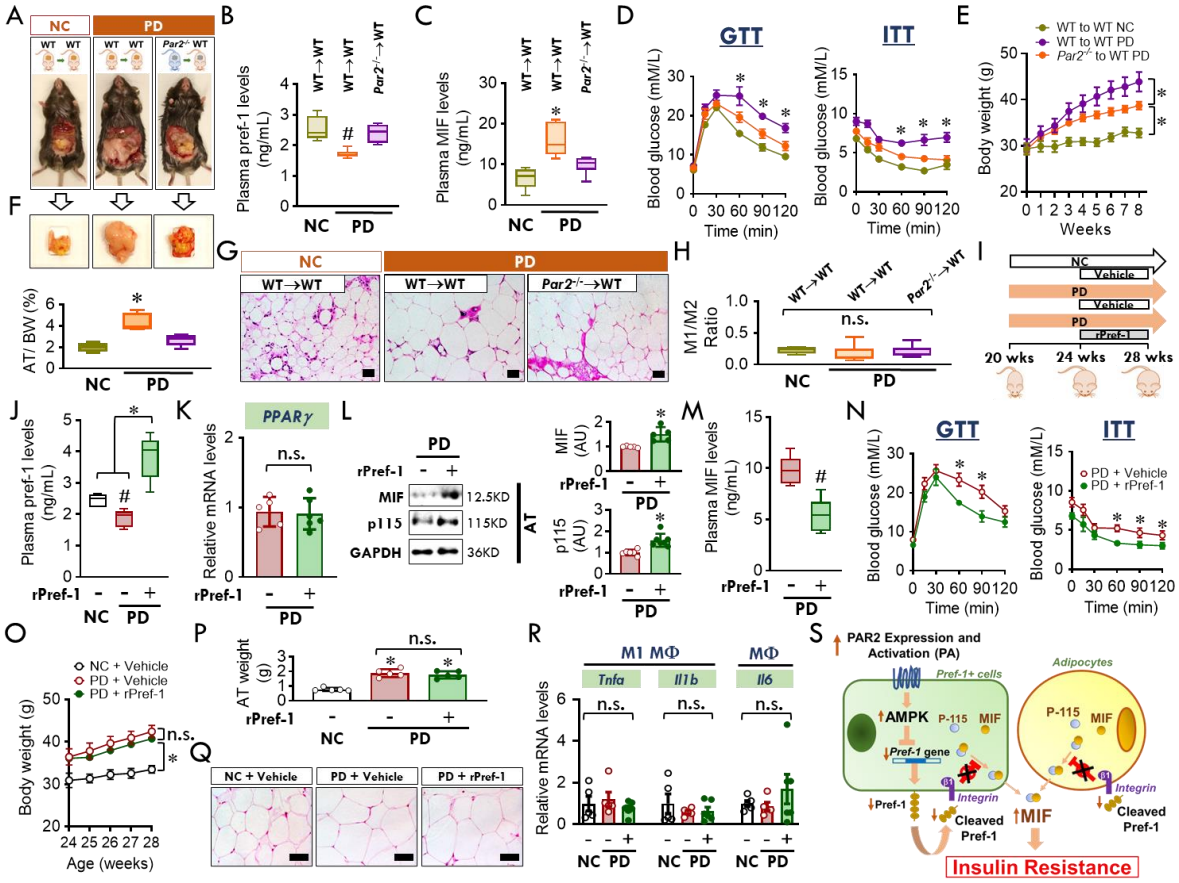

Figure 2-6. PAR2 deficiency in WAT or addition of Pref-1 decreases non-inflammatory adipose MIF release and improves insulin sensitivity. (**A**) WT mice at 18 weeks were anesthetized and transplanted with WT or *Par2*$^{-/-}$ visceral epididymal adipose tissue. Following 2-week recovery, these mice at 20 weeks will be fed with NC or PD for 8 weeks. (**B**-**H**) Plasma Pref-1 (**B**) and MIF (**C**) levels in the mice transplanted with WT or *Par2*$^{-/-}$ adipose tissue following NC or PD diet feeding. Insulin resistance was assessed by GTT and ITT (**D**). Body weight gain, adipose weight (AT)/body weight (BW) ratio, adipocyte size and M1/M2 ratio in adipose tissue were measured in these mice as well (**E** to **H**) (Scale bars, 20 μm in **G**). (**I**) WT mice at 20 weeks were fed with NC or PD for 8 weeks. During the last 4 weeks, the mice were infused with vehicle or rPref-1 protein (24μg/day/kg) by osmotic pump. (**J**-**R**) Plasma Pref-1 levels, PPARγ gene expression, adipose MIF and p115 contents and plasma MIF levels were subsequently evaluated from (**J**) to (**M**). IR was assessed by GTT and ITT in (**N**). Body weight gain, adipose tissue (AT) weight, adipocyte size and expression of inflammatory factors were quantified from (**O**) to (**R**) (Scale bars, 20 μm in **Q**). (**S**) Schematic diagram for the mechanism of PAR2/AMPK/Pref-1/MIF release signaling pathway. Pref-1 is expressed and released in Pref-1+ cells with characteristics of M2 macrophages, endothelial cells or progenitors. Pref-1 inhibits MIF release from both Pref-1+ cells and adipocytes by binding with cell membrane integrin β1 and inhibiting the mobilization of p115, a cofactor for MIF release. High PA induces PAR2 expression in Pref-1+ cells, leading to the downregulation of Pref-1 expression and its release in an AMPK-dependent manner. When Pref-1 secretion is reduced, Pref-1+ cells and adipocytes increase MIF release and its plasma content, resulting in IR. All data are presented as mean ± SD. n=6 each animal group. *P ≤ 0.05 increase vs. other groups in (**C**, **D**, **F** and **J**); vs. WT to WT NC or *Par2*$^{-/-}$ to WT PD in (**E**); vs. NC in (**O**) and (**P**). $^{\#}$P ≤ 0.05 reduction vs. other groups in (**B**); vs. NC in (**J**); vs. PD + Vehicle in (**M**) and (**N**). The n.s. represents no significance.

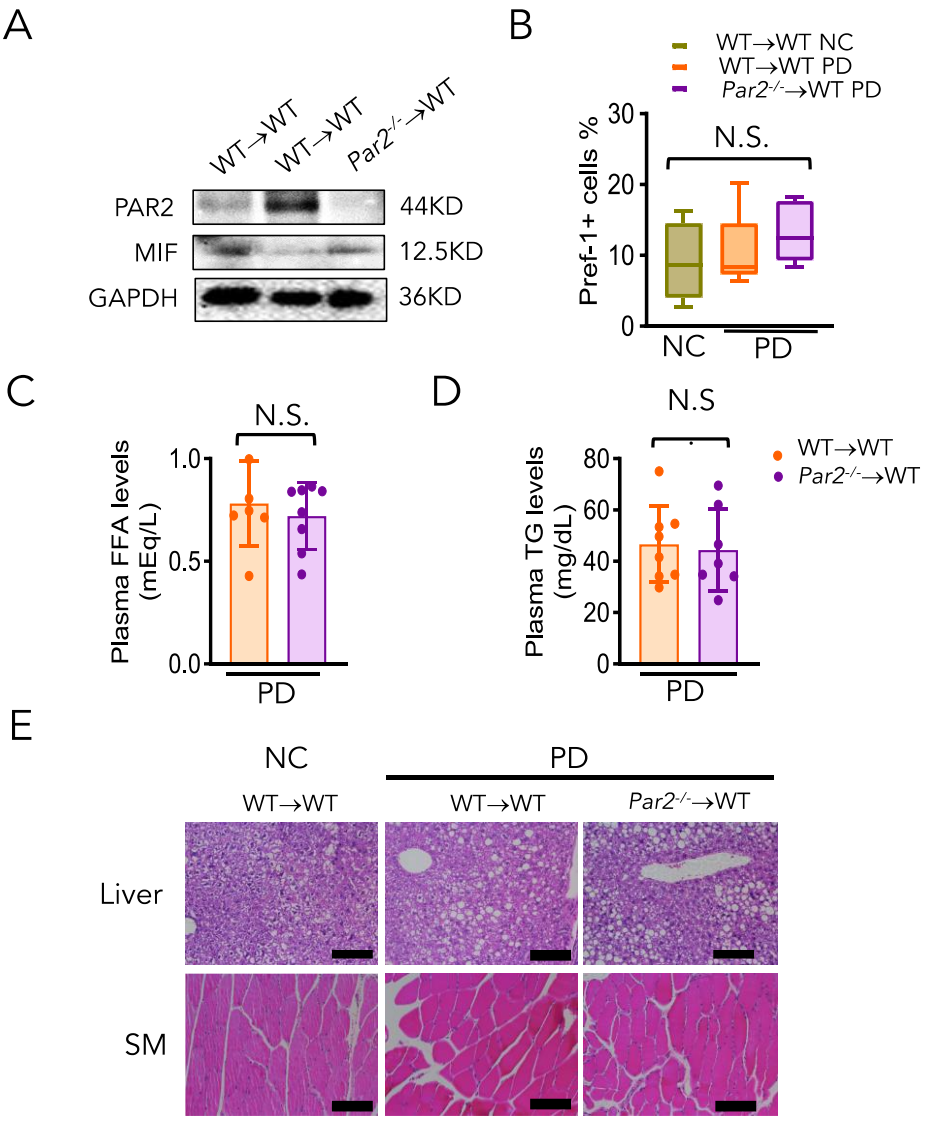

Figure S2-14. The metabolic characteristics of WT mice transplanted with Par2$^{-/-}$ visceral adipose tissue following high palmitic acid diet feeding. WT mice at 18 weeks were anesthetized and their visceral adipose tissues (epididymal) were removed. Visceral adipose tissues (epididymal) from WT or *Par2*$^{-/-}$ donors were transplanted into these WT mice. Following 2-week recovery, these mice at 20 weeks were fed with NC or PD for 8 weeks. PAR2 and MIF protein expression was evaluated in the transplanted adipose tissues by western blot (A). The components of pref-1+ cells were quantified by flow-cytometry (B). The levels of plasma FFA (C) and TG (D) were also quantified and lipid storage in liver and skeletal muscle (SM) (E) was identified by HE staining. Mean ± SD in all the panels; the n.s. represents no significance.

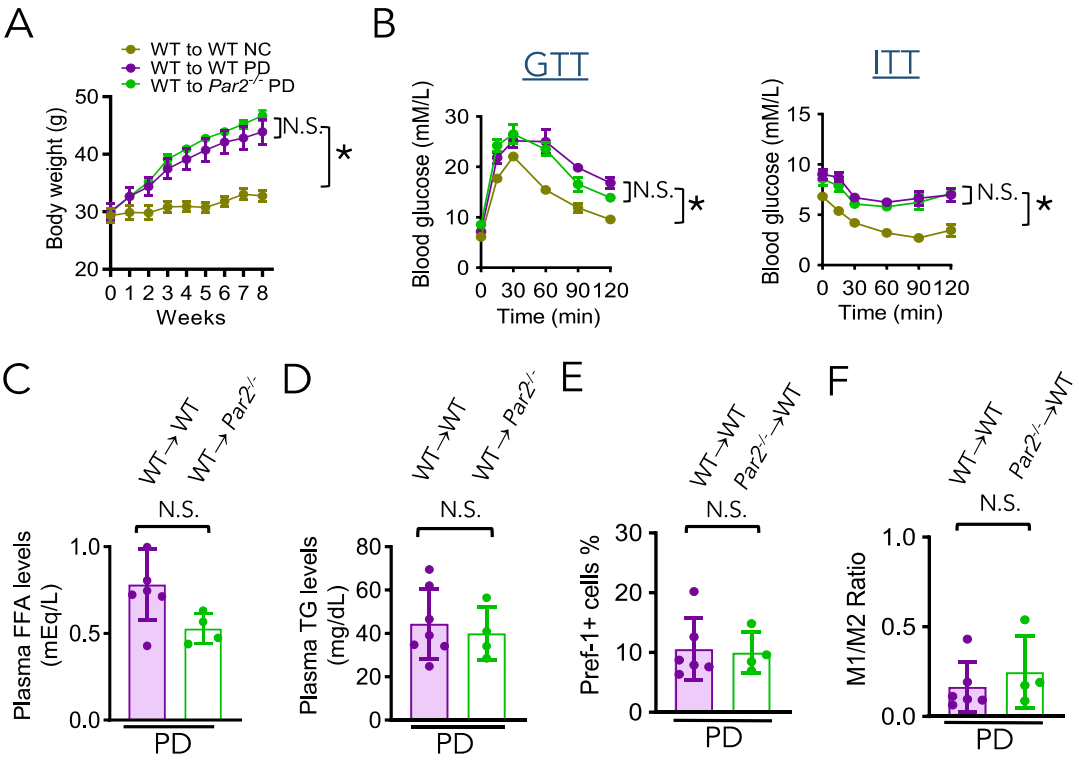

Figure S2-15. The metabolic characteristics of Par2$^{-/-}$ mice transplanted with WT visceral adipose tissue following high palmitic acid diet feeding. WT and *Par2*$^{-/-}$ mice at 18 weeks were anesthetized and transplanted with WT visceral adipose tissue (epididymal). Following 2-week recovery, these mice at 20 weeks were fed with NC or PD for 8 weeks. Body weight gain was monitored in (A) and IR was quantified by i.p. glucose tolerance and insulin tolerance tests (B). Plasma FFA and TG levels were measured in (C) and (D). The components of adipose pref-1+ cells and M1/M2 ratio were evaluated by flow-cytometry (E and F). Mean ± SD in all the panels; *P< 0.05 increase vs WT to WT NC, the n.s. represents no significance.

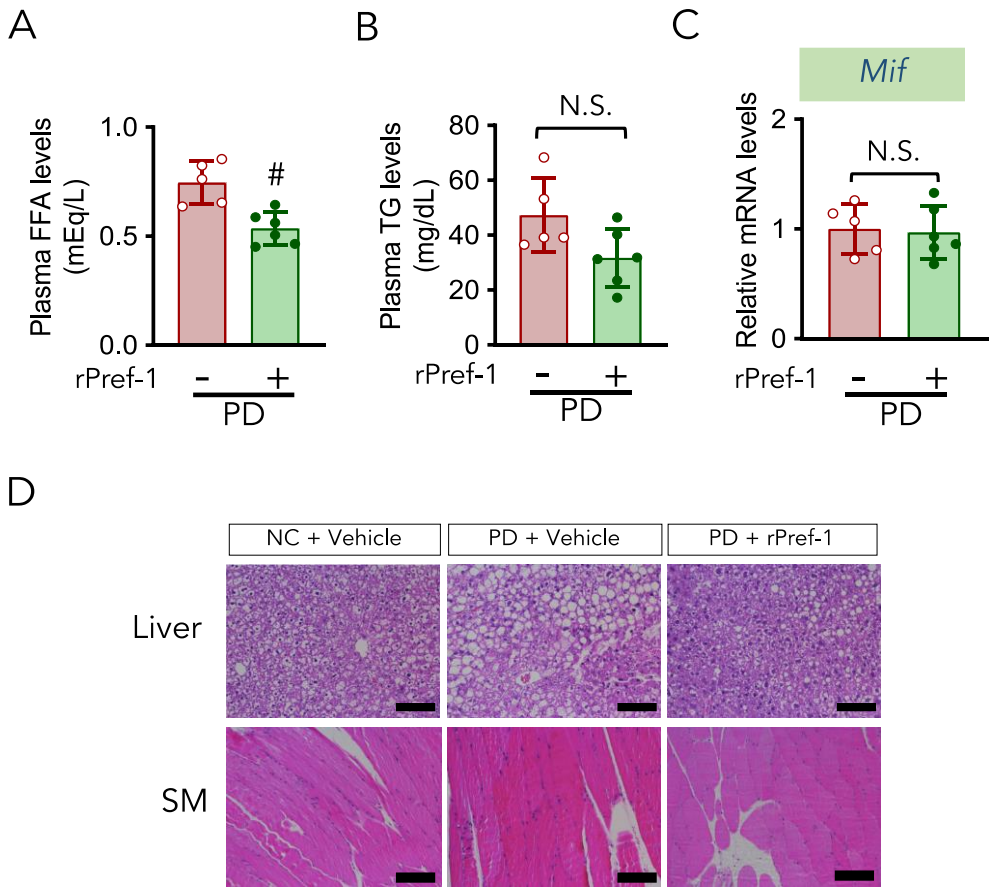

Figure S2-16. The effects of pref-1 infusion on high palmitic acid diet induced metabolic dysfunction. WT mice at 20 weeks were fed with NC or PD for 8 weeks. During the last 4 weeks, the mice were infused with vehicle or recombinant pref-1 protein by osmotic pump. Plasma levels of FFA and TG were measured in (A) and (B). *Mif* gene expression was quantified by qPCR (C) and lipid storage in liver and SM were evaluated by HE staining in (D, Scale bars: 100 μM). Mean ± SD in all the panels; #P< 0.05 reduction vs vehicle, the n.s. represents no significance.

2.4 DISCUSSION

Accumulating evidence suggests that non-inflammatory mechanisms may initiate IR (3, 89). We describe a Pref-1 mediated pathway involving the crosstalk between cells expressing Pref-1 (Pref-1+) and adipocytes that regulates MIF secretion from WAT in response to high PA exposure. The molecular pathway underlying this crosstalk is initiated by PAR2, whose expression is induced by HFD; PAR2 downregulates Pref-1 expression and release from Pref-1+ cells in an AMPK-dependent manner. Normally, Pref-1, derived from Pref-1+ cells, inhibits MIF release from both Pref-1+ cells and adipocytes by binding to integrin β1 and inhibiting the action of p115, a necessary cofactor for MIF secretion. However, in the context of non-inflammatory obesity, the ability of Pref-1 to inhibit MIF release from Pref-1+ cells and adipocytes is impaired; consequently, circulating plasma MIF levels are increased. This finding is significant given MIF's maladaptive action to cause metabolic dysfunction and IR in obesity, as evidenced in experimental results in mice as well as human subjects with functionally variant *MIF* alleles (154, 177, 196).

WAT is known to be an important site of MIF production, and circulating MIF levels correlate positively with increased body weight (172). Early studies attributed the upregulation of adipose MIF secretion to macrophage infiltration (177, 184). One prior study reported that high caloric diet feeding induces an increase in adipose macrophages and *Mif* gene expression, leading to an elevation in plasma MIF levels (177). In metabolic dysfunction associated with treatment with the antipsychotic olanzapine, high plasma MIF levels are accompanied by an increase in both MIF gene and protein expression in WAT (154). Increased MIF expression also was associated with increased expression of IL-6 and IL-1β (154), further supporting an inflammatory etiology for adipose MIF secretion with olanzapine treatment. In contrast, the current study provides the first evidence for a non-inflammatory pathway of MIF secretion in WAT. Animals fed a HFD for 8 weeks showed increased MIF secretion by WAT in the absence of

increased *Mif* mRNA expression or a significant, associated inflammatory response. Thus, our findings support the existence of a mechanism of MIF secretion that is metabolically controlled and independent of adipose macrophage infiltration or inflammatory activation.

The current results also demonstrate that non-inflammatory MIF release from WAT is mediated by cellular crosstalk driven by Pref-1. Pref-1 was expressed and released by Pref-1+ cells, which included M2 macrophage (an anti-inflammatory phenotype), endothelial cell, and progenitor populations. Pref-1 inhibited MIF release from both Pref-1+ cells and adipocytes. Accordingly, the activation and secretion of Pref-1 may reduce non-inflammatory MIF secretion from WAT and improve metabolic dysfunction. Indeed, *pref-1* overexpression improved glucose homeostasis and insulin sensitivity (189). It should be noted that Pref-1 was originally identified to regulate adipogenesis (186). Mice with high levels of Pref-1 in adipose tissue have reduced fat mass and hypertriglyceridemia due to impaired storage in adipose tissue (187). In contrast, mice lacking Pref-1 show augmented fat deposition and obesity (188). However, our current findings indicate that while Pref-1 expression and release by WAT were downregulated following high fat feeding, this occurred in the absence of changes in adipose maturation. Thus, the effect of Pref-1 described herein reflects an early phase of metabolic dysfunction; and it is possible that actions on adipogenesis may be detected in a more chronic obesity model.

We found that Pref-1 significantly inhibited basal and/or LPS-induced MIF release from Pref-1+ cells and adipocytes through p115. The Golgi-associated protein, p115 is a binding partner of MIF that facilitates MIF transport from the perinuclear ring to the plasma membrane and subsequent export from monocytes/macrophages (158). p115 is necessary for the release of MIF but not other cytokines (158). Pref-1 signaling is associated with the activation of the classic fibronectin receptors, integrins $\alpha5\beta1$ (193), but only ITGB1 is highly expressed in both Pref-1+ cells and adipocytes. Our current findings indicated that Pref-1 modulates p115 and MIF release by binding to ITGB1 in both Pref-1+ cells and adipocytes. Thus, a Pref-1/ITGB1/p115

pathway appears to be a key mechanism that regulates non-inflammatory MIF release from WAT, leading to HFD-induced IR. Indeed, infusion of rPref-1 in mice significantly upregulated the cytosolic content of MIF and p115 in WAT, and that this effect was associated with a reduction in plasma MIF levels and decreased IR. The MIF release and insulin sensitivity modulated by Pref-1 did not appear to be related to adipose inflammation, further supporting our hypothesis that MIF is a key regulator of non-inflammatory mechanisms of IR.

Our findings also demonstrate that the expression and activation of PAR2 negatively regulates Pref-1 expression and release from Pref-1+ cells in WAT. PAR2 is a seven transmembrane receptor expressed by endothelial cells and macrophages (197, 198). We also showed that PAR2 is highly expressed in Pref-1+ cells rather than adipocytes. PAR2 is known to activate AMPK through Ca^{2+}/CaMKKβ signaling (194), and we found that AMPK is required for the PAR2-mediated downregulation of both *pref-1* expression and Pref-1 release in Pref-1+ cells in WAT. Thus, the absence of PAR2 expression in WAT significantly increased Pref-1 expression and release. PAR2 expression was upregulated by PA. Following short-term treatment with a PD diet, PAR2 expression and activation in Pref-1+ cells occurred without concomitant alterations in adipose cytokine gene expression, and pharmacologic activation of PAR2 in turn stimulated MIF release rather than *Mif* gene expression. Downregulation of Pref-1 following PAR2 activation prevented its inhibitory action on MIF release in Pref-1+ cells and adipocytes, leading to increased plasma MIF levels. We therefore conclude that PAR2/Pref-1 mediates a novel pathway for autocrine/paracrine signaling between Pref-1+ cells and adipocytes that influences circulating MIF levels in the absence of inflammation.

Recent experimental work is also consistent with the hypothesis that IR occurs prior to systemic or adipose inflammation (3). Clinical research indicates that adipose inflammation is not causally linked to IR (89) and targeting TNFα fails to provide beneficial effect on systemic insulin sensitivity (99). Immunocompromised animal models are also not protected from IR induced by

a short-term HFD (90). Thus, elucidating the proximate role of non-inflammatory mechanisms in the initiation of IR is potentially important. We found that alterations in Pref-1 in the regulation of adipose MIF secretion may have an early role in the development of HFD-induced IR prior to the inflammatory activation of adipose tissue macrophages. Furthermore, PAR2 appears to be critical in the inhibition of Pref-1 secretion. These data together suggest that Pref-1 and its upstream regulator, PAR2, could be a tractable therapeutical target for early, non-inflammatory IR. Whether PAR2 has additional distinct actions on lipid metabolism independent of its effects on Pref-1 and MIF against obesity will also be of interest for further studies.

In conclusion, we have identified a novel autocrine/paracrine mechanism mediated by secreted Pref-1 that contributes to high fat-induced metabolic dysfunction and is independent of adipose macrophage infiltration and inflammation. PAR2 is highly expressed in various adipose tissues, including subcutaneous and visceral adipose tissues (199). PAR2 expression and activation downregulate Pref-1 expression and release from Pref-1+ cells in WAT. Strategies to block FA-induced PAR2 expression and/or to augment Pref-1 expression, activation or secretion may reduce WAT MIF secretion and improve metabolic dysfunction. Further work is warranted to investigate the therapeutic applicability of these strategies in the clinical settings of obesity and type 2 diabetes.

2.4.1 Limitations of the Study

The focus of this study was to identify the mechanisms underlying IR in the absence of inflammation. We found that pref-1 regulates non-inflammatory MIF release from WAT, which was previously recognized as a risk factor for IR. However, although PAR2 and Pref-1 co-localize in Pref-1+ cells, our study did not demonstrate the role of PAR2 in mediating Pref-1 expression and release in Pref-1+ cells by specifically knocking down PAR2 in Pref-1+ cells in animal models.

2.5. CONTRIBUTIONS OF AUTHORS

Yiheng Huang performed the major experiments. Liujun Chen, Haibin Tong, Yadan Qi, Jinjie Xu, Xiang Gao, Kathleen E. Fifield, and Lingyan Wang participated in animal studies. Jacqueline L. Vanderluit contributed to immunofluorescence. Guang Sun provided human samples, and Guang Sun, Donghong Cui, and Suixin Liu conducted human data analysis. Grace K. Muller, Hong Wu, Zhengyuan Xia, Lin Leng, Lawrence H. Young, and Richard Bucala contributed validated research reagents, assisted with data interpretations, and edited the manuscript. Yadan Qi and John McGuire contributed to preparing the animal models. Lawrence H. Young, and Richard Bucala provided overall scientific support for the research project and Dake Qi designed and managed the research.

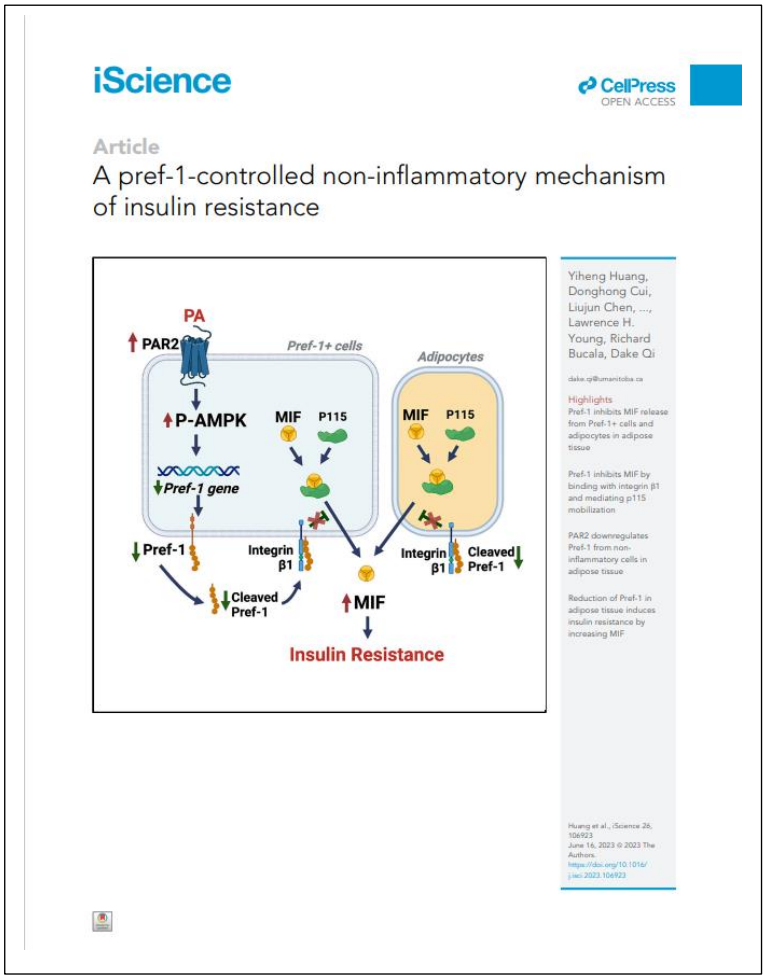

CHAPTER 3 DOWNREGULATION OF ADIPOSE LIPOPROTEIN LIPASE BY PROTEASE-ACTIVATED RECEPTOR 2 CONTRIBUTES TO THE DEVELOPMENT OF HYPERTRIGLYCERIDEMIA

3.1 INTRODUCTION

LPL plays a key role in breaking down plasma triglycerides and promoting lipid storage in adipose tissue. LPL is ubiquitously expressed in WAT including both subcutaneous and visceral adipose tissues (200). Transgenic defects in LPL in adipose tissue are associated with elevated plasma TG levels (7), suggesting a critical role for adipose LPL in regulating hypertriglyceridemia. LPL activity is attenuated in human subcutaneous adipose tissue associated with metabolic dysfunction (149) while weight loss results in increased LPL activity and expression (201). To date, the molecular mechanisms that regulate LPL in WAT and how they contribute to the regulation of hypertriglyceridemia remain unclear.

MIF is an evolutionarily conserved cytokine (179) that is highly expressed in visceral and subcutaneous adipose tissue. MIF is positively correlated with waist circumference or body fat percentage in obese subjects (173, 174). Initially, MIF expression in WAT was thought to arise from infiltrating macrophages (177, 184). However, non-immune cells such as adipose progenitors and adipocytes in WAT also release MIF under physiologic and pathologic conditions (175, 185). Circulating MIF levels are associated with metabolic dysfunction in the presence or absence of inflammation (177, 202) but its role in regulating hypertriglyceridemia is currently unknown.

PARs belong to a unique class of GPRs expressed on various cell types, including endothelial cells (203) and adipocytes (202, 204). Following N-terminal cleavage, PARs activate intracellular G-protein signaling cascades (205). A cell-penetrating, lipidated PAR2 inhibitor, PZ-235 reduces fatty liver steatosis and hypertriglyceridemia by up to 50% (206), suggesting an inverse relationship between PAR2 and hypertriglyceridemia. Interestingly, PAR2 activation also

induces *MIF* mRNA expression in human endothelial cells (207). Herein, in the present study, we investigated a novel hypothesis that PAR2 regulates hypertriglyceridemia through MIF. Our data indicate that increased PAR2 expression upregulates circulating MIF levels which downregulate LPL expression in WAT. Alterations in LPL were associated with impaired clearance of plasma triglyceride, which was associated with hypertriglyceridemia. Loss of PAR2 reduced plasma MIF levels, thereby abrogating the inhibitory effect of MIF on adipose LPL expression. Thus, loss of PAR2 increased plasma triglyceride clearance and fat storage in WAT.

Hypothesis: To demonstrate the role of PAR2/MIF signaling pathway in regulating LPL and plasma TG levels.

Objective 1: To elucidate the molecular mechanism by which PAR2 regulates LPL and contributes to hypertriglyceridemia.

Objective 2: To identify the signaling pathway through which PAR2 suppresses LPL expression via MIF.

Objective 3: To confirm the role of adipose-derived MIF in regulating LPL and the development of hypertriglyceridemia in animal models.

3.2 METHODS

3.2.1 Human Subjects

Human mRNA samples were obtained from a previous overfeeding study to investigate the effects of a positive energy balance on endocrine factors and glucose and lipid metabolism, which has been approved by Newfoundland and Labrador HREB (19). We also obtained an ethic approval for a secondary use of these samples for the current study (Research portal File# 20200635). Plasma MIF level was determined with an ELISA method according to the protocol from R&D Systems, USA. Human PCR data were analyzed using t-test. All significant levels were two-tailed tested, and a P value of less than 0.05 was considered as statistically significant.

3.2.2 Experimental Animals

Par2$^{-/-}$, *Mif* Lung Tg (208), *Cd74*$^{-/-}$ and WT littermate male mice on a pure C57BL/6 background (from 4-28 weeks of age) were bred at the Health Science Center Animal Facility in Memorial University of Newfoundland or the Animal Care Centre of University of Manitoba, Canada. They were housed in IVCs with an artificial 12:12 h light: dark cycle at room temperature and fed with either NC or PD (41% palmitic oil; #170100, Envigo Teklad Diets) for 8 weeks. All experiments were conducted in accordance with the Guide for the Care and Use of Laboratory Animals of the National Institutes of Health and were approved by the Internal Animal Committee Review Board of Memorial University of Newfoundland or University of Manitoba.

3.2.3 Recombinant Mouse Macrophage Migration Inhibitory Factor Infusion and Macrophage Migration Inhibitory Factor Neutralization

WT and Mouse *Par2*$^{-/-}$ mice at 20 weeks were initially fed with PD for 4 weeks. Jugular vein was then cannulated and rMIF (24 μg/day/kg) or vehicle was injected via a mini-osmotic pump implanted in a subcutaneous pocket (Alzet model 1004) into the mice accompanied with

PD feeding for the following 4 weeks. In a separate experiment, plasma MIF was neutralized with anti-MIF antibody (20 mg/kg, i.p. twice a week) during PD feeding.

3.2.4 3T3-L1 Cell Culture

3T3-L1 cells were purchased from ATCC and passage 6-15 of these cells were used in the study. 3T3-L1 adipocytes were cultured and differentiated as described previously. Before all experiments, cells were briefly serum-starved in DMEM-0.5% FBS for 8 hr.

3.2.5 Antibodies and Reagents

Antibodies against LPL, PAR2, phosphor-Akt (Ser^{473}) and total Akt, and MIF were purchased from Abcam, Invitrogen, Cell Signaling and Torrey Pines Biolabs, respectively. Recombinant mouse MIF was purified from a high yield *E. coli* expression system by fast protein liquid chromatography (FPLC) followed by C8 chromatography to remove endotoxin (209). Mouse MIF concentrations were measured by a one-step sandwich ELISA from R&D systems as previously described (202). Plasma levels of TG and FFA were measured by L-type Triglyceride M assay kit and non-esterified fatty acid assay kit from FUJIFILM Wako Diagnostics, USA. LPL activity was detected by the LPL assay kit from Abcam, USA. The CXCR2 inhibitor SB225002, CXCR4 inhibitor WZ811 and insulin were purchased from Sigma-Aldrich, USA.

3.2.6 Expression and Phosphorylation Analyses

The transcript level for human gene of *F2RL1, LPL and b-actin* and mouse gene of *F2rl1, Mif*, *Lpl, Tnfa, Il6, Il1b and Gapdh* (Table S3-1 and S3-2) were measured by qPCR (154). PAR2, LPL, β-tubulin, GAPDH and phosphorylation and total levels of Akt in WAT or cells were evaluated by Western blot.

3.2.7 Histology

HE staining was performed to identify adipocyte hypertrophy in WAT as described previously (154).

3.2.8 Statistics

One-way ANOVA with Tukey's post-hoc tests or student t-test was used to determine differences between group mean values. The level of statistical significance was set at $P<0.05$.

3.2.9 Study Approval

The human study was approved by Newfoundland and Labrador HREB (Research portal File# 20200635) and all human experiments were conducted in accordance with the Declaration of Helsinki. All study-related procedures were carried out with written informed consent. All experiments involving mice were conducted in accordance with the Guide for the Care and Use of Laboratory Animals of the National Institutes of Health and were approved by the Internal Animal Committee Review Board of Memorial University of Newfoundland and University of Manitoba.

Table S3-1. List of human PCR primer sequences.

Gene Name	Sequences (5' – 3')
F2RL1	GGG TTT GCC AAG TAA CGG C CGG AAC CAG ATG ACA GAG AGG
LPL	AGA GCC AAA AGA AGC AG GGC AGA GTG AAT GGG AT
ACTB (b-actin)	CCT GTA CGC CAA CAC AGT GC ATA CTC CTG CTT GCT GAT CC

Table S3-2. List of mouse PCR primer sequences.

Gene Name	Sequences (5' – 3')
F2rl1	AAC ATC ACC ACC TGT CAC GA CAC GTA GGC AGA CGC AGT AA
Mif	CGG ACC GGG TCT ACA TAC A TCA AGC GAA GGT GGA ACC GTT
Lpl	AAT TTG CTT TCG ATG TCT GAG AA CAG AGT TTG ACC GCC TTC C
Tnfa	CAG GCG GTG CCT ATG TCT C CGA TCA CCC CGA AGT TCA GTA G
Il6	GAG GAT ACC ACT CCC AAC AGA CC AAG TGC ATC ATC GTT GTT CAT ACA
Il1b	TGG TGT GTG ACG TTC CCA TT CAG CAC GAG GCT TTT TTG TTG
Gapdh	ATG TGT CCG TCG TGG ATC TGA TGC CTG CTT CAC CAC CTT CTT

3.3 RESULTS

3.3.1 Human Obesity Increases Adipose Protease-activated Receptor 2 Expression, Which Is Associated with Downregulation of Lipoprotein Lipase Expression and Hypertriglyceridemia

We initially sought to establish the clinical relevance of PAR2 and LPL in WAT. Therefore, we sampled abdominal adipose tissue from lean (age: 23.08 ± 2.15; BMI<25kg/m^2) and obese (age: 24.6 ± 3.39; BMI>30kg/m^2) human subjects with metabolic dysfunction (Table S3-3). We found that obesity was associated with increased expression of the PAR2 gene, *F2RL1* (Figure 3-1A) and decreased expression of the *LPL* gene (Figure 3-1B). *F2RL1* expression was inversely correlated with *LPL* gene expression (Figure 3-1C), which was inversely correlated with plasma TG levels (Figure 3-1D). These data suggest that *F2RL1* expression during obesity may repress adipose LPL, resulting in hypertriglyceridemia.

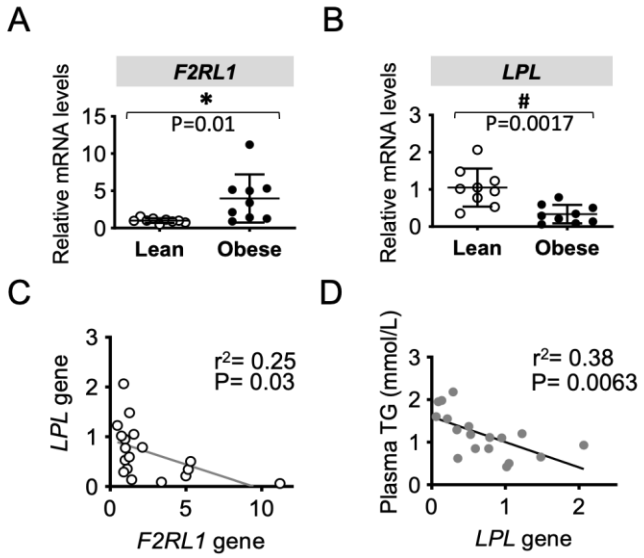

Figure 3-1. Human obesity increases adipose PAR2 expression which is associated with downregulation of LPL expression and hypertriglyceridemia. (**A** and **B**) *F2RL1* and *LPL* mRNA expression in biopsied WAT from male subjects including lean (age: 23.08 ± 2.15; BMI ≤ 25 kg/m^2) and obese individuals (age: 24.6 ± 3.39; BMI > 30 kg/m^2). (**C** and **D**) The correlation between *F2RL1* and *LPL* mRNA expression was shown in (**C**) while the correlation between *LPL* mRNA expression and plasma TG levels was shown in (**D**). N = 9 each group; all data are presented as mean ± SD. *P ≤ 0.05 increase vs. lean group in (**A**); $^{\#}$P ≤ 0.05 reduction vs. lean group in (**B**).

Table S3-3. General characteristics of human subjects.

	Lean	Obese	*P*-value
Age (years)	23.08±2.15	24.60±3.39	0.2717
BMI (kg/m^2)	21.50±1.62	33.01±3.54	<0.0001
Glucose (mmol/L)	5.10±0.43	5.69±0.78	0.0670
Insulin (pmol/L)	32.35±17.07	123.01±80.01	0.0050
TG (mmol/L)	0.87±0.29	1.63±0.38	0.0009
HDL (mmol/L)	1.47±0.31	1.10±0.35	0.0173
LDL (mmol/L)	2.40±0.69	3.10±0.85	0.1243

3.3.2 Elevated Protease-activated Receptor 2 Gene Expression Is Associated with Reduced Lipoprotein Lipase Expression in White Adipose Tissue and Hypertriglyceridemia Following High Palmitic Acid Diet Feeding

We fed male WT and *Par2*$^{-/-}$ mice (20 weeks) a PD for 8 weeks. PD significantly upregulated PAR2 gene (*F2rl1*) and protein expression (Figure 3-2A-B), with increased PAR2 downstream readout, ERK phosphorylation (Figure S3-1A) in WAT. However, PAR2 expression and activation were not associated with any changes in circulating levels of tissue factor (Figure S3-1B), suggesting the upregulation of PAR2 activation is probably not associated with tissue factor. Increased PAR2 expression correlated with decreased LPL expression and activity (Figure 3-2C-E). In the absence of PAR2, PD was unable to reduce LPL (Figure 3-2C-E). While PD significantly upregulated LPL expression in the heart, LPL was not affected by PAR2 deficiency (Figure 3-2F). In addition, LPL protein contents in the liver and skeletal muscle were unchanged following either PD feeding or PAR 2 knockout (Figure 3-2F). These data collectively suggest that PAR2 expression specifically downregulates LPL in WAT rather than in the heart, liver and skeletal muscle.

Suppression of adipose LPL following PAR2 expression was associated with hypertriglyceridemia and was reversed in *Par2*$^{-/-}$ mice (Figure 3-2G). Interestingly, this regulation of plasma TG occurred in the absence of changes in plasma FFA concentrations and liver and skeletal muscle lipid content (Figure 3-2H and Figure S3-2A-B). These results suggest that PAR2 expression in WAT may reduce plasma TG clearance by modulating LPL following HFD feeding in mice.

3.3.3 Protease-activated Receptor 2 Gene Expression Increases Adipose Macrophage Migration Inhibitory Factor Release and Circulating Macrophage Migration Inhibitory Factor Levels, Thereby Downregulating Lipoprotein Lipase Expression and Activation in White Adipose Tissue

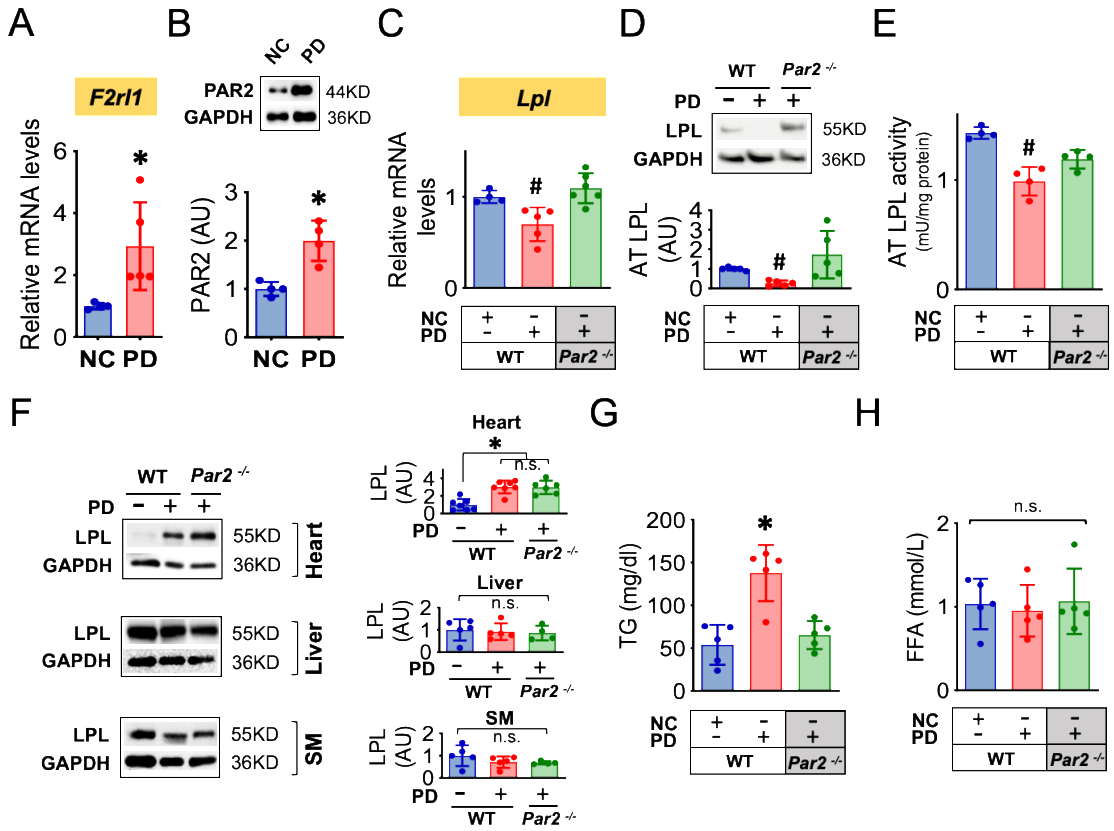

Figure 3-2. The elevation of PAR2 gene expression following high palmitic acid diet feeding is associated with a reduction of LPL expression in WAT and hypertriglyceridemia. WT and *Par2*$^{-/-}$ mice (20-week-old) were fed with a NC or PD for 8 weeks. (**A** and **B**) Measurement of *F2rl1* mRNA and PAR2 protein levels in WAT by qPCR and western blot. Quantification of adipose LPL mRNA, protein level and activity (AT LPL) in (**C** to **E**). (**F**) LPL protein levels in heart, liver and SM were evaluated by western blot. (**G** and **H**) Plasma TG and FFA levels of NC and PD mice. n=4-7 each animal group. All data are presented as mean ± SD. *P ≤ 0.05 increase vs. NC in (**A**, **B** and **F**) or vs. other groups in (**G**); #P ≤ 0.05 reduction vs. other groups in (**C**-**E**). n.s. represents no significance.

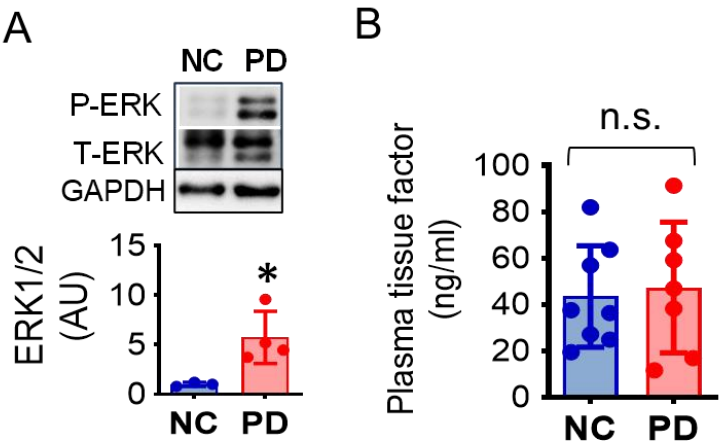

Figure S3-1 High palmitic acid diet upregulates ERK phosphorylation but not affect circulating levels of tissue factor. The WT and *Par2* $^{-/-}$ mice at 20 weeks were fed with NC or PD for 8 weeks and the phosphorylation of ERK in adipose tissue (**A**) was evaluated by western blot. The levels of tissue factor were quantified in plasma by ELISA kit (**B**). n=4-8 for each group. Mean ± SD in all the panels. 2-tailed Student's *t* test was performed for statistical analysis. The n.s. represents no significance.

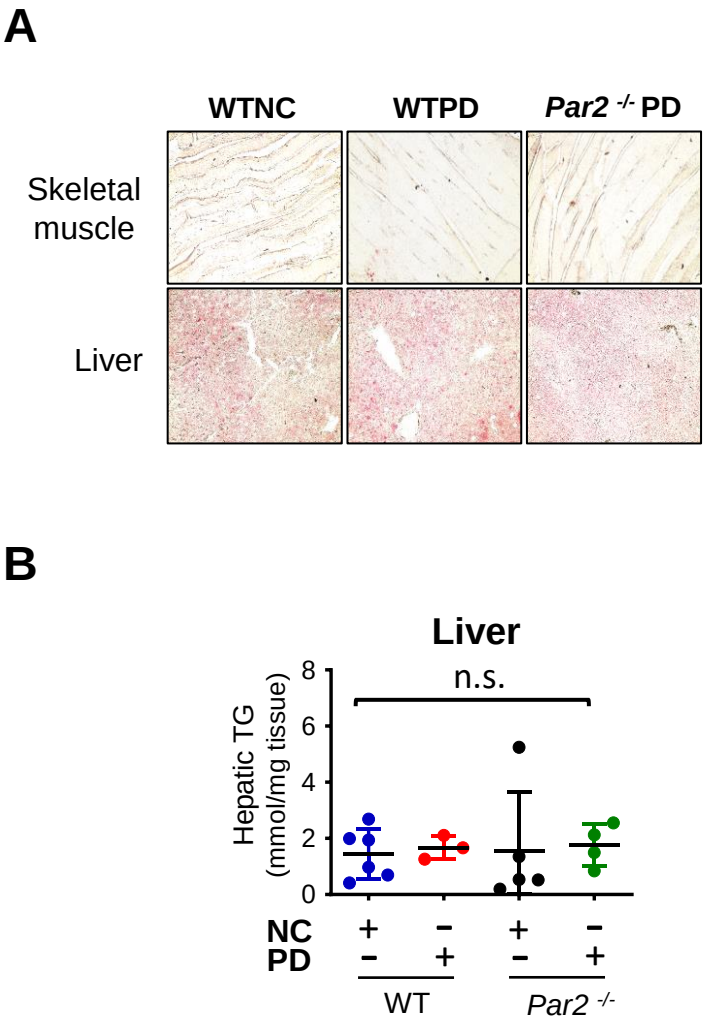

Figure S3-2. PD feeding for 8 weeks did not affect lipid storage in liver and skeletal muscle in WT and Par2 $^{-/-}$ mice. The WT and *Par2* $^{-/-}$ mice at 20 weeks were fed with NC or PD for 8 weeks and the lipid storage in skeletal muscle and liver was quantified by oil red O staining (**A**) or enzymatic methods (**B**). n=3-5 for each group. Mean ± SD in all the panels; One-way ANOVA was performed for statistical analysis in (**B**). The n.s. represents no significance.

We found that *F2rl1* expression in WAT is age dependent. WAT from older mice (20-25 weeks) showed higher levels of *F2rl1* gene expression compared to 4-week-old mice (Figure 3-3A). Our recent study showed that PAR2 expression upregulates the release of MIF in WAT (202). Accordingly, higher levels of PAR2 expression at 25 weeks were associated with increased plasma MIF levels (Figure 3-3B) and accompanied by decreased adipose MIF content but unchanged *Mif* gene expression (Figure S3-3A-C). High circulating MIF levels at 25 weeks were also associated with decreased LPL expression and activity compared with 4 weeks (Figure 3-3C-D). Plasma MIF levels were further increased in 20-week WT mice fed a PD (Figure 3-3E). In the absence of adipose PAR2, elevated plasma MIF levels were suppressed in aged mice or mice fed a PD (Figure 3-3B and E), accompanied by reversed LPL expression and activities (Figure 3-3C-D and Figure 3-2C-E). In PD fed WT mice, inhibition of LPL expression was abolished by neutralizing the MIF effect with anti-MIF antibody (Figure 3-3F). MIF neutralization did not affect *F2rl1* gene expression (Figure 3-3G). These results collectively suggest that MIF may mediate PAR2-downregulated LPL in WAT.

3.3.4 Macrophage Migration Inhibitory Factor Downregulates Lipoprotein Lipase Expression in White Adipose Tissue Through a CXC Chemokine Receptor/Akt Signaling Pathway

We next investigated the direct effect of MIF on LPL expression in adipocytes. Recombinant mouse MIF protein (400 ng/ml) was incubated with 3T3-L1 differentiated adipocytes for 24 hours. LPL gene and protein expression and its activity were significantly suppressed (Figure 3-4A-C). To further investigate the mechanism by which MIF downregulates LPL, we isolated adipocytes from WT and MIF receptor, CD74 knockout (*Cd74*$^{-/-}$) mice and subsequently treated with recombinant MIF for 24 hours. Interestingly, MIF-downregulated *Lpl* expression was not reversed by the deficiency of CD74 (Figure 3-4D). However, in 3T3-L1 adipocytes, the CXCR2 and 4 inhibitors, SB225002 and WZ811, respectively blocked MIF-induced

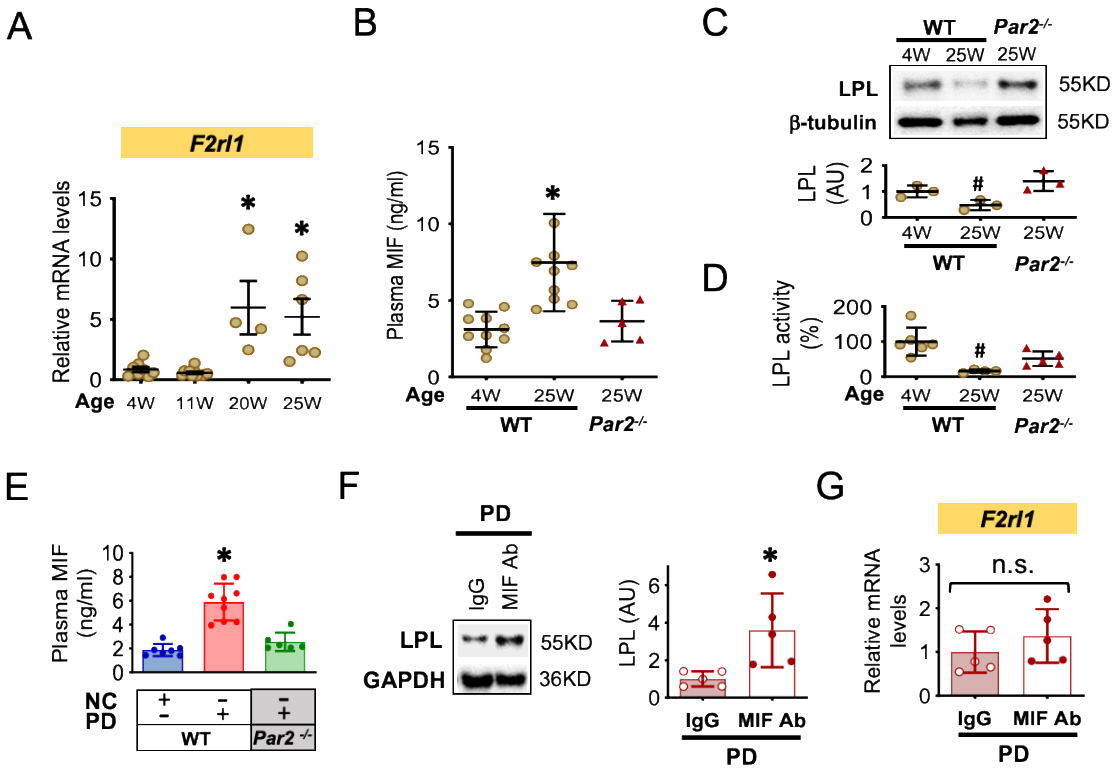

Figure 3-3. PAR2 gene expression increases circulating MIF levels which downregulate LPL expression and activation in WAT. (**A**-**D**) WAT were collected from C57BL/6 WT mice at 4-to-25-week age with NC feeding. *F2rl1* gene was measured by qPCR (**A**). Plasma MIF levels were evaluated in 4- and 25-week WT or *Par2*$^{-/-}$ mice by ELISA (**B**) and LPL protein expression and activity were measured in (**C** and **D**). (**E**-**G**) WT and *Par2*$^{-/-}$ mice at 20 weeks were fed with NC or PD feeding for 8 weeks. Plasma MIF levels were quantified subsequently in (**E**). LPL expression (**F**) and *F2rl1* gene (**G**) were quantified in WT mice with PD feeding following MIF neutralization with anti-MIF antibody (20 mg/kg, i.p. twice a week). n=3-9 each animal group. All data are presented as mean ± SD. *P ≤ 0.05 increase vs. 4 weeks in (**A**), vs. other groups in (**B** and **E**), or vs. IgG in (**F**); $^{\#}$P ≤ 0.05 reduction vs. other groups in (**C** and **D**). n.s. represents no significance.

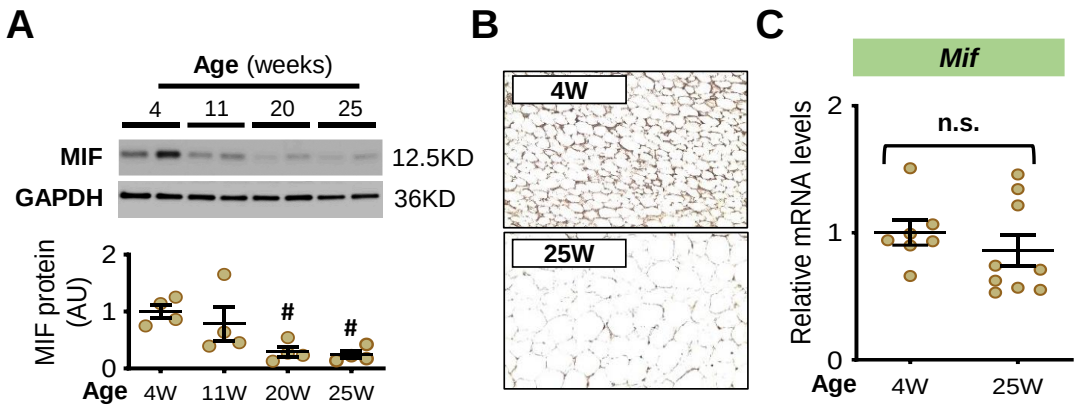

Figure S3-3. Alterations of MIF contents in WAT with age. The WT mice from 4 to 25 weeks were euthanized and the MIF gene and protein levels in WAT were quantified by Western blot (**A**), immunohistochemistry (**B**), or qPCR (**C**) (n=4-8 each group). Mean ± SD in all the panels; One-way ANOVA and 2-tailed Student's *t* test were performed for statistical analysis. #P<0.05 reduction vs. 4 weeks. The n.s. represents no significance.

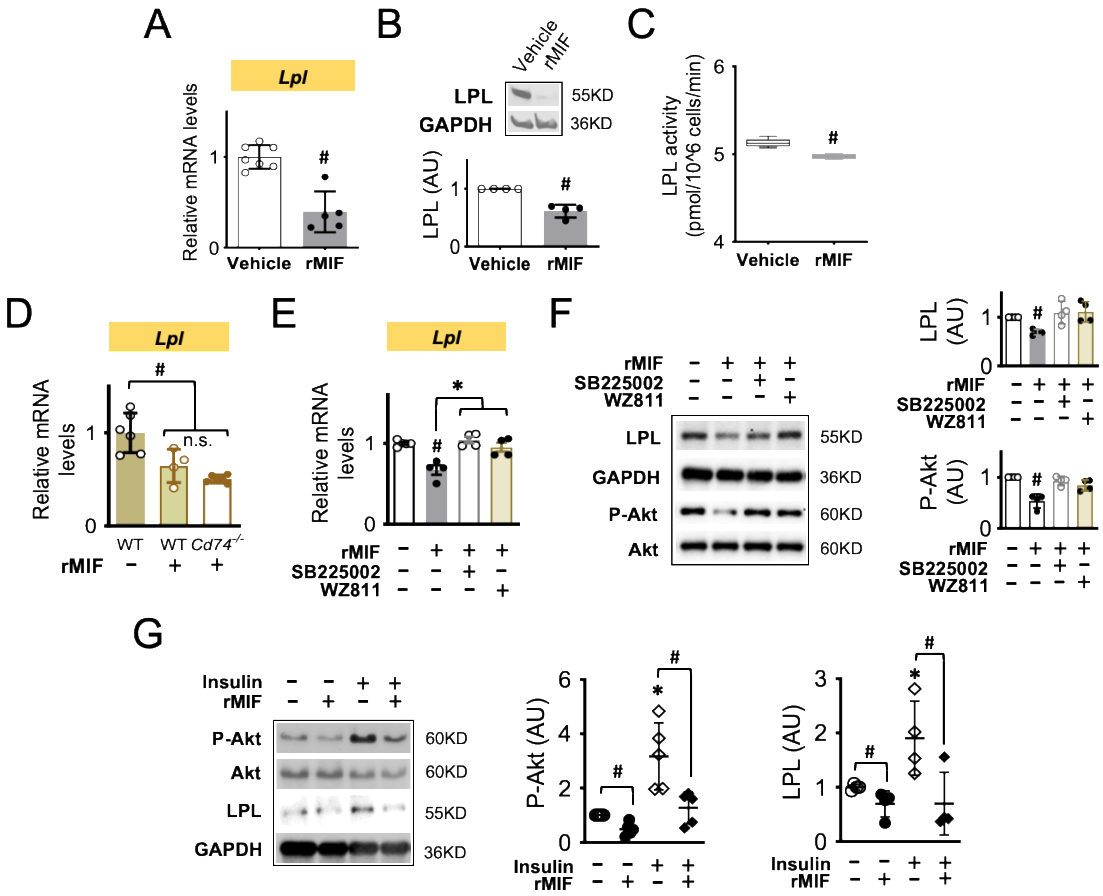

Figure 3-4 MIF inhibits LPL expression in adipocytes through a CXCR/Akt signaling pathway. (**A**-**C**) Recombinant mouse MIF protein (rMIF, 400 ng/ml) was incubated with differentiated 3T3-L1 adipocytes for 24 hours, and LPL expression and activity were measured. Mature adipocytes were initially isolated from WT and *Cd74*$^{-/-}$ mice and suspended cells were treated with vehicle or rMIF (400ng/ml) for 24 hours. *Lpl* gene was quantified by qPCR in (**D**). In 3T3-L1 adipocytes, rMIF was incubated with the CXCR2 or CXCR4 inhibitors, SB225002 (400nM) and WZ811 (5μM). The levels of *Lpl* gene and proteins (**E** and **F**) and Akt phosphorylation were subsequently evaluated. MIF regulated Akt phosphorylation and LPL protein expression in the presence of insulin were assessed by Western blot (**G**). All data are presented as mean ± SD. *P ≤ 0.05 increase vs. rMIF group in (**E**), vs. Other groups in (**G**); $^{\#}$P ≤ 0.05 reduction vs. Vehicle in (**A**-**D** and **G**), vs. other groups in (**F**), vs. insulin in (**G**). n.s. represents no significance.

downregulation of LPL expression (Figure 3-4E and F). Taken together, these data suggest that MIF regulates LPL expression through binding with its non-cognate CXCR2 and 4 receptors but not CD74 in adipocytes. Previous studies have shown that Akt upregulates LPL gene expression in human adipocytes as well as liver and mouse macrophages (210-212). Thus, we examined whether MIF regulates LPL expression through Akt. We found that MIF-induced downregulation of LPL expression was associated with a reduction in Akt phosphorylation that could be reversed by inhibition of CXCR2 and 4 (Figure 3-4F). Interestingly, LPL expression was significantly upregulated with activation of Akt following insulin treatment and was reversed by MIF (Figure 3-4G), suggesting that Akt may be an important mediator in modulating MIF-induced reduction of LPL expression in adipocytes.

3.3.5 Macrophage Migration Inhibitory Factor Overexpression Induces High Circulating Macrophage Migration Inhibitory Factor Levels, Thereby Suppressing Adipose Lipoprotein Lipase and Inducing Hypertriglyceridemia

To further examine whether MIF downregulates LPL in WAT *in vivo*, we used a transgenic mouse model that over-expresses MIF in the lung (*Mif* lung Tg mice) (208). Plasma MIF levels were increased 2-fold in *Mif* lung Tg mice compared to WT littermates (Figure 3-5A). High circulating plasma MIF concentrations were associated with inhibited Akt phosphorylation (Figure 3-5B) and reduced expression of *Lpl* gene and LPL protein in WAT (Figure 3-5C-D), but not in liver and skeletal muscle (Figure S3-4), suggesting that MIF specifically inhibits adipose LPL expression. Indeed, *Mif* lung Tg mice also had no detectable alterations in histological appearance and lipid storage of liver and skeletal muscle (Figure S3-5). The reduction in adipose LPL expression further was reflected by attenuated LPL activity (Figure 3-5E). Downregulation of LPL in WAT was associated with increased plasma TG levels (Figure 3-5F), although plasma FFA levels were unchanged (Figure 3-5G). These findings overall suggest that MIF inhibition of LPL in WAT contributes to the development of hypertriglyceridemia.

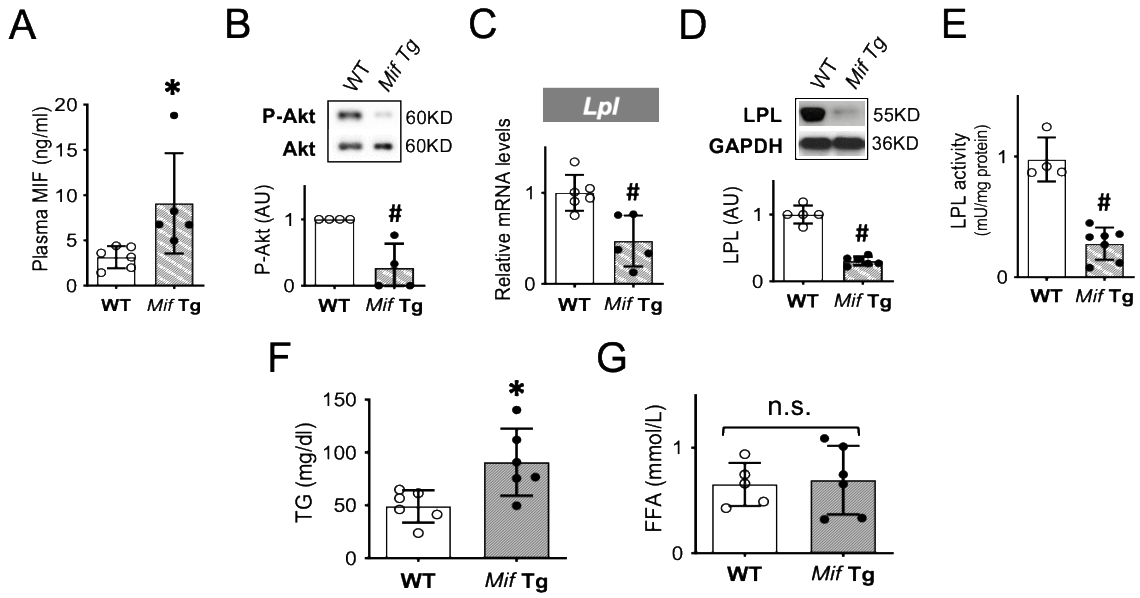

Figure 3-5. High circulating MIF levels in MIF transgenic overexpression model (*Mif* Tg) downregulate LPL in WAT which is associated with hyperlipidemia. (**A**) Plasma MIF levels were quantified by ELISA in WT and *Mif* lung Tg mice (25-week old). (**B**-**E**) Akt phosphorylation, *Lpl* mRNA and protein expression, and LPL activity were evaluated in their WAT. (**F** and **G**) Plasma TG and FFA levels in WT and *Mif* Tg mice. N=4-6 each animal group. All data are presented as mean ± SD. *P ≤ 0.05 increase vs. WT in (**A** and **F**); #P ≤ 0.05 reduction vs. WT in (**B**-**E**). n.s. represents no significance.

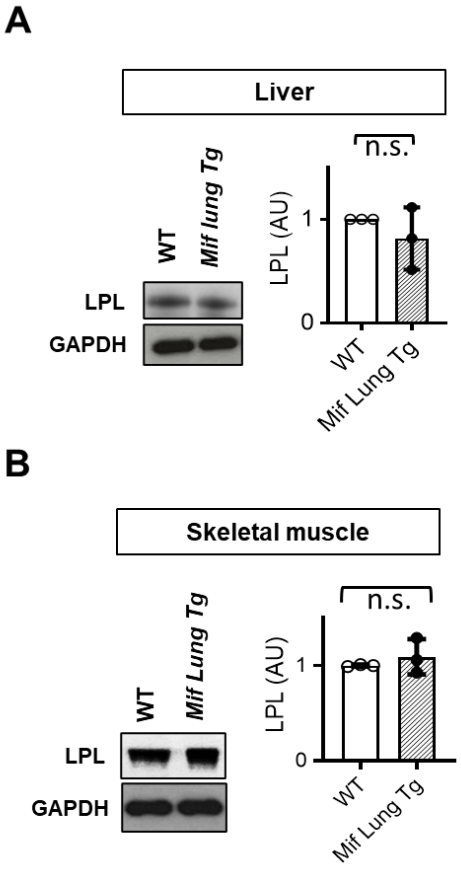

Figure S3-4. *Mif* lung Tg mice have unchanged LPL protein levels in liver and skeletal muscle. The WT (littermates) and *Mif* lung Tg mice at 25 weeks were euthanized and the LPL protein levels in liver (**A**) and skeletal muscle (**B**) were quantified by Western blot (n=3 each group). Mean ± SD in all the panels; 2-tailed Student's *t* test was performed for statistical analysis. The n.s. represents no significance.

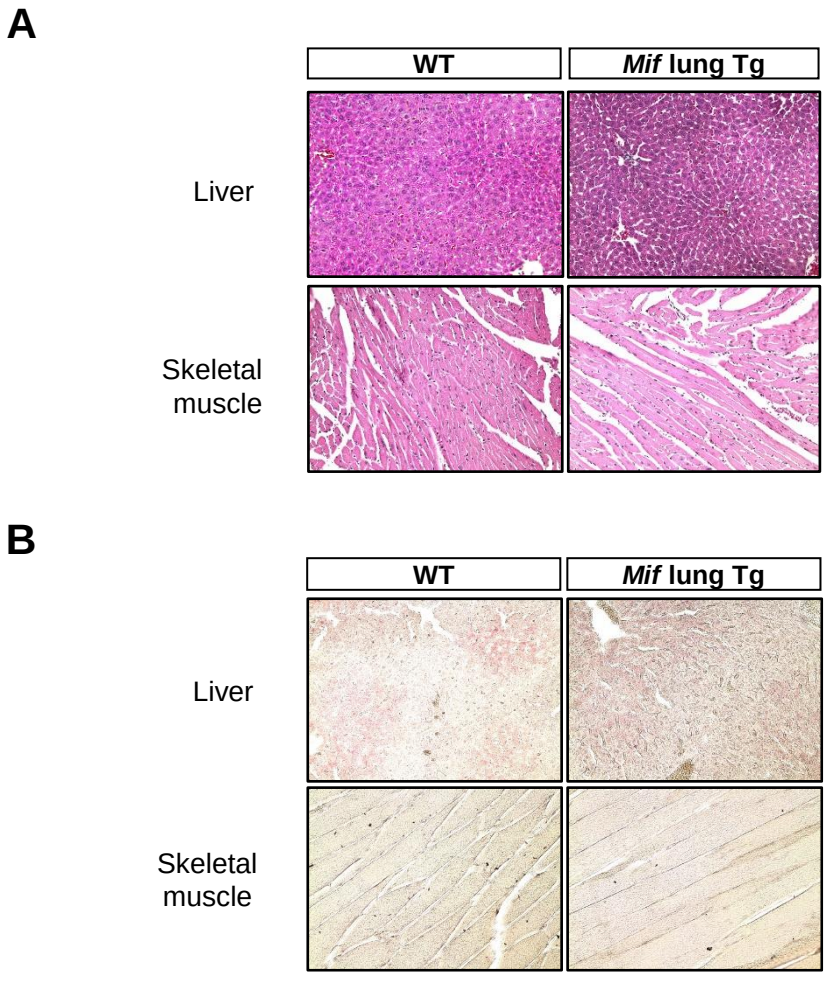

Figure S3-5. The histological characteristics of WT and *Mif* lung Tg mice. Skeletal muscle and liver were isolated from WT and *Mif* lung Tg mice at 25 weeks for HE (**A**) and oil red O staining (**B**).

3.3.6 Restoration of High Plasma Macrophage Migration Inhibitory Factor Levels Reverses High Lipoprotein Lipase in White Adipose Tissue of Protease-activated Receptor 2 Deficient Mice, Resulting in Hypertriglyceridemia

Par2 $^{-/-}$ mice were fed with a PD and received vehicle or recombinant MIF via osmotic pump during the final four-week feeding period (Figure 3-6A). MIF infusion reversed plasma MIF levels (Figure 3-6B). Akt phosphorylation (Figure 3-6C) and LPL expression and activity (Figure 3-6D-F) in WAT was decreased after MIF infusion in *Par2* $^{-/-}$ mice. Alterations in LPL were associated with attenuated plasma TG clearance (Figure 3-6G) and reduced lipid storage and adipocyte size in WAT (Figure 3-6I), although plasma FFA levels were unchanged (Figure 3-6H). Under these conditions, MIF infusion did not affect the expression of inflammatory factors, *TNFα*, *IL-6* and *IL-1β* in WAT (Figure S3-6). These data suggest that MIF plays a key role in the regulation of PAR2-mediated adipose LPL expression and the development of hypertriglyceridemia.

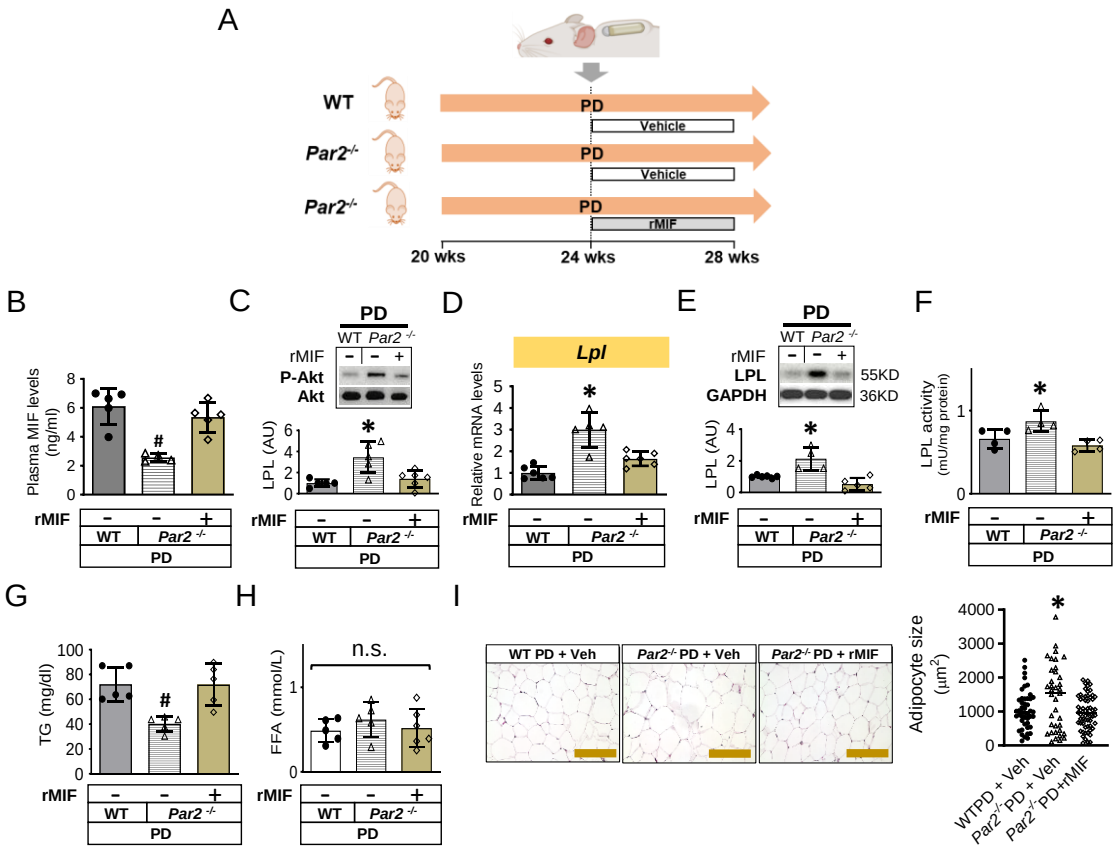

Figure 3-6. Restoring high plasma MIF levels reverses the high LPL in WAT in PAR2 deficient mice resulting in hypertriglyceridemia. (**A**-**H**) Vehicle or rMIF (24 μg/day/kg) was administered intravenously by an osmotic pump to WT or *Par2* $^{-/-}$ mice half-way through the PD regiment (at the last 4 weeks) (**A**). Plasma MIF levels were quantified by ELISA in (**B**). Adipose Akt phosphorylation (**C**), *Lpl* mRNA (**D**), protein (**E**), and activity (**F**), plasma TG (**G**), FFA (**H**), HE staining of adipose tissue and adipocyte size (**I**) were also evaluated. The yellow bars represent 100μM. n=4-6 each animal group. All data are presented as mean ± SD. *P ≤ 0.05 increase vs. other groups in (**C**-**F** and **I**); $^{\#}$P ≤ 0.05 reduction vs. other groups in (**B** and **G**). n.s. represents no significance.

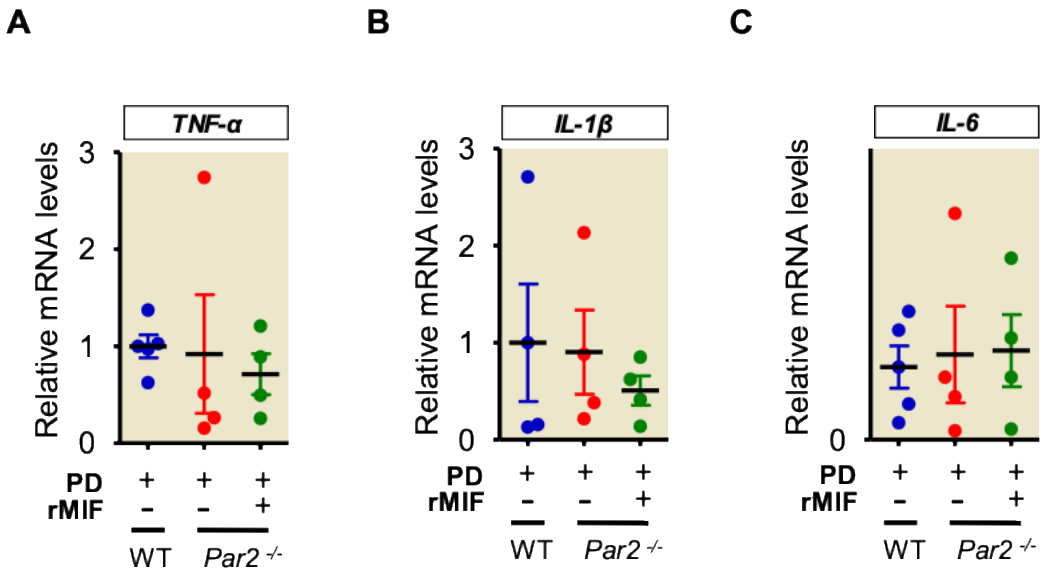

Figure S3-6. The gene expression of inflammatory factors in WAT from WT and Par2 $^{-/-}$ mice following PD feeding with or without MIF infusion. The WT and *Par2* $^{-/-}$ mice at 20 weeks were fed with NC or PD for 4 weeks. rMIF (24 g/day/kg) were given by osmotic pump with PD for 4 weeks. The gene expression of *TNF-α* (**A**), *IL-1β* (**B**) and *IL-6* (**C**) in WAT was quantified by qPCR. N=5 for each group.

3.4 DISCUSSION

Obesity is inversely correlated with LPL in WAT. However, the molecular mechanisms mediating LPL during obesity are largely unknown. Our current study identifies a novel regulatory mechanism of LPL in WAT which contributes to hypertriglyceridemia. We found that the expression of PAR2 was significantly increased in WAT isolated from human obese subjects and was inversely correlated with the *LPL* gene. Reduced LPL expression was also negatively correlated with elevated plasma TG levels, suggesting that adipose PAR2 may contribute to the development of hyperlipidemia through downregulation of LPL. In animal models, adipose PAR2 expression was associated with high plasma MIF, a cytokine that downregulates LPL expression and activity through binding with CXCR2/4 and inhibiting Akt phosphorylation in adipocytes. Thus, following HFD feeding, PAR2 deficiency attenuated the rise in plasma MIF levels, reversed LPL expression and activity in WAT, and thus corrected hypertriglyceridemia. These data together suggest that downregulation of adipose LPL by PAR2/MIF is an important mechanism for the development of hypertriglyceridemia.

Hypertriglyceridemia is an important biomarker of metabolic dysfunction in abdominal obesity (213). It also increases the risk of cardiovascular disease even in the presence of optimized LDL-C levels (214). Hypertriglyceridemia is associated with the activation of LPL, which hydrolyzes plasma TG to release FFA (215). Decreased LPL, for instance, leads to increased plasma TG concentrations in type 2 diabetic patients (202). LPL is produced by many tissues, including adipose tissue, skeletal muscle and heart. Overexpression of LPL in skeletal muscle protects against excess weight gain by increasing TG accumulation in skeletal muscle (216). LPL deficiency in the heart results in hypertriglyceridemia and cardiac dysfunction (217). Adipose tissue is a key organ for lipid storage, so adipose LPL acts as a gatekeeper for directing TG to adipose tissue. Indeed, adipose LPL is impaired in obesity (218), and underexpression of adipose

LPL reduces FA entry into adipose tissue (219). Our current study shows that manipulation of LPL in WAT but not in skeletal muscle, liver and heart is associated with hypertriglyceridemia.

LPL can be regulated at transcriptional, posttranscriptional, and posttranslational levels. The present study identifies a novel transcriptional regulation of LPL by PAR2, a member of the GPR family. PAR2 is expressed in various cell types, including endothelial cells (203) and adipocytes (202, 204). Our clinical data demonstrate that obesity upregulates PAR2 expression in WAT, which inversely correlates with *Lpl* gene expression, leading to hypertriglyceridemia. A HFD successfully mimics all genotypes and metabolic phenotypes in mouse models that can be abolished by PAR2 knockout. Although a previous study indicated that PAR2 accelerates adipocyte differentiation (220), our recent data did not observe any difference in the expression of adipogenesis marker, PPARγ between lean and obese subjects or WT and *Par2*$^{-/-}$ mice with HFD feeding (202). Thus, PAR2 may have a differentiation-independent effect on regulating LPL in adipose tissue. Furthermore, it should be noted that increased PAR2 expression may be related to cleavage and activation of PAR2 by proteases, such as plasmin. A recent study indeed demonstrated that ANGPTL 4/8 complex mediates plasmin generation, thereby upregulating LPL activity and postprandial TG hydrolysis (221). However, it is unclear whether plasmin is also involved in the regulation of *Lpl* gene expression by upregulating PAR2 activation and concomitantly increasing PAR2 expression.

MIF is an evolutionarily conserved cytokine generally recognized as an upstream regulator of the innate immune response (179). Other work has highlighted the role of MIF in promoting metabolic dysfunction (222). However, whether MIF regulates LPL and hypertriglyceridemia was previously unknown. Our present data indicate that MIF directly represses the transcription of LPL in adipocytes. High plasma MIF concentrations in the MIF overexpression model reduced adipose but not liver or skeletal muscle LPL expression. Interestingly, while the inflammatory state may affect pre-heparin LPL mass in rheumatoid arthritis (223), MIF-regulated LPL

transcription is independent of inflammation. Together, these data suggest a direct relationship between MIF and LPL expression in the absence of inflammation in WAT.

LPL transcription was upregulated by Akt in human adipocytes and in liver and mouse macrophages (210-212). MIF downregulates Akt phosphorylation in adipocytes in the presence or absence of insulin. Our data further demonstrate that MIF inhibits *Lpl* gene expression by downregulating Akt, and this effect was associated with the classical chemokine receptors CXCR2/4, which are both non-cognate receptors for MIF. Although CXCR2/4 and CD74 both have been identified as the MIF receptors in immune cells, CD74 is considered to be the primary receptor regulating MIF cell functions in non-immune cells, including cardiomyocytes, hepatocytes and renal cells (167, 168, 224). Our recent studies also have shown that MIF inhibits HSL and lipolysis by binding to CD74 in adipocytes (225). However, the inhibitory effect of MIF on Akt/LPL signaling in adipocytes depends on CXCR2/4 but not CD74. The downstream mechanism (s) by which MIF activates CXCR2/4 in adipocytes to inhibit LPL is currently unclear but is deserving of further investigation.

PAR2 activation induces *MIF* mRNA expression in human endothelial cells (207), suggesting a possible link between PAR2 activity and regulation of MIF expression. However, our recent study showed that the expression and activation of PAR2 promotes the release of MIF but not its expression in WAT in the absence of inflammation (202). Thus, PAR2 activation may repress LPL gene and activity in WAT by mediating adipose MIF release. Indeed, antibody neutralization of plasma MIF following HFD feeding demonstrated a reversal of LPL expression, while maintaining high levels of PAR2 expression, suggesting that a critical role for MIF in PAR2-mediated LPL expression in WAT.

PAR2 knockout mice with reduced plasma MIF levels are protected from hypertriglyceridemia, an effect associated with adipocyte hypertrophy, indicating increased FA uptake and storage. Plasma TG are absorbed by WAT, which reduces lipid accumulation and

potential toxicity in the liver and skeletal muscle (226). Although we did not observe differences in lipid storage in liver or skeletal muscle, MIF-mediated changes may be important later in the disease, such as the development of steatosis.

In conclusion, we have identified a novel role for PAR2 in regulating hypertriglyceridemia. Blocking FA induced PAR2 expression and/or reducing MIF secretion from WAT would be an important strategy to restore LPL expression in WAT. Optimization of LPL expression and activity in WAT will reduce plasma TG levels which can ultimately reduce the incidence of cardiovascular disease in conjunction with successful LDL-C reduction (214). Further work is needed to investigate the therapeutic applicability of these strategies in clinical settings for patients with obesity or type 2 diabetes.

3.4.1 Limitations of the Study

We found that PAR2 expression is associated with increased PAR2 activation in adipocytes and that FA induced upregulation of PAR2 transcription likely increases PAR2 activation by augmenting the amount of cell surface PAR2 (197). Interestingly, our data show that circulating levels of tissue factor are not accompanied with alterations in adipose PAR2, suggesting that tissue factor may not be the protease to cleave and activate PAR2 in mouse models. Given the evidence that obesity is often associated with high levels of circulating proteases, such as thrombin and tryptase (227, 228), targeting specific proteases that may contribute to PAR2 activation will be of interest for our future study.

3.5. CONTRIBUTIONS OF AUTHORS

Yiheng Huang performed the major experiments. Liujun Chen, Lisha Li, Sukhinder Cheema, Jinjie Xu and Yadan Qi participated in animal studies. Haibin Tong, Hong Wu, Lin Leng, Zhengyuan Xia, Brian Rodrigues and Richard Bucala contributed intellectually to data analysis and manuscript editing. John McGuire contributed to preparing the animal models. Guang Sun provided key supports in human studies. Lawrence Young and Richard Bucala provided overall scientific support for the research project, and Dake Qi designed and managed the research. All authors read and approved the final manuscript. Dake Qi is the guarantor of this work and, as such, had full access to all the data in the study and takes responsibility for the integrity of the data and the accuracy of the data analysis.

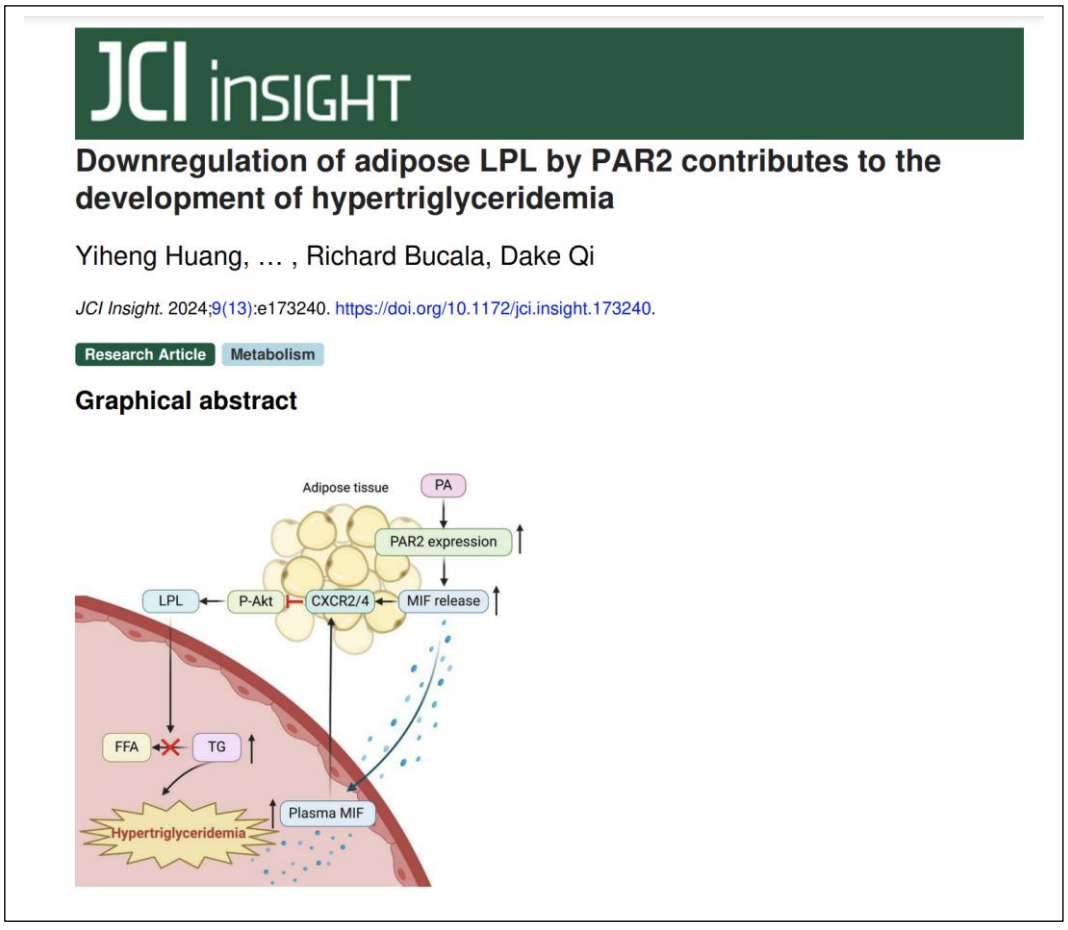

CHAPTER 4 DISCUSSION AND CONCLUSION

4.1 GENERAL DISCUSSION AND CONCLUSION

Metabolic syndrome contains a cluster of symptoms including abdominal obesity, hyperglycemia, hypertension and hyperlipidemia (229). The patients with metabolic syndrome have higher risks of type 2 diabetes, cardiovascular disease, hepatic steatosis and so on (230), which causes severe health and social issues in Canada and worldwide. IR and hyperlipidemia are the core symptoms of metabolic syndrome with limited clinical therapeutic approaches (1). Therefore, my PhD study investigated the molecular mechanisms of the regulation of IR and hypertriglyceridemia to nominate potential therapeutic targets for treating metabolic dysfunction.

WAT is a key organ system for maintaining whole-body metabolic homeostasis by regulating lipid storage and catabolism as well as releasing adipokines, such as leptin, adiponectin and cytokines. MIF is one of the cytokines released from WAT. Interestingly, MIF is the most sensitive biomarker of the onset of IR and can directly induce IR in adipocytes (154, 178). In accords with previous research regarding the pathogenesis of obesity, MIF expression in WAT is thought to arise from infiltrating macrophages (177, 184). However, non-immune cells such as adipocyte progenitors and adipocytes also release MIF under both physiologic and pathologic conditions (175, 185), indicating an independent role for non-inflammatory mechanisms of adipose MIF production. The pathways mediating non-inflammatory MIF release as well as their roles in mediating metabolic dysfunction remain unclear.

Therefore, my first study identified a novel autocrine/paracrine mechanism of non-inflammatory adipose MIF release mediated by secreted Pref-1, resulting in IR in human obese subjects and a PD fed mice (202). Pref-1 is a transmembrane protein highly expressed in non-adipocyte cells of WAT. Pref-1 is cleaved by TNFα-converting enzyme to generate a soluble form that acts as an autocrine/paracrine factor (231). Pref-1 was originally reported to regulate

metabolism by inhibiting *PPARγ* expression and adipogenesis (186). However, other investigators have reported that *pref-1* overexpression may improve glucose homeostasis during metabolic stress without changing adipogenesis (189). We found that non-inflammatory human obese subjects have a reduction in adipose *PREF-1* gene expression which is associated with high circulating IR inducible factor MIF, suggesting the association between adipose Pref-1 expression and MIF release (202).

In detail, we found a novel crosstalk mechanism between a group of pref-1 expressing cells (pref-1+ cells) and adipocytes that regulates MIF release in the absence of inflammation in WAT (202). Unlike adipocytes, adipose Pref-1+ cells include many non-adipocyte cell types, such as M2 macrophages, endothelial cells or progenitors that are also specifically express PAR2, a unique GPR. The molecular pathway underlying the crosstalk is initiated by PAR2, whose expression is induced by PD; PAR2 downregulates Pref-1 expression and release from Pref-1+ cells in an AMPK-dependent manner. Normally, Pref-1, derived from Pref-1+ cells, inhibits MIF release from both Pref-1+ cells and adipocytes by binding to integrin β1 and inhibiting the action of p115, a necessary cofactor for MIF secretion. However, in the context of non-inflammatory obesity, the ability of Pref-1 to inhibit MIF release from Pref-1+ cells and adipocytes is impaired; consequently, circulating plasma MIF levels are increased leading to IR. This finding is significant given MIF's non-inflammatory action to cause metabolic dysfunction and IR in early obesity, as evidenced in experimental results in mice as well as human subjects with functionally variant *MIF* alleles (154, 177, 196).

In addition to IR, hypertriglyceridemia is another core symptom of the metabolic syndrome which is also independently associated with an increased risk of atherosclerotic cardiovascular diseases (135, 136). LPL breaks down plasma TG to release FFA, thereby playing a key role in regulating plasma TG levels. Interestingly, LPL deficiency in adipose tissue increased plasma TG levels (7), suggesting the importance of adipose LPL in regulating plasma TG levels.

My second study showed that adipose derived MIF may also regulate hypertriglyceridemia through inhibiting LPL and facilitating lipid storage in WAT. WAT isolated from non-inflammatory human obese subjects exhibited increased expression of *PAR2*, which was inversely correlated with the *LPL* gene. Decreased LPL expression was also inversely correlated with elevated plasma TG levels, suggesting that adipose PAR2 may regulate hypertriglyceridemia by downregulating LPL. In mice, aging and PD increased PAR2 expression in WAT, which was associated with a high level of plasma MIF. MIF reduced LPL expression and activity in adipocytes. In a MIF overexpression model, high circulating MIF levels suppressed adipose LPL which was associated with increased plasma TG but not FFA. Following PD feeding, adipose LPL expression and activity were significantly reduced, and this reduction was reversed in $Par2^{-/-}$ mice. Recombinant MIF perfusion restored high plasma MIF levels in $Par2^{-/-}$ mice, which decreased LPL and attenuated adipocyte lipid storage leading to hypertriglyceridemia. Thus, high levels of PA increased activation of PAR2, facilitating adipose MIF secretion, and then resulted in LPL-induced hypertriglyceridemia.

In conclusion, these data together hint that adipose non-inflammatory MIF has direct effects in regulating IR and hypertriglyceridemia. Strategies to block PA-induced PAR2 expression and/or to augment Pref-1 expression or secretion may reduce adipose MIF secretion and improve metabolic dysfunction.

4.2 LIMITATIONS

In my first study, the alteration of MIF release occurred in both pref-1+ cells and adipocytes in WAT, while the adipose derived MIF is the focus in the second study. Because of the limitation of transgenic mice technology, it is currently impossible to generate Pref-1+ cells specific MIF knockout mice or adipose tissue specific MIF knockout mice. Therefore, it is technically difficult to prove the metabolic effects of adipose derived MIF by using transgenic mice model. In the first study, we used anti-MIF antibody treatment to demonstrate that circulating MIF played a crucial

role in the development of IR (Figure 2-1T). In the second study, anti-MIF antibody treatment reversed PD-induced LPL reduction (Figure 3-3F), suggesting that circulating MIF is an important mediator of adipose LPL expression and hypertriglyceridemia. Both experiments suggest the significant roles of circulating MIF in regulating metabolic dysfunction.

4.3 FUTURE WORK

Further work is warranted to investigate therapeutic applicability of these strategies in the clinical settings of metabolic syndrome. PA facilitates PAR2 activation in multiple cell types, including Pref-1+ cells and macrophages (197, 202). Thus, future work may investigate the binding between PA and PAR2 or the mechanism of palmitic acid induced PAR2 activation. Although MIF directly induces IR only in WAT rather than skeletal muscle and liver (232), the function of brain MIF in mediating metabolic homeostasis deserves further investigation. Moreover, anti-MIF antibody can reduce bodyweight gain and IR levels in PD feeding mice. The neutralization of circulating MIF may be an effective therapeutic strategy in treating obesity and metabolic syndrome in the future.

BIBLIOGRAPHY

1. Monzillo LU, Hamdy O, Horton ES, Ledbury S, Mullooly C, Jarema C, et al. Effect of lifestyle modification on adipokine levels in obese subjects with insulin resistance. *Obes Res.* 2003;11(9):1048-54.
2. Samaras K, Botelho NK, Chisholm DJ, and Lord RV. Subcutaneous and visceral adipose tissue gene expression of serum adipokines that predict type 2 diabetes. *Obesity (Silver Spring).* 2010;18(5):884-9.
3. Shimobayashi M, Albert V, Woelnerhanssen B, Frei IC, Weissenberger D, Meyer-Gerspach AC, et al. Insulin resistance causes inflammation in adipose tissue. *J Clin Invest.* 2018;128(4):1538-50.
4. Gao ZG, and Ye JP. Why do anti-inflammatory therapies fail to improve insulin sensitivity? *Acta Pharmacol Sin.* 2012;33(2):182-8.
5. Goldfine AB, and Shoelson SE. Therapeutic approaches targeting inflammation for diabetes and associated cardiovascular risk. *J Clin Invest.* 2017;127(1):83-93.
6. Mead JR, Irvine SA, and Ramji DP. Lipoprotein lipase: structure, function, regulation, and role in disease. *J Mol Med (Berl).* 2002;80(12):753-69.
7. Garcia-Arcos I, Hiyama Y, Drosatos K, Bharadwaj KG, Hu Y, Son NH, et al. Adipose-specific lipoprotein lipase deficiency more profoundly affects brown than white fat biology. *J Biol Chem.* 2013;288(20):14046-58.
8. Richard AJ, White U, Elks CM, and Stephens JM. In: Feingold KR, Anawalt B, Boyce A, Chrousos G, de Herder WW, Dhatariya K, et al. eds. *Endotext*. South Dartmouth (MA); 2000.
9. Raje V, Ahern KW, Martinez BA, Howell NL, Oenarto V, Granade ME, et al. Adipocyte lipolysis drives acute stress-induced insulin resistance. *Sci Rep.* 2020;10(1):18166.
10. Girousse A, Tavernier G, Valle C, Moro C, Mejhert N, Dinel AL, et al. Partial inhibition of adipose tissue lipolysis improves glucose metabolism and insulin sensitivity without alteration of fat mass. *PLoS Biol.* 2013;11(2):e1001485.
11. Hoy AJ, Bruce CR, Turpin SM, Morris AJ, Febbraio MA, and Watt MJ. Adipose triglyceride lipase-null mice are resistant to high-fat diet-induced insulin resistance despite reduced energy expenditure and ectopic lipid accumulation. *Endocrinology.* 2011;152(1):48-58.
12. Kienesberger PC, Lee D, Pulinilkunnil T, Brenner DS, Cai L, Magnes C, et al. Adipose triglyceride lipase deficiency causes tissue-specific changes in insulin signaling. *J Biol Chem.* 2009;284(44):30218-29.
13. Claus TH, Lowe DB, Liang Y, Salhanick AI, Lubeski CK, Yang L, et al. Specific inhibition of hormone-sensitive lipase improves lipid profile while reducing plasma glucose. *J Pharmacol Exp Ther.* 2005;315(3):1396-402.
14. Makowski L, Boord JB, Maeda K, Babaev VR, Uysal KT, Morgan MA, et al. Lack of macrophage fatty-acid-binding protein aP2 protects mice deficient in apolipoprotein E against atherosclerosis. *Nat Med.* 2001;7(6):699-705.
15. Sun L, Nicholson AC, Hajjar DP, Gotto AM, Jr., and Han J. Adipogenic differentiating agents regulate expression of fatty acid binding protein and CD36 in the J744 macrophage cell line. *J Lipid Res.* 2003;44(10):1877-86.
16. Hotamisligil GS, Johnson RS, Distel RJ, Ellis R, Papaioannou VE, and Spiegelman BM. Uncoupling of obesity from insulin resistance through a targeted mutation in aP2, the adipocyte fatty acid binding protein. *Science.* 1996;274(5291):1377-9.
17. Frangioudakis G, and Cooney GJ. Acute elevation of circulating fatty acids impairs downstream insulin signalling in rat skeletal muscle in vivo independent of effects on stress signalling. *J Endocrinol.* 2008;197(2):277-85.

18. Jiao P, Ma J, Feng B, Zhang H, Diehl JA, Chin YE, et al. FFA-induced adipocyte inflammation and insulin resistance: involvement of ER stress and IKKbeta pathways. *Obesity (Silver Spring).* 2011;19(3):483-91.
19. Kersten S. Mechanisms of nutritional and hormonal regulation of lipogenesis. *EMBO Rep.* 2001;2(4):282-6.
20. Coburn CT, Knapp FF, Jr., Febbraio M, Beets AL, Silverstein RL, and Abumrad NA. Defective uptake and utilization of long chain fatty acids in muscle and adipose tissues of CD36 knockout mice. *J Biol Chem.* 2000;275(42):32523-9.
21. Chirala SS, and Wakil SJ. Structure and function of animal fatty acid synthase. *Lipids.* 2004;39(11):1045-53.
22. Tong L. Acetyl-coenzyme A carboxylase: crucial metabolic enzyme and attractive target for drug discovery. *Cell Mol Life Sci.* 2005;62(16):1784-803.
23. Song Z, Xiaoli AM, and Yang F. Regulation and Metabolic Significance of De Novo Lipogenesis in Adipose Tissues. *Nutrients.* 2018;10(10).
24. Panarotto D, Remillard P, Bouffard L, and Maheux P. Insulin resistance affects the regulation of lipoprotein lipase in the postprandial period and in an adipose tissue-specific manner. *Eur J Clin Invest.* 2002;32(2):84-92.
25. Walton RG, Zhu B, Unal R, Spencer M, Sunkara M, Morris AJ, et al. Increasing adipocyte lipoprotein lipase improves glucose metabolism in high fat diet-induced obesity. *J Biol Chem.* 2015;290(18):11547-56.
26. Bonen A, Tandon NN, Glatz JF, Luiken JJ, and Heigenhauser GJ. The fatty acid transporter FAT/CD36 is upregulated in subcutaneous and visceral adipose tissues in human obesity and type 2 diabetes. *Int J Obes (Lond).* 2006;30(6):877-83.
27. Kuwasako T, Hirano K, Sakai N, Ishigami M, Hiraoka H, Yakub MJ, et al. Lipoprotein abnormalities in human genetic CD36 deficiency associated with insulin resistance and abnormal fatty acid metabolism. *Diabetes Care.* 2003;26(5):1647-8.
28. Love-Gregory L, Sherva R, Sun L, Wasson J, Schappe T, Doria A, et al. Variants in the CD36 gene associate with the metabolic syndrome and high-density lipoprotein cholesterol. *Hum Mol Genet.* 2008;17(11):1695-704.
29. Love-Gregory L, Sherva R, Schappe T, Qi JS, McCrea J, Klein S, et al. Common CD36 SNPs reduce protein expression and may contribute to a protective atherogenic profile. *Hum Mol Genet.* 2011;20(1):193-201.
30. Corpeleijn E, van der Kallen CJ, Kruijshoop M, Magagnin MG, de Bruin TW, Feskens EJ, et al. Direct association of a promoter polymorphism in the CD36/FAT fatty acid transporter gene with Type 2 diabetes mellitus and insulin resistance. *Diabet Med.* 2006;23(8):907-11.
31. Pietka TA, Schappe T, Conte C, Fabbrini E, Patterson BW, Klein S, et al. Adipose and muscle tissue profile of CD36 transcripts in obese subjects highlights the role of CD36 in fatty acid homeostasis and insulin resistance. *Diabetes Care.* 2014;37(7):1990-7.
32. Yang J, Park KW, and Cho S. Inhibition of the CD36 receptor reduces visceral fat accumulation and improves insulin resistance in obese mice carrying the BDNF-Val66Met variant. *J Biol Chem.* 2018;293(34):13338-48.
33. Ranganathan G, Unal R, Pokrovskaya I, Yao-Borengasser A, Phanavanh B, Lecka-Czernik B, et al. The lipogenic enzymes DGAT1, FAS, and LPL in adipose tissue: effects of obesity, insulin resistance, and TZD treatment. *J Lipid Res.* 2006;47(11):2444-50.
34. Hou XG, Moser S, Sarr MG, Thompson GB, Que FG, and Jensen MD. Visceral and subcutaneous adipose tissue diacylglycerol acyltransferase activity in humans. *Obesity (Silver Spring).* 2009;17(6):1129-34.
35. Chitraju C, Walther TC, and Farese RV, Jr. The triglyceride synthesis enzymes DGAT1 and DGAT2 have distinct and overlapping functions in adipocytes. *J Lipid Res.* 2019;60(6):1112-20.

36. Chitraju C, Mejhert N, Haas JT, Diaz-Ramirez LG, Grueter CA, Imbriglio JE, et al. Triglyceride Synthesis by DGAT1 Protects Adipocytes from Lipid-Induced ER Stress during Lipolysis. *Cell Metab.* 2017;26(2):407-18 e3.
37. Roberts R, Hodson L, Dennis AL, Neville MJ, Humphreys SM, Harnden KE, et al. Markers of de novo lipogenesis in adipose tissue: associations with small adipocytes and insulin sensitivity in humans. *Diabetologia.* 2009;52(5):882-90.
38. Mayas MD, Ortega FJ, Macias-Gonzalez M, Bernal R, Gomez-Huelgas R, Fernandez-Real JM, et al. Inverse relation between FASN expression in human adipose tissue and the insulin resistance level. *Nutr Metab (Lond).* 2010;7:3.
39. Sievert H, Krause C, Geissler C, Grohs M, El-Gammal AT, Wolter S, et al. Epigenetic Downregulation of FASN in Visceral Adipose Tissue of Insulin Resistant Subjects. *Exp Clin Endocrinol Diabetes.* 2021;129(9):674-82.
40. Berndt J, Kovacs P, Ruschke K, Kloting N, Fasshauer M, Schon MR, et al. Fatty acid synthase gene expression in human adipose tissue: association with obesity and type 2 diabetes. *Diabetologia.* 2007;50(7):1472-80.
41. Guilherme A, Pedersen DJ, Henchey E, Henriques FS, Danai LV, Shen Y, et al. Adipocyte lipid synthesis coupled to neuronal control of thermogenic programming. *Mol Metab.* 2017;6(8):781-96.
42. Lodhi IJ, Yin L, Jensen-Urstad AP, Funai K, Coleman T, Baird JH, et al. Inhibiting adipose tissue lipogenesis reprograms thermogenesis and PPARgamma activation to decrease diet-induced obesity. *Cell Metab.* 2012;16(2):189-201.
43. Paz-Filho G, Mastronardi C, Wong ML, and Licinio J. Leptin therapy, insulin sensitivity, and glucose homeostasis. *Indian J Endocrinol Metab.* 2012;16(Suppl 3):S549-55.
44. Shimomura I, Hammer RE, Ikemoto S, Brown MS, and Goldstein JL. Leptin reverses insulin resistance and diabetes mellitus in mice with congenital lipodystrophy. *Nature.* 1999;401(6748):73-6.
45. Kahn CR, Wang G, and Lee KY. Altered adipose tissue and adipocyte function in the pathogenesis of metabolic syndrome. *J Clin Invest.* 2019;129(10):3990-4000.
46. Trujillo ME, and Scherer PE. Adipose tissue-derived factors: impact on health and disease. *Endocrine reviews.* 2006;27(7):762-78.
47. Yang RZ, Lee MJ, Hu H, Pray J, Wu HB, Hansen BC, et al. Identification of omentin as a novel depot-specific adipokine in human adipose tissue: possible role in modulating insulin action. *Am J Physiol Endocrinol Metab.* 2006;290(6):E1253-61.
48. Arita Y, Kihara S, Ouchi N, Takahashi M, Maeda K, Miyagawa J, et al. Paradoxical decrease of an adipose-specific protein, adiponectin, in obesity. *Biochem Biophys Res Commun.* 1999;257(1):79-83.
49. de Souza Batista CM, Yang RZ, Lee MJ, Glynn NM, Yu DZ, Pray J, et al. Omentin plasma levels and gene expression are decreased in obesity. *Diabetes.* 2007;56(6):1655-61.
50. Shih YL, Huang TC, Shih CC, and Chen JY. Relationship between Leptin and Insulin Resistance among Community-Dwelling Middle-Aged and Elderly Populations in Taiwan. *J Clin Med.* 2022;11(18).
51. Nieva-Vazquez A, Perez-Fuentes R, Torres-Rasgado E, Lopez-Lopez JG, and Romero JR. Serum resistin levels are associated with adiposity and insulin sensitivity in obese Hispanic subjects. *Metab Syndr Relat Disord.* 2014;12(2):143-8.
52. Buechler C, Feder S, Haberl EM, and Aslanidis C. Chemerin Isoforms and Activity in Obesity. *Int J Mol Sci.* 2019;20(5).
53. Bozaoglu K, Curran JE, Stocker CJ, Zaibi MS, Segal D, Konstantopoulos N, et al. Chemerin, a novel adipokine in the regulation of angiogenesis. *J Clin Endocrinol Metab.* 2010;95(5):2476-85.

54. Fatima SS, Rehman R, Baig M, and Khan TA. New roles of the multidimensional adipokine: chemerin. *Peptides.* 2014;62:15-20.
55. Qatanani M, Szwergold NR, Greaves DR, Ahima RS, and Lazar MA. Macrophage-derived human resistin exacerbates adipose tissue inflammation and insulin resistance in mice. *J Clin Invest.* 2009;119(3):531-9.
56. Banerjee RR, Rangwala SM, Shapiro JS, Rich AS, Rhoades B, Qi Y, et al. Regulation of fasted blood glucose by resistin. *Science.* 2004;303(5661):1195-8.
57. Okuno M, Caraveo VE, Goodman DS, and Blaner WS. Regulation of adipocyte gene expression by retinoic acid and hormones: effects on the gene encoding cellular retinol-binding protein. *J Lipid Res.* 1995;36(1):137-47.
58. Moraes-Vieira PM, Yore MM, Dwyer PM, Syed I, Aryal P, and Kahn BB. RBP4 activates antigen-presenting cells, leading to adipose tissue inflammation and systemic insulin resistance. *Cell Metab.* 2014;19(3):512-26.
59. Janke J, Engeli S, Boschmann M, Adams F, Bohnke J, Luft FC, et al. Retinol-binding protein 4 in human obesity. *Diabetes.* 2006;55(10):2805-10.
60. Park HS, Park JY, and Yu R. Relationship of obesity and visceral adiposity with serum concentrations of CRP, TNF-alpha and IL-6. *Diabetes Res Clin Pract.* 2005;69(1):29-35.
61. Febbraio MA. Role of interleukins in obesity: implications for metabolic disease. *Trends Endocrinol Metab.* 2014;25(6):312-9.
62. Syed I, Lee J, Moraes-Vieira PM, Donaldson CJ, Sontheimer A, Aryal P, et al. Palmitic Acid Hydroxystearic Acids Activate GPR40, Which Is Involved in Their Beneficial Effects on Glucose Homeostasis. *Cell Metab.* 2018;27(2):419-27 e4.
63. Yore MM, Syed I, Moraes-Vieira PM, Zhang T, Herman MA, Homan EA, et al. Discovery of a class of endogenous mammalian lipids with anti-diabetic and anti-inflammatory effects. *Cell.* 2014;159(2):318-32.
64. Lynes MD, Leiria LO, Lundh M, Bartelt A, Shamsi F, Huang TL, et al. The cold-induced lipokine 12,13-diHOME promotes fatty acid transport into brown adipose tissue. *Nat Med.* 2017;23(5):631-7.
65. Stanford KI, Lynes MD, Takahashi H, Baer LA, Arts PJ, May FJ, et al. 12,13-diHOME: An Exercise-Induced Lipokine that Increases Skeletal Muscle Fatty Acid Uptake. *Cell Metab.* 2018;27(6):1357.
66. Wu H, and Ballantyne CM. Metabolic Inflammation and Insulin Resistance in Obesity. *Circ Res.* 2020;126(11):1549-64.
67. Hotamisligil GS. Inflammation and metabolic disorders. *Nature.* 2006;444(7121):860-7.
68. Hotamisligil GS. Inflammation, metaflammation and immunometabolic disorders. *Nature.* 2017;542(7640):177-85.
69. Xue W, Fan Z, Li L, Lu J, Zhai Y, and Zhao J. The chemokine system and its role in obesity. *J Cell Physiol.* 2019;234(4):3336-46.
70. Wu H, Ghosh S, Perrard XD, Feng L, Garcia GE, Perrard JL, et al. T-cell accumulation and regulated on activation, normal T cell expressed and secreted upregulation in adipose tissue in obesity. *Circulation.* 2007;115(8):1029-38.
71. Weisberg SP, Hunter D, Huber R, Lemieux J, Slaymaker S, Vaddi K, et al. CCR2 modulates inflammatory and metabolic effects of high-fat feeding. *The Journal of clinical investigation.* 2006;116(1):115-24.
72. Talukdar S, Oh DY, Bandyopadhyay G, Li D, Xu J, McNelis J, et al. Neutrophils mediate insulin resistance in mice fed a high-fat diet through secreted elastase. *Nat Med.* 2012;18(9):1407-12.
73. Kintscher U, Hartge M, Hess K, Foryst-Ludwig A, Clemenz M, Wabitsch M, et al. T-lymphocyte infiltration in visceral adipose tissue: a primary event in adipose tissue inflammation and the development of obesity-mediated insulin resistance. *Arterioscler Thromb Vasc Biol.* 2008;28(7):1304-10.

74. Khan IM, Perrard XY, Brunner G, Lui H, Sparks LM, Smith SR, et al. Intermuscular and perimuscular fat expansion in obesity correlates with skeletal muscle T cell and macrophage infiltration and insulin resistance. *Int J Obes (Lond).* 2015;39(11):1607-18.
75. Fujisaka S. The role of adipose tissue M1/M2 macrophages in type 2 diabetes mellitus. *Diabetol Int.* 2021;12(1):74-9.
76. Wernstedt Asterholm I, Tao C, Morley TS, Wang QA, Delgado-Lopez F, Wang ZV, et al. Adipocyte inflammation is essential for healthy adipose tissue expansion and remodeling. *Cell Metab.* 2014;20(1):103-18.
77. Xu F, Burk D, Gao Z, Yin J, Zhang X, Weng J, et al. Angiogenic deficiency and adipose tissue dysfunction are associated with macrophage malfunction in SIRT1-/- mice. *Endocrinology.* 2012;153(4):1706-16.
78. Cinti S, Mitchell G, Barbatelli G, Murano I, Ceresi E, Faloia E, et al. Adipocyte death defines macrophage localization and function in adipose tissue of obese mice and humans. *J Lipid Res.* 2005;46(11):2347-55.
79. Nguyen KD, Qiu Y, Cui X, Goh YP, Mwangi J, David T, et al. Alternatively activated macrophages produce catecholamines to sustain adaptive thermogenesis. *Nature.* 2011;480(7375):104-8.
80. Cho CH, Koh YJ, Han J, Sung HK, Jong Lee H, Morisada T, et al. Angiogenic role of LYVE-1-positive macrophages in adipose tissue. *Circ Res.* 2007;100(4):e47-57.
81. Strissel KJ, Stancheva Z, Miyoshi H, Perfield JW, 2nd, DeFuria J, Jick Z, et al. Adipocyte death, adipose tissue remodeling, and obesity complications. *Diabetes.* 2007;56(12):2910-8.
82. Kosteli A, Sugaru E, Haemmerle G, Martin JF, Lei J, Zechner R, et al. Weight loss and lipolysis promote a dynamic immune response in murine adipose tissue. *J Clin Invest.* 2010;120(10):3466-79.
83. Qiu Y, Nguyen KD, Odegaard JI, Cui X, Tian X, Locksley RM, et al. Eosinophils and type 2 cytokine signaling in macrophages orchestrate development of functional beige fat. *Cell.* 2014;157(6):1292-308.
84. Hotamisligil GS. Mechanisms of TNF-alpha-induced insulin resistance. *Exp Clin Endocrinol Diabetes.* 1999;107(2):119-25.
85. Memon RA, Feingold KR, Moser AH, Fuller J, and Grunfeld C. Regulation of fatty acid transport protein and fatty acid translocase mRNA levels by endotoxin and cytokines. *Am J Physiol.* 1998;274(2):E210-7.
86. Tian XY, Ganeshan K, Hong C, Nguyen KD, Qiu Y, Kim J, et al. Thermoneutral Housing Accelerates Metabolic Inflammation to Potentiate Atherosclerosis but Not Insulin Resistance. *Cell Metab.* 2016;23(1):165-78.
87. Turner N, Kowalski GM, Leslie SJ, Risis S, Yang C, Lee-Young RS, et al. Distinct patterns of tissue-specific lipid accumulation during the induction of insulin resistance in mice by high-fat feeding. *Diabetologia.* 2013;56(7):1638-48.
88. Lowry JE, Tumurbaatar B, D'Agostino C, Main E, Wright TJ, Dillon EL, et al. Effect of high-fat diet on peripheral blood mononuclear cells and adipose tissue in early stages of diet-induced weight gain. *Br J Nutr.* 2019;122(12):1359-67.
89. Espinosa De Ycaza AE, Sondergaard E, Morgan-Bathke M, Lytle K, Delivanis DA, Ramos P, et al. Adipose Tissue Inflammation Is Not Related to Adipose Insulin Resistance in Humans. *Diabetes.* 2022;71(3):381-93.
90. Lee YS, Li P, Huh JY, Hwang IJ, Lu M, Kim JI, et al. Inflammation is necessary for long-term but not short-term high-fat diet-induced insulin resistance. *Diabetes.* 2011;60(10):2474-83.
91. Ventre J, Doebber T, Wu M, MacNaul K, Stevens K, Pasparakis M, et al. Targeted disruption of the tumor necrosis factor-alpha gene: metabolic consequences in obese and nonobese mice. *Diabetes.* 1997;46(9):1526-31.

92. Schreyer SA, Chua SC, Jr., and LeBoeuf RC. Obesity and diabetes in TNF-alpha receptor- deficient mice. *J Clin Invest.* 1998;102(2):402-11.
93. Dominguez H, Storgaard H, Rask-Madsen C, Steffen Hermann T, Ihlemann N, Baunbjerg Nielsen D, et al. Metabolic and vascular effects of tumor necrosis factor-alpha blockade with etanercept in obese patients with type 2 diabetes. *J Vasc Res.* 2005;42(6):517-25.
94. Lo J, Bernstein LE, Canavan B, Torriani M, Jackson MB, Ahima RS, et al. Effects of TNF-alpha neutralization on adipocytokines and skeletal muscle adiposity in the metabolic syndrome. *Am J Physiol Endocrinol Metab.* 2007;293(1):E102-9.
95. Ofei F, Hurel S, Newkirk J, Sopwith M, and Taylor R. Effects of an engineered human anti-TNF-alpha antibody (CDP571) on insulin sensitivity and glycemic control in patients with NIDDM. *Diabetes.* 1996;45(7):881-5.
96. Rosenvinge A, Krogh-Madsen R, Baslund B, and Pedersen BK. Insulin resistance in patients with rheumatoid arthritis: effect of anti-TNFalpha therapy. *Scand J Rheumatol.* 2007;36(2):91-6.
97. Paquot N, Castillo MJ, Lefebvre PJ, and Scheen AJ. No increased insulin sensitivity after a single intravenous administration of a recombinant human tumor necrosis factor receptor: Fc fusion protein in obese insulin-resistant patients. *J Clin Endocrinol Metab.* 2000;85(3):1316-9.
98. Stanley TL, Zanni MV, Johnsen S, Rasheed S, Makimura H, Lee H, et al. TNF-alpha antagonism with etanercept decreases glucose and increases the proportion of high molecular weight adiponectin in obese subjects with features of the metabolic syndrome. *J Clin Endocrinol Metab.* 2011;96(1):E146-50.
99. Wascher TC, Lindeman JH, Sourij H, Kooistra T, Pacini G, and Roden M. Chronic TNF-alpha neutralization does not improve insulin resistance or endothelial function in "healthy" men with metabolic syndrome. *Mol Med.* 2011;17(3-4):189-93.
100. van den Oever IAM, Baniaamam M, Simsek S, Raterman HG, van Denderen JC, van Eijk IC, et al. The effect of anti-TNF treatment on body composition and insulin resistance in patients with rheumatoid arthritis. *Rheumatol Int.* 2021;41(2):319-28.
101. Corrado A, Colia R, Rotondo C, Sanpaolo E, and Cantatore FP. Changes in serum adipokines profile and insulin resistance in patients with rheumatoid arthritis treated with anti-TNF-alpha. *Curr Med Res Opin.* 2019;35(12):2197-205.
102. Stagakis I, Bertsias G, Karvounaris S, Kavousanaki M, Virla D, Raptopoulou A, et al. Anti-tumor necrosis factor therapy improves insulin resistance, beta cell function and insulin signaling in active rheumatoid arthritis patients with high insulin resistance. *Arthritis Res Ther.* 2012;14(3):R141.
103. Matthews VB, Allen TL, Risis S, Chan MH, Henstridge DC, Watson N, et al. Interleukin-6-deficient mice develop hepatic inflammation and systemic insulin resistance. *Diabetologia.* 2010;53(11):2431-41.
104. Franckhauser S, Elias I, Rotter Sopasakis V, Ferre T, Nagaev I, Andersson CX, et al. Overexpression of Il6 leads to hyperinsulinaemia, liver inflammation and reduced body weight in mice. *Diabetologia.* 2008;51(7):1306-16.
105. Sadagurski M, Norquay L, Farhang J, D'Aquino K, Copps K, and White MF. Human IL6 enhances leptin action in mice. *Diabetologia.* 2010;53(3):525-35.
106. van Hall G, Steensberg A, Sacchetti M, Fischer C, Keller C, Schjerling P, et al. Interleukin-6 stimulates lipolysis and fat oxidation in humans. *J Clin Endocrinol Metab.* 2003;88(7):3005-10.
107. Carey AL, Steinberg GR, Macaulay SL, Thomas WG, Holmes AG, Ramm G, et al. Interleukin-6 increases insulin-stimulated glucose disposal in humans and glucose uptake and fatty acid oxidation in vitro via AMP-activated protein kinase. *Diabetes.* 2006;55(10):2688-97.

108. Castaneda S, Remuzgo-Martinez S, Lopez-Mejias R, Genre F, Calvo-Alen J, Llorente I, et al. Rapid beneficial effect of the IL-6 receptor blockade on insulin resistance and insulin sensitivity in non-diabetic patients with rheumatoid arthritis. *Clin Exp Rheumatol.* 2019;37(3):465-73.
109. Lagathu C, Yvan-Charvet L, Bastard JP, Maachi M, Quignard-Boulange A, Capeau J, et al. Long-term treatment with interleukin-1beta induces insulin resistance in murine and human adipocytes. *Diabetologia.* 2006;49(9):2162-73.
110. Gao D, Madi M, Ding C, Fok M, Steele T, Ford C, et al. Interleukin-1beta mediates macrophage-induced impairment of insulin signaling in human primary adipocytes. *Am J Physiol Endocrinol Metab.* 2014;307(3):E289-304.
111. Nov O, Kohl A, Lewis EC, Bashan N, Dvir I, Ben-Shlomo S, et al. Interleukin-1beta may mediate insulin resistance in liver-derived cells in response to adipocyte inflammation. *Endocrinology.* 2010;151(9):4247-56.
112. McGillicuddy FC, Harford KA, Reynolds CM, Oliver E, Claessens M, Mills KH, et al. Lack of interleukin-1 receptor I (IL-1RI) protects mice from high-fat diet-induced adipose tissue inflammation coincident with improved glucose homeostasis. *Diabetes.* 2011;60(6):1688-98.
113. Stienstra R, Joosten LA, Koenen T, van Tits B, van Diepen JA, van den Berg SA, et al. The inflammasome-mediated caspase-1 activation controls adipocyte differentiation and insulin sensitivity. *Cell Metab.* 2010;12(6):593-605.
114. Cavelti-Weder C, Babians-Brunner A, Keller C, Stahel MA, Kurz-Levin M, Zayed H, et al. Effects of gevokizumab on glycemia and inflammatory markers in type 2 diabetes. *Diabetes Care.* 2012;35(8):1654-62.
115. Dagdeviren S, Jung DY, Friedline RH, Noh HL, Kim JH, Patel PR, et al. IL-10 prevents aging-associated inflammation and insulin resistance in skeletal muscle. *FASEB J.* 2017;31(2):701-10.
116. Kowalski GM, Nicholls HT, Risis S, Watson NK, Kanellakis P, Bruce CR, et al. Deficiency of haematopoietic-cell-derived IL-10 does not exacerbate high-fat-diet-induced inflammation or insulin resistance in mice. *Diabetologia.* 2011;54(4):888-99.
117. den Boer MA, Voshol PJ, Schroder-van der Elst JP, Korsheninnikova E, Ouwens DM, Kuipers F, et al. Endogenous interleukin-10 protects against hepatic steatosis but does not improve insulin sensitivity during high-fat feeding in mice. *Endocrinology.* 2006;147(10):4553-8.
118. Kohl A, Gogebakan O, Mohlig M, Osterhoff M, Isken F, Pfeiffer AF, et al. Increased interleukin-10 but unchanged insulin sensitivity after 4 weeks of (1, 3)(1, 6)-beta-glycan consumption in overweight humans. *Nutr Res.* 2009;29(4):248-54.
119. Williamson RT. On the Treatment of Glycosuria and Diabetes Mellitus with Sodium Salicylate. *Br Med J.* 1901;1(2100):760-2.
120. Reid J, Macdougall AI, and Andrews MM. Aspirin and diabetes mellitus. *Br Med J.* 1957;2(5053):1071-4.
121. Perry CG, Spiers A, Cleland SJ, Lowe GD, Petrie JR, and Connell JM. Glucocorticoids and insulin sensitivity: dissociation of insulin's metabolic and vascular actions. *J Clin Endocrinol Metab.* 2003;88(12):6008-14.
122. Chan DC, Watts GF, Barrett PH, Beilin LJ, and Mori TA. Effect of atorvastatin and fish oil on plasma high-sensitivity C-reactive protein concentrations in individuals with visceral obesity. *Clin Chem.* 2002;48(6 Pt 1):877-83.
123. Preiss D, Seshasai SR, Welsh P, Murphy SA, Ho JE, Waters DD, et al. Risk of incident diabetes with intensive-dose compared with moderate-dose statin therapy: a meta-analysis. *JAMA.* 2011;305(24):2556-64.

124. Morley TS, Xia JY, and Scherer PE. Selective enhancement of insulin sensitivity in the mature adipocyte is sufficient for systemic metabolic improvements. *Nat Commun.* 2015;6:7906.
125. McCurdy CE, Schenk S, Holliday MJ, Philp A, Houck JA, Patsouris D, et al. Attenuated Pik3r1 expression prevents insulin resistance and adipose tissue macrophage accumulation in diet-induced obese mice. *Diabetes.* 2012;61(10):2495-505.
126. Shearin AL, Monks BR, Seale P, and Birnbaum MJ. Lack of AKT in adipocytes causes severe lipodystrophy. *Mol Metab.* 2016;5(7):472-9.
127. Su D, Coudriet GM, Hyun Kim D, Lu Y, Perdomo G, Qu S, et al. FoxO1 links insulin resistance to proinflammatory cytokine IL-1beta production in macrophages. *Diabetes.* 2009;58(11):2624-33.
128. Boren J, and Taskinen MR. In: von Eckardstein A, and Binder CJ eds. *Prevention and Treatment of Atherosclerosis: Improving State-of-the-Art Management and Search for Novel Targets*. Cham (CH); 2022:133-56.
129. Barrows BR, and Parks EJ. Contributions of different fatty acid sources to very low-density lipoprotein-triacylglycerol in the fasted and fed states. *J Clin Endocrinol Metab.* 2006;91(4):1446-52.
130. Tamura S, and Shimomura I. Contribution of adipose tissue and de novo lipogenesis to nonalcoholic fatty liver disease. *J Clin Invest.* 2005;115(5):1139-42.
131. Adiels M, Olofsson SO, Taskinen MR, and Boren J. Overproduction of very low-density lipoproteins is the hallmark of the dyslipidemia in the metabolic syndrome. *Arterioscler Thromb Vasc Biol.* 2008;28(7):1225-36.
132. Goldberg IJ. Lipoprotein lipase and lipolysis: central roles in lipoprotein metabolism and atherogenesis. *J Lipid Res.* 1996;37(4):693-707.
133. Miksztowicz V, Lucero D, Zago V, Cacciagiu L, Lopez G, Gonzalez Ballerga E, et al. Hepatic lipase activity is increased in non-alcoholic fatty liver disease beyond insulin resistance. *Diabetes Metab Res Rev.* 2012;28(6):535-41.
134. Dallinga-Thie GM, Franssen R, Mooij HL, Visser ME, Hassing HC, Peelman F, et al. The metabolism of triglyceride-rich lipoproteins revisited: new players, new insight. *Atherosclerosis.* 2010;211(1):1-8.
135. Patel A, Barzi F, Jamrozik K, Lam TH, Ueshima H, Whitlock G, et al. Serum triglycerides as a risk factor for cardiovascular diseases in the Asia-Pacific region. *Circulation.* 2004;110(17):2678-86.
136. Sarwar N, Danesh J, Eiriksdottir G, Sigurdsson G, Wareham N, Bingham S, et al. Triglycerides and the risk of coronary heart disease: 10,158 incident cases among 262,525 participants in 29 Western prospective studies. *Circulation.* 2007;115(4):450-8.
137. Boren J, Watts GF, Adiels M, Soderlund S, Chan DC, Hakkarainen A, et al. Kinetic and Related Determinants of Plasma Triglyceride Concentration in Abdominal Obesity: Multicenter Tracer Kinetic Study. *Arterioscler Thromb Vasc Biol.* 2015;35(10):2218-24.
138. Taskinen MR, Adiels M, Westerbacka J, Soderlund S, Kahri J, Lundbom N, et al. Dual metabolic defects are required to produce hypertriglyceridemia in obese subjects. *Arterioscler Thromb Vasc Biol.* 2011;31(9):2144-50.
139. Ooi EM, Russell BS, Olson E, Sun SZ, Diffenderfer MR, Lichtenstein AH, et al. Apolipoprotein B-100-containing lipoprotein metabolism in subjects with lipoprotein lipase gene mutations. *Arterioscler Thromb Vasc Biol.* 2012;32(2):459-66.
140. Young SG, Davies BS, Voss CV, Gin P, Weinstein MM, Tontonoz P, et al. GPIHBP1, an endothelial cell transporter for lipoprotein lipase. *J Lipid Res.* 2011;52(11):1869-84.
141. Peterfy M, Ben-Zeev O, Mao HZ, Weissglas-Volkov D, Aouizerat BE, Pullinger CR, et al. Mutations in LMF1 cause combined lipase deficiency and severe hypertriglyceridemia. *Nat Genet.* 2007;39(12):1483-7.

142. Doolittle MH, Ehrhardt N, and Peterfy M. Lipase maturation factor 1: structure and role in lipase folding and assembly. *Curr Opin Lipidol.* 2010;21(3):198-203.
143. Rios JJ, Shastry S, Jasso J, Hauser N, Garg A, Bensadoun A, et al. Deletion of GPIHBP1 causing severe chylomicronemia. *J Inherit Metab Dis.* 2012;35(3):531-40.
144. Hegele RA. Multidimensional regulation of lipoprotein lipase: impact on biochemical and cardiovascular phenotypes. *J Lipid Res.* 2016;57(9):1601-7.
145. Mach F, Baigent C, Catapano AL, Koskinas KC, Casula M, Badimon L, et al. 2019 ESC/EAS Guidelines for the management of dyslipidaemias: lipid modification to reduce cardiovascular risk. *Eur Heart J.* 2020;41(1):111-88.
146. Reitman M, and Gavrilova O. A-ZIP/F-1 mice lacking white fat: a model for understanding lipoatrophic diabetes. *International Journal of Obesity.* 2000;24(S4):S11.
147. Gavrilova O, Marcus-Samuels B, Graham D, Kim JK, Shulman GI, Castle AL, et al. Surgical implantation of adipose tissue reverses diabetes in lipoatrophic mice. *The Journal of clinical investigation.* 2000;105(3):271-8.
148. Adiels M, Boren J, Caslake MJ, Stewart P, Soro A, Westerbacka J, et al. Overproduction of VLDL1 driven by hyperglycemia is a dominant feature of diabetic dyslipidemia. *Arterioscler Thromb Vasc Biol.* 2005;25(8):1697-703.
149. Reynisdottir S, Angelin B, Langin D, Lithell H, Eriksson M, Holm C, et al. Adipose tissue lipoprotein lipase and hormone-sensitive lipase. Contrasting findings in familial combined hyperlipidemia and insulin resistance syndrome. *Arterioscler Thromb Vasc Biol.* 1997;17(10):2287-92.
150. Bessesen DH, Robertson AD, and Eckel RH. Weight reduction increases adipose but decreases cardiac LPL in reduced-obese Zucker rats. *Am J Physiol.* 1991;261(2 Pt 1):E246-51.
151. David JR. Delayed hypersensitivity in vitro: its mediation by cell-free substances formed by lymphoid cell-antigen interaction. *Proc Natl Acad Sci U S A.* 1966;56(1):72-7.
152. Bernhagen J, Calandra T, Mitchell RA, Martin SB, Tracey KJ, Voelter W, et al. MIF is a pituitary-derived cytokine that potentiates lethal endotoxaemia. *Nature.* 1993;365(6448):756-9.
153. Calandra T, and Roger T. Macrophage migration inhibitory factor: a regulator of innate immunity. *Nat Rev Immunol.* 2003;3(10):791-800.
154. Cui D, Peng Y, Zhang C, Li Z, Su Y, Qi Y, et al. Macrophage migration inhibitory factor mediates metabolic dysfunction induced by atypical antipsychotic therapy. *J Clin Invest.* 2018;128(11):4997-5007.
155. Bacher M, Meinhardt A, Lan HY, Dhabhar FS, Mu W, Metz CN, et al. MIF expression in the rat brain: implications for neuronal function. *Mol Med.* 1998;4(4):217-30.
156. Willis MS, Carlson DL, Dimaio JM, White MD, White DJ, Adams GAt, et al. Macrophage migration inhibitory factor mediates late cardiac dysfunction after burn injury. *Am J Physiol Heart Circ Physiol.* 2005;288(2):H795-804.
157. Flieger O, Engling A, Bucala R, Lue H, Nickel W, and Bernhagen J. Regulated secretion of macrophage migration inhibitory factor is mediated by a non-classical pathway involving an ABC transporter. *FEBS Lett.* 2003;551(1-3):78-86.
158. Merk M, Baugh J, Zierow S, Leng L, Pal U, Lee SJ, et al. The Golgi-associated protein p115 mediates the secretion of macrophage migration inhibitory factor. *J Immunol.* 2009;182(11):6896-906.
159. Leng L, Metz CN, Fang Y, Xu J, Donnelly S, Baugh J, et al. MIF signal transduction initiated by binding to CD74. *J Exp Med.* 2003;197(11):1467-76.
160. Bernhagen J, Krohn R, Lue H, Gregory JL, Zernecke A, Koenen RR, et al. MIF is a noncognate ligand of CXC chemokine receptors in inflammatory and atherogenic cell recruitment. *Nat Med.* 2007;13(5):587-96.

161. Tarnowski M, Grymula K, Liu R, Tarnowska J, Drukala J, Ratajczak J, et al. Macrophage migration inhibitory factor is secreted by rhabdomyosarcoma cells, modulates tumor metastasis by binding to CXCR4 and CXCR7 receptors and inhibits recruitment of cancer-associated fibroblasts. *Mol Cancer Res.* 2010;8(10):1328-43.
162. Burger-Kentischer A, Goebel H, Seiler R, Fraedrich G, Schaefer HE, Dimmeler S, et al. Expression of macrophage migration inhibitory factor in different stages of human atherosclerosis. *Circulation.* 2002;105(13):1561-6.
163. Al-Abed Y, Dabideen D, Aljabari B, Valster A, Messmer D, Ochani M, et al. ISO-1 binding to the tautomerase active site of MIF inhibits its pro-inflammatory activity and increases survival in severe sepsis. *J Biol Chem.* 2005;280(44):36541-4.
164. Baugh JA, Chitnis S, Donnelly SC, Monteiro J, Lin X, Plant BJ, et al. A functional promoter polymorphism in the macrophage migration inhibitory factor (MIF) gene associated with disease severity in rheumatoid arthritis. *Genes Immun.* 2002;3(3):170-6.
165. Das R, LaRose MI, Hergott CB, Leng L, Bucala R, and Weiser JN. Macrophage migration inhibitory factor promotes clearance of pneumococcal colonization. *J Immunol.* 2014;193(2):764-72.
166. Li S, Nie K, Zhang Q, Guo M, Qiu Y, Li Y, et al. Macrophage Migration Inhibitory Factor Mediates Neuroprotective Effects by Regulating Inflammation, Apoptosis and Autophagy in Parkinson's Disease. *Neuroscience.* 2019;416:50-62.
167. Miller EJ, Li J, Leng L, McDonald C, Atsumi T, Bucala R, et al. Macrophage migration inhibitory factor stimulates AMP-activated protein kinase in the ischaemic heart. *Nature.* 2008;451(7178):578-82.
168. Stoppe C, Averdunk L, Goetzenich A, Soppert J, Marlier A, Kraemer S, et al. The protective role of macrophage migration inhibitory factor in acute kidney injury after cardiac surgery. *Sci Transl Med.* 2018;10(441).
169. Benigni F, Atsumi T, Calandra T, Metz C, Echtenacher B, Peng T, et al. The proinflammatory mediator macrophage migration inhibitory factor induces glucose catabolism in muscle. *J Clin Invest.* 2000;106(10):1291-300.
170. Dandona P, Aljada A, Ghanim H, Mohanty P, Tripathy C, Hofmeyer D, et al. Increased plasma concentration of macrophage migration inhibitory factor (MIF) and MIF mRNA in mononuclear cells in the obese and the suppressive action of metformin. *J Clin Endocrinol Metab.* 2004;89(10):5043-7.
171. Ghanim H, Aljada A, Hofmeyer D, Syed T, Mohanty P, and Dandona P. Circulating mononuclear cells in the obese are in a proinflammatory state. *Circulation.* 2004;110(12):1564-71.
172. Church TS, Willis MS, Priest EL, Lamonte MJ, Earnest CP, Wilkinson WJ, et al. Obesity, macrophage migration inhibitory factor, and weight loss. *Int J Obes (Lond).* 2005;29(6):675-81.
173. Gonzalez-Muniesa P, Marrades MP, Martinez JA, and Moreno-Aliaga MJ. Differential proinflammatory and oxidative stress response and vulnerability to metabolic syndrome in habitual high-fat young male consumers putatively predisposed by their genetic background. *Int J Mol Sci.* 2013;14(9):17238-55.
174. Alvehus M, Buren J, Sjostrom M, Goedecke J, and Olsson T. The human visceral fat depot has a unique inflammatory profile. *Obesity (Silver Spring).* 2010;18(5):879-83.
175. Skurk T, Herder C, Kraft I, Muller-Scholze S, Hauner H, and Kolb H. Production and release of macrophage migration inhibitory factor from human adipocytes. *Endocrinology.* 2005;146(3):1006-11.
176. Atsumi T, Cho YR, Leng L, McDonald C, Yu T, Danton C, et al. The proinflammatory cytokine macrophage migration inhibitory factor regulates glucose metabolism during systemic inflammation. *J Immunol.* 2007;179(8):5399-406.

177. Finucane OM, Reynolds CM, McGillicuddy FC, Harford KA, Morrison M, Baugh J, et al. Macrophage migration inhibitory factor deficiency ameliorates high-fat diet induced insulin resistance in mice with reduced adipose inflammation and hepatic steatosis. *PLoS One.* 2014;9(11):e113369.
178. Herder C, Kolb H, Koenig W, Haastert B, Muller-Scholze S, Rathmann W, et al. Association of systemic concentrations of macrophage migration inhibitory factor with impaired glucose tolerance and type 2 diabetes: results from the Cooperative Health Research in the Region of Augsburg, Survey 4 (KORA S4). *Diabetes Care.* 2006;29(2):368-71.
179. Kang I, and Bucala R. The immunobiology of MIF: function, genetics and prospects for precision medicine. *Nat Rev Rheumatol.* 2019;15(7):427-37.
180. Lumeng CN, and Saltiel AR. Inflammatory links between obesity and metabolic disease. *J Clin Invest.* 2011;121(6):2111-7.
181. Amouzou C, Breuker C, Fabre O, Bourret A, Lambert K, Birot O, et al. Skeletal Muscle Insulin Resistance and Absence of Inflammation Characterize Insulin-Resistant Grade I Obese Women. *PLoS One.* 2016;11(4):e0154119.
182. Qi D, Hu X, Wu X, Merk M, Leng L, Bucala R, et al. Cardiac macrophage migration inhibitory factor inhibits JNK pathway activation and injury during ischemia/reperfusion. *J Clin Invest.* 2009;119(12):3807-16.
183. Qi D, and Young LH. AMPK: energy sensor and survival mechanism in the ischemic heart. *Trends Endocrinol Metab.* 2015;26(8):422-9.
184. Verschuren L, Kooistra T, Bernhagen J, Voshol PJ, Ouwens DM, van Erk M, et al. MIF deficiency reduces chronic inflammation in white adipose tissue and impairs the development of insulin resistance, glucose intolerance, and associated atherosclerotic disease. *Circ Res.* 2009;105(1):99-107.
185. Fain JN, Tichansky DS, and Madan AK. Most of the interleukin 1 receptor antagonist, cathepsin S, macrophage migration inhibitory factor, nerve growth factor, and interleukin 18 release by explants of human adipose tissue is by the non-fat cells, not by the adipocytes. *Metabolism.* 2006;55(8):1113-21.
186. Hudak CS, and Sul HS. Pref-1, a gatekeeper of adipogenesis. *Front Endocrinol (Lausanne).* 2013;4:79.
187. Lee K, Villena JA, Moon YS, Kim KH, Lee S, Kang C, et al. Inhibition of adipogenesis and development of glucose intolerance by soluble preadipocyte factor-1 (Pref-1). *J Clin Invest.* 2003;111(4):453-61.
188. Moon YS, Smas CM, Lee K, Villena JA, Kim KH, Yun EJ, et al. Mice lacking paternally expressed Pref-1/Dlk1 display growth retardation and accelerated adiposity. *Mol Cell Biol.* 2002;22(15):5585-92.
189. Charalambous M, Da Rocha ST, Radford EJ, Medina-Gomez G, Curran S, Pinnock SB, et al. DLK1/PREF1 regulates nutrient metabolism and protects from steatosis. *Proc Natl Acad Sci U S A.* 2014;111(45):16088-93.
190. Shea J, French CR, Bishop J, Martin G, Roebothan B, Pace D, et al. Changes in the transcriptome of abdominal subcutaneous adipose tissue in response to short-term overfeeding in lean and obese men. *Am J Clin Nutr.* 2009;89(1):407-15.
191. O'Connell J, Lynch L, Hogan A, Cawood TJ, and O'Shea D. Preadipocyte factor-1 is associated with metabolic profile in severe obesity. *J Clin Endocrinol Metab.* 2011;96(4):E680-4.
192. Mitchell R, Bacher M, Bernhagen J, Pushkarskaya T, Seldin MF, and Bucala R. Cloning and characterization of the gene for mouse macrophage migration inhibitory factor (MIF). *J Immunol.* 1995;154(8):3863-70.
193. Wang Y, Zhao L, Smas C, and Sul HS. Pref-1 interacts with fibronectin to inhibit adipocyte differentiation. *Mol Cell Biol.* 2010;30(14):3480-92.

194. Wang P, Jiang Y, Wang Y, Shyy JY, and DeFea KA. Beta-arrestin inhibits CAMKKbeta-dependent AMPK activation downstream of protease-activated-receptor-2. *BMC Biochem.* 2010;11:36.
195. Tran TT, and Kahn CR. Transplantation of adipose tissue and stem cells: role in metabolism and disease. *Nat Rev Endocrinol.* 2010;6(4):195-213.
196. Sakaue S, Ishimaru S, Hizawa N, Ohtsuka Y, Tsujino I, Honda T, et al. Promoter polymorphism in the macrophage migration inhibitory factor gene is associated with obesity. *Int J Obes (Lond).* 2006;30(2):238-42.
197. Lim J, Iyer A, Liu L, Suen JY, Lohman RJ, Seow V, et al. Diet-induced obesity, adipose inflammation, and metabolic dysfunction correlating with PAR2 expression are attenuated by PAR2 antagonism. *FASEB J.* 2013;27(12):4757-67.
198. McGuire JJ, Hollenberg MD, Bennett BM, and Triggle CR. Hyperpolarization of murine small caliber mesenteric arteries by activation of endothelial proteinase-activated receptor 2. *Can J Physiol Pharmacol.* 2004;82(12):1103-12.
199. Li M, Yang X, Zhang Y, Chen L, Lu H, Li X, et al. Activation of proteaseactivated receptor2 is associated with increased expression of inflammatory factors in the adipose tissues of obese mice. *Mol Med Rep.* 2015;12(4):6227-34.
200. Ruge T, Sukonina V, Myrnas T, Lundgren M, Eriksson JW, and Olivecrona G. Lipoprotein lipase activity/mass ratio is higher in omental than in subcutaneous adipose tissue. *Eur J Clin Invest.* 2006;36(1):16-21.
201. Kern PA, Ong JM, Saffari B, and Carty J. The effects of weight loss on the activity and expression of adipose-tissue lipoprotein lipase in very obese humans. *N Engl J Med.* 1990;322(15):1053-9.
202. Huang Y, Cui D, Chen L, Tong H, Wu H, Muller GK, et al. A pref-1-controlled non-inflammatory mechanism of insulin resistance. *iScience.* 2023;26(6):106923.
203. Ramachandran R, Noorbakhsh F, Defea K, and Hollenberg MD. Targeting proteinase-activated receptors: therapeutic potential and challenges. *Nat Rev Drug Discov.* 2012;11(1):69-86.
204. Li M, Yang X, Zhang Y, Chen L, Lu H, Li X, et al. Activation of protease-activated receptor-2 is associated with increased expression of inflammatory factors in the adipose tissues of obese mice. *Mol Med Rep.* 2015;12(4):6227-34.
205. Adams MN, Ramachandran R, Yau MK, Suen JY, Fairlie DP, Hollenberg MD, et al. Structure, function and pathophysiology of protease activated receptors. *Pharmacol Ther.* 2011;130(3):248-82.
206. Shearer AM, Rana R, Austin K, Baleja JD, Nguyen N, Bohm A, et al. Targeting Liver Fibrosis with a Cell-penetrating Protease-activated Receptor-2 (PAR2) Pepducin. *J Biol Chem.* 2016;291(44):23188-98.
207. Shimizu T, Nishihira J, Watanabe H, Abe R, Honda A, Ishibashi T, et al. Macrophage migration inhibitory factor is induced by thrombin and factor Xa in endothelial cells. *J Biol Chem.* 2004;279(14):13729-37.
208. Sreih AG, Ezzedine R, Leng L, Fan J, Yao J, Reid D, et al. Role of Macrophage Migration Inhibitory Factor in Granulomatosis With Polyangiitis. *Arthritis Rheumatol.* 2018;70(12):2077-86.
209. Bernhagen J, Mitchell RA, Calandra T, Voelter W, Cerami A, and Bucala R. Purification, bioactivity, and secondary structure analysis of mouse and human macrophage migration inhibitory factor (MIF). *Biochemistry.* 1994;33(47):14144-55.
210. Kim SJ, Nian C, and McIntosh CH. GIP increases human adipocyte LPL expression through CREB and TORC2-mediated trans-activation of the LPL gene. *J Lipid Res.* 2010;51(11):3145-57.

211. Kanaki M, and Kardassis D. Regulation of the human lipoprotein lipase gene by the forkhead box transcription factor FOXA2/HNF-3beta in hepatic cells. *Biochim Biophys Acta Gene Regul Mech.* 2017;1860(3):327-36.
212. Li B, Fang J, He T, Yin S, Yang M, Cui H, et al. Resistin up-regulates LPL expression through the PPARgamma-dependent PI3K/AKT signaling pathway impacting lipid accumulation in RAW264.7 macrophages. *Cytokine.* 2019;119:168-74.
213. Li Z, Deng ML, Tseng CH, and Heber D. Hypertriglyceridemia is a practical biomarker of metabolic syndrome in individuals with abdominal obesity. *Metab Syndr Relat Disord.* 2013;11(2):87-91.
214. Sampson UK, Fazio S, and Linton MF. Residual cardiovascular risk despite optimal LDL cholesterol reduction with statins: the evidence, etiology, and therapeutic challenges. *Curr Atheroscler Rep.* 2012;14(1):1-10.
215. Preiss-Landl K, Zimmermann R, Hammerle G, and Zechner R. Lipoprotein lipase: the regulation of tissue specific expression and its role in lipid and energy metabolism. *Curr Opin Lipidol.* 2002;13(5):471-81.
216. Jensen DR, Schlaepfer IR, Morin CL, Pennington DS, Marcell T, Ammon SM, et al. Prevention of diet-induced obesity in transgenic mice overexpressing skeletal muscle lipoprotein lipase. *Am J Physiol.* 1997;273(2 Pt 2):R683-9.
217. Augustus A, Yagyu H, Haemmerle G, Bensadoun A, Vikramadithyan RK, Park SY, et al. Cardiac-specific knock-out of lipoprotein lipase alters plasma lipoprotein triglyceride metabolism and cardiac gene expression. *J Biol Chem.* 2004;279(24):25050-7.
218. Nilsson-Ehle P. Impaired regulation of adipose tissue lipoprotein lipase in obesity. *Int J Obes.* 1981;5(6):695-9.
219. Weinstock PH, Levak-Frank S, Hudgins LC, Radner H, Friedman JM, Zechner R, et al. Lipoprotein lipase controls fatty acid entry into adipose tissue, but fat mass is preserved by endogenous synthesis in mice deficient in adipose tissue lipoprotein lipase. *Proc Natl Acad Sci U S A.* 1997;94(19):10261-6.
220. Park YJ, Lee B, Kim DH, Kwon EB, Go Y, Ha S, et al. PAR2 Deficiency Induces Mitochondrial ROS Generation and Dysfunctions, Leading to the Inhibition of Adipocyte Differentiation. *Oxid Med Cell Longev.* 2021;2021:6683033.
221. Zhen EY, Chen YQ, Russell AM, Ehsani M, Siegel RW, Qian Y, et al. Angiopoietin-like protein 4/8 complex-mediated plasmin generation leads to cleavage of the complex and restoration of LPL activity. *Proc Natl Acad Sci U S A.* 2023;120(7):e2214081120.
222. Morrison MC, and Kleemann R. Role of Macrophage Migration Inhibitory Factor in Obesity, Insulin Resistance, Type 2 Diabetes, and Associated Hepatic Co-Morbidities: A Comprehensive Review of Human and Rodent Studies. *Front Immunol.* 2015;6:308.
223. Wallberg-Jonsson S, Dahlen G, Johnson O, Olivecrona G, and Rantapaa-Dahlqvist S. Lipoprotein lipase in relation to inflammatory activity in rheumatoid arthritis. *J Intern Med.* 1996;240(6):373-80.
224. Heinrichs D, Knauel M, Offermanns C, Berres ML, Nellen A, Leng L, et al. Macrophage migration inhibitory factor (MIF) exerts antifibrotic effects in experimental liver fibrosis via CD74. *Proc Natl Acad Sci U S A.* 2011;108(42):17444-9.
225. Chen L, Li L, Cui D, Huang Y, Tong H, Zabihi H, et al. Extracellular macrophage migration inhibitory factor (MIF) downregulates adipose hormone-sensitive lipase (HSL) and contributes to obesity. *Mol Metab.* 2023;79:101834.
226. Guilherme A, Virbasius JV, Puri V, and Czech MP. Adipocyte dysfunctions linking obesity to insulin resistance and type 2 diabetes. *Nat Rev Mol Cell Biol.* 2008;9(5):367-77.
227. Ay L, Kopp HP, Brix JM, Ay C, Quehenberger P, Schernthaner GH, et al. Thrombin generation in morbid obesity: significant reduction after weight loss. *J Thromb Haemost.* 2010;8(4):759-65.

228. Moreno M, Puig J, Serrano M, Moreno-Navarrete JM, Ortega F, Ricart W, et al. Circulating tryptase as a marker for subclinical atherosclerosis in obese subjects. *PLoS One.* 2014;9(5):e97014.
229. Eckel RH, Grundy SM, and Zimmet PZ. The metabolic syndrome. *Lancet.* 2005;365(9468):1415-28.
230. Mendrick DL, Diehl AM, Topor LS, Dietert RR, Will Y, La Merrill MA, et al. Metabolic Syndrome and Associated Diseases: From the Bench to the Clinic. *Toxicol Sci.* 2018;162(1):36-42.
231. Wang Y, and Sul HS. Ectodomain shedding of preadipocyte factor 1 (Pref-1) by tumor necrosis factor alpha converting enzyme (TACE) and inhibition of adipocyte differentiation. *Mol Cell Biol.* 2006;26(14):5421-35.
232. Lan H, Wang N, Chen Y, Wang X, Gong Y, Qi X, et al. Macrophage migration inhibitory factor (MIF) promotes rat airway muscle cell proliferation and migration mediated by ERK1/2 and FAK signaling. *Cell Biol Int.* 2018;42(1):75-83.